DESIGN OF IMMUNOACTIVE BIOMATERIALS FOR THERAPEUTIC APPLICATIONS

A Dissertation
Presented to
The Academic Faculty

by

Ni Su

In Partial Fulfillment
of the Requirements for the Degree
of Doctor of Philosophy in the
Wallace H. Coulter Department of Biomedical Engineering

Georgia Institute of Technology
Emory University
August 2018

DESIGN OF IMMUNOACTIVE BIOMATERIALS FOR THERAPEUTIC APPLICATIONS

Approved by:

Dr. Ying Luo, Advisor
Department of Biomedical Engineering
Peking University

Dr. Krishnendu Roy, Advisor
Department of Biomedical EEngineering
Georgia Institute of Technology

Dr. Huaiqiu Zhu
Department of Biomedical Engineering
Peking University

Dr. Haifeng Chen
Department of Biomedical Engineering
Peking University

Dr. Jingwei Xiong
Department of Molecular Science
Peking University

Dr. Weiping Gao
Department of Biomedical Engineering
Tsinghua University

Dr. Jin Zhou
Department of Tissue Engineering
Academy of Military Medical Sciences

Date Approved: [June 5th, 2018]

I dedicate this dissertation to my loving families and my respectable advisors.

ACKNOWLEDGEMENTS

First and foremost, I wish to express my gratitude to my advisors, Dr. Ying Luo and Dr. Krishnendu Roy, for their great help, support and mentoring throughout my graduate studies. To each of the members of my thesis committee, I am thankful for their advice on the research. I'd like to thank my amazing lab mates in both Beijing and Atlanta, who shared experiences and inspirations in both research and life with me. At last, I would like to express my sincere gratitude to my family. Their unconditional love and encouragement have always been the greatest support for me.

TABLE OF CONTENTS

LIST OF FIGURES

LIST OF SYMBOLS AND ABBREVIATIONS

MSC	Mesenchymal stromal cell
DC	Dendritic cell
Treg	Regulatory T cell
Th1	T helper 1
Th2	T helper 2
IFN γ	Interferon gamma
IL17	Interleukin 17
IL4	Interleukin 4
M1	Classically-activated macrophage
M2	Alternatively-activated macrophage
IGF-1	Insulin-like growth factor-1
VEGF	Vascular endothelial growth factor
IL10	Interleukin 10
TGF-β	Transforming growth factor beta
CCL1	C-C Motif Chemokine Ligand 1
CCL22	C-C Motif Chemokine Ligand 22
IDO	Indoleamine-2, 3- dioxygenase
PGE2	prostaglandin E2
TNF-α	tumor necrosis factor α
TSG-6	tumor necrosis factor α-stimulated gene 6 (TSG-6)
EV	Extracellular vesicle

MV	Micro-vesicles
PD-L1	Programmed cell death ligand-1
PD-1	Programmed cell death protein-1
Gal-1	Galectin-1
PLGA	Poly(lactide coglycolide)
PEG	poly(ethylene glycol)
PVA	poly(vinyl alcohol)
FBGC	Foreign body giant cell
EF	Electrospun fiber
ECM	Extracellular matrix
GM-CSF	Granulocyte-macrophage colony-stimulating factor
PEI	Polyethylenimine
PCL	Polycaprolactone
M-CSF	Macrophage colony-stimulating factor
TLR	Toll like receptor
APC	Antigen-presenting cell
Texo	Tumor-derived exosomes
NHL	Non-Hodgkin lymphoma
DLBCL	Diffuse large B cell lymphoma
BMDCs	Bone marrow derived dendritic cells
BMDM	Bone marrow derived macrophage
LN	Lymph nodes

SUMMARY

Immune system is a highly organized network, consisting of innate and adaptive immune responses. The immune system has a critical role in the health of organisms and can be either a cure or cause of disease. In recent years, with the expanded knowledge of immunology that both innate and adaptive immune cells are the key mediators in cancer immunotherapy and tissue repair/regeneration, immunomodulatory biomaterial design provides a new direction for related therapeutics. Therefore, the overall goal of this dissertation is to design biomaterials to modulate or qualitatively shape the immune response, which could be ultimately used for biomedical applications of cancer immunotherapy and regenerative medicine. On the side of cancer immunotherapy, we first designed a cancer vaccine based on tumor-derived exosome, and demonstrated both cellular and humoral anti-tumor immunity could be induced by immunization of the vaccine. The designed vaccine showed a long-term protection against pre-established lethal challenges of B-cell lymphoma in mice. On the side of regenerative medicine, mesenchymal stromal cells (MSCs) are known as the sensor and switch of inflammation. Their widely achieved therapeutic effects for degenerative diseases are mainly contributed by their secretion behavior. We then designed fibrous scaffolds with the aim to potentiate the paracrine function of MSCs for tissue regeneration. It's proved that MSCs showed enhanced secretion of anti-inflammatory and elevated capacities to induce pro-regenerative macrophage phenotype, when potentiated by scaffolds. The conditioned medium from MSCs-scaffolds are demonstrated to promote skin wound healing of mice. Based on the knowledge and experience from the previous two studies, we designed a MSC exosomes

loaded fibrous scaffolds material to directly interact with the immune system for regenerative immunomodulation. The results proved our hypothesis that the scaffolds could recruit immune cells to the transplant site and the loaded exosomes provide them with regenerative immunomodulatory signals, together generating pro-regenerative innate and adaptive immune responses locally and systemically. This dissertation brings new insights and inspirations for the design of therapeutic immunomodulatory biomaterial.

CHAPTER 1. INTRODUCTION

Design of immunoactive biomaterials for therapeutic application of cancer immunotherapy and regenerative medicine is the overall goal of this dissertation. Before going through detailed motivation and objectives of this dissertation, the background information of basic concept of immune system, their role in treating cancer and favoring tissue regeneration/repair, current biomaterial strategies to interfere with the immune system will be introduced in the first chapter.

1.1 Immune system

The immune system has a critical role in the health of organisms and can be either a cure or cause of disease. The immune system is best known as the first line of defense against invading pathogens. The immune system consists of two parts: innate and adaptive system. The innate immune system is the first line of defense, involving polymorphonuclear cells (such as neutrophils, basophils and eosinophils), macrophages and dendritic cells (DCs). They were the first responder towards challenge (infection/wound) and are responsible for killing and phagocytose pathogens or debris from wound. The antigen presenting cells (DCs/macrophages) then carry the signals to the adaptive immune cells to initiate specific response against the existing challenge.

Adaptive immunity consists of B and T lymphocytes bearing highly diverse antigen-specific receptors that enable the immune system to recognize foreign antigen. B-cells mediated humoral immune response that secrete antibodies that can target pathogens for degradation. They could also maintain memory B cells in the bone marrow and circulating

blood to protect against re-infection. T cells could be divided into T helper (Th) cells and cytotoxic T cells. Cytotoxic T cells can mediate direct specific killing against pathogens. While, T helper cells can be polarized into many subtypes, including Th1 cells, Th2 cells, Th17 cells, regulatory T cells (Tregs), and are capable of affecting other innate and adaptive immune cells by cytokine secretion. T helper 1 (Th1) cells secreting IFNγ, is associated with intracellular bacterial infections. Th17 cells secreting IL17, could induce secretion of antimicrobial peptides and defends against extracellular bacteria. Th2 cells secreting IL4, is related to multicellular parasites and has a role in wound healing. Finally, regulatory T cells (Tregs) are modulatory T cells that prevents over activation of the other immune polarizations and play a role in tissue regeneration.

Though the immune system is best known as the first line of defense against invading pathogens, but is also essential to tissue development, homeostasis cancer immunotherapy and wound repair. Actually, cells of the immune system, from innate immune system to adaptive immune system can sense the signals from the surrounding environment and together orchestrated an immunological network to create adequate response for the local tissue microenvironment, either to eliminate pathogen invasion, to clear the cancer cells or to favor tissue repair/regeneration. In the next part, the relationship between immune system and regeneration will be discussed.

1.2 Immune system and regeneration

Centuries ago, scientists were amazed by the ability of organisms such as salamanders to regrowth perfect copies of amputated body parts. It's also astonishing that mice in embryo stage showed the ability to regenerate fully functioned heart tissue post

myocardium infarction, which was lost in adult mice.[1] A widespread idea indicates that the change in the immune system during species revolution or individual development is responsible for differed outcome of regeneration. Actually, the immune system and the immunological environment they orchestrated is crucial to determine the quality of the repair response, including the behavior of stem/progenitor cells, process of angiogenesis, extent of scarring, and the restoration of organ structure and function by lots of studies in different tissue and organisms. And many key mediators in the immune system were identified that interfere the process of tissue repair/regeneration involving both innate immune cells and adaptive immune cells, which will be further introduced below. [2]

1.2.1 Macrophage

Macrophage is one of the most vital and well-studied mediators in immune-mediated regeneration because they are the first responder and final effector cells to the wound site as well as they have highly programming possibilities.[3] (Fig. 1.1) Once injury happens, the local macrophages and the recruited monocytes will massively accumulate in the wound sites in the following few days. After conditioning by the inflammatory stimuli including local growth factors and cytokines, macrophages polarize into classically activated (M1) or alternatively activated (M2) subtypes based on their markers, function, and cytokine profiles. Typically, M1 cells produce high levels of pro-inflammatory cytokines that aid in host defense, debris clearance and stem/progenitor cell recruitment and proliferation, but can also damage healthy tissue. On the contrary, M2 macrophages mediate wound healing, tissue repair, and the resolution of inflammation.[4] Specifically, the cytokine secreted by M2 macrophage, including interleukin-10 (IL-10), insulin-like growth factos-1 (IGF-1), vascular endothelial growth factor (VEGF), IL-4 etc., would

function as mitigating the inflammation at the early stage post injury, recruiting and supporting the proliferation of tissue progenitor cells, inducing vascularization and avoiding fibrosis.[5]

The convert of macrophage from M1 to M2 phenotype is therefore essential for proper wound healing and tissue regeneration. Worth mentioning, the timing of the convert should also be seriously considered, as shown in other study that early infiltration of M2 macrophage to the skin wound will even hinder the process of wound closure.[6] Actually, M1 macrophage and their secretomes in the early time point post injury may be essential for progenitor cell accumulation and proliferation due to their behavior of debris clearance and release of inflammatory cytokines and chemo-attractive cytokines.[7] Due to the natural pro-inflammatory environment in the injury site driven by cell debris and danger signals, the presence of M1 macrophage in the wound site could naturally be achieved without artificial interference. Especially, the living individuals are forced to face with more and more severe survival environment, when evolution from water to land or development from fetus to adult. Therefore, the immune system is prompted to be more intensive in driving inflammatory immune response post injury, in order to seal the wounds efficiently and facilitate individual survival. In such circumstances, strategies to convert M1 to M2 macrophage is still one of the major strategies to generate a pro-regenerative immune environment.

1.2.2 T cells

Other than innate immune cells, adaptive immune cells are also proved to be key mediators in establishment of regenerative immune micro-environment in recent years.

Especially, T cells are proved by many studies to have a crucial role in tissue repair/regeneration.

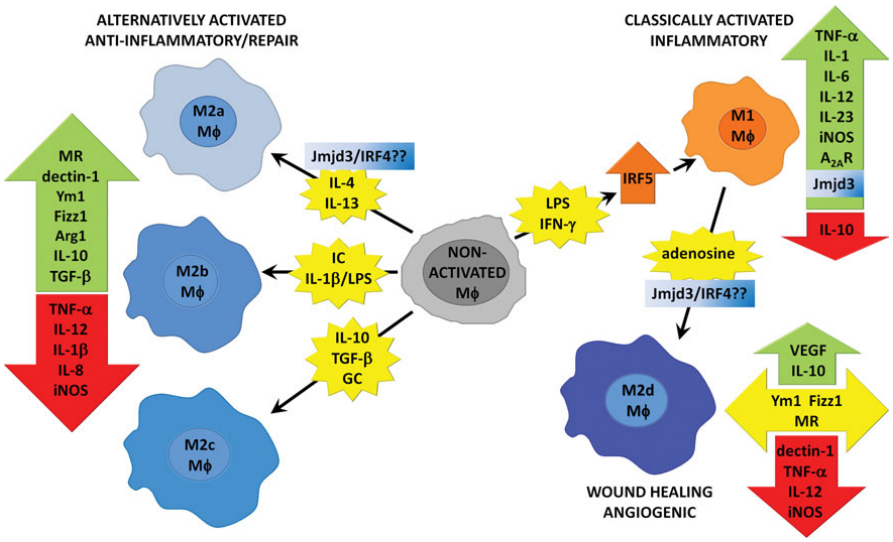

Figure 1.1 The highly programming possibilities of macrophages. (Ferrante et al., Advanced in wound care, 2012, volume1, No.1)

T cells have different subtypes as mentioned above and their role and underlying mechanisms in tissue regeneration/repair is very different and seem to vary from tissue to tissue. . Though some mechanisms have been revealed, the exact function of different type of T cells are largely unknown, which needs more investigation. The following part will discuss current findings of each specific T cell types and their role in tissue repair/regeneration.

Regulatory T cells (Tregs)

Tregs are considered as a pro-regenerative type of immune cells. Tregs may be identified by the co-expression of CD4 and CD25 and by the transcription factor FoxP3.

They produce regulatory cytokines IL-10 and transforming growth factor beta (TGF-β), exhibiting the ability to suppress proliferation of activated T cells and modulate the activity of macrophages towards M2 pehnotype, thereby can indirectly influence the regenerative process.[8] For example, the muscle Tregs are proved to participate muscle regeneration through mediating myotube differentiation, M1 to M2 polarization, and attenuation of excessive T lymphocyte responses.[9, 10] Tregs can also secret growth factors such as amphiregulin, which is beneficial for progenitor cells proliferation and differentiation.[11] Actually, the pro-regenerative role of Tregs has been proved to be critical for the repair and regeneration of several tissues including skin[12], gut[13], skeletal muscle[14], and neuron[15]. The underlying mechanisms based on current knowledge depends on the two pathways mentioned above: immunomodulatory properties on other immune cells (especially macrophage) to form regenerative immune micro-environment and secretion of growth factors directly interact with progenitor cells to induce tissue regrowth.

T helper cells and effector T cells

T helper cells are capable of secreting a diverse range of cytokines and growth factors, which have beneficial or inhibitory effects on tissue healing.[16] The CD4+ T helper 1 (Th1), secreting IFNγ and TNFα, are usually considered as T cell subsets that inhibit regeneration, while the The CD4+ T helper 2 (Th2), secreting IL-4 and IL-10, are recognized as pro-regenerative. The Th1 cells secret pro-inflammatory molecules that forms a positive feedback loop to increase M1 macrophage commitment and ultimately drive chronic inflammation that hinder regeneration. Type 2 immune polarization, which is important in the response to multicellular parasites and wound healing, could drive M2

macrophage differentiation and directly mediate progenitor cell differentiation, thus contributes to tissue regeneration. [17]

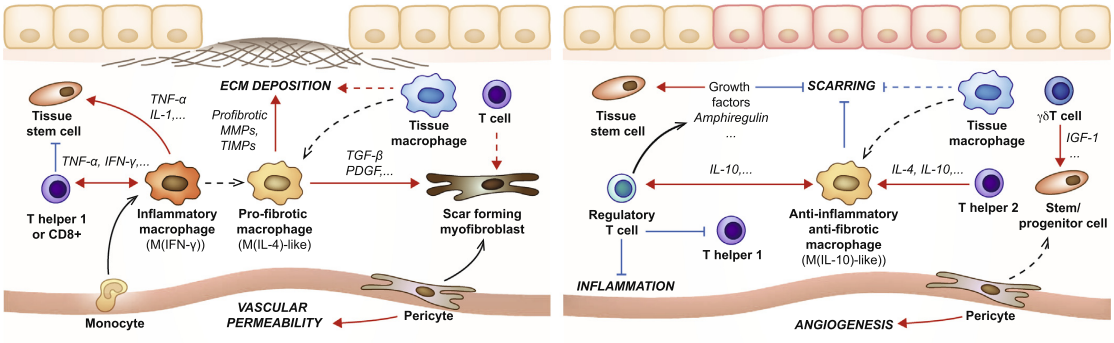

Figure 1.2 Overview of the immune mechanisms that can impair or promote tissue healing or drive scarring and fibrosis. Inflammatory macrophages stimulate effector T cells in a positive-feedback loop. Effector T cells may also inhibit the regenerative capacity of tissue resident stem/progenitor cells via inflammatory cytokines. On contrary, a critical amount of macrophages displaying an anti-inflammatory/anti-fibrotic phenotype contribute to regeneration through a crosstalk with Tregs, which in turn help sustain the anti-inflammatory/anti-fibrotic phenotype via secretion of anti-inflammatory cytokines such as IL-10. Tregs may also enhance the regenerative capacity of endogenous stem/progenitor cells through secretion of growth factors. Th2 cells induce/maintain anti-fibrotic/anti-inflammatory macrophages. (Z. Julier et al. Acta biomaterialia, 2017)

CD8+ (cytotoxic) T cell subsets are considered to inhibit regeneration. For example, fracture healing is accelerated when CD8+ T cells are depleted. On a mechanistic level, it has been demonstrated that Th1 cells inhibits MSC-driven bone formation in the mouse via IFNγ and TNFα. Similar research in humans showed that that delayed fracture healing significantly correlated with enhanced levels of terminally differentiated CD8+ effector memory T.[18] Actually, the inflammatory cytokines secreted by CD8+ T cells exhibited similar mechanism as Th1 immune cells

To conclude, the whole immune system including both innate and adaptive immune response forms a network and together orchestrated the microenvironment for tissue

regeneration. (Fig. 1.2) Though many mechanisms of immune-mediated regeneration remains to be elucidated, the close relationship between immune cells and tissue regeneration has been largely proved. Therefore, modulating the polarization of the immune response becomes a promising strategy to induce tissue regeneration.

1.3 Immunomodulatory properties of MSCs

Mesenchymal stromal cells (MSCs) are widely used in clinical treatment for degenerative diseases. Their secretomes consist of bioactive components with the function of immunomodulation, pro-angiogenesis, anti-apoptosis etc. Especially, MSCs could sense the immune environment and modulate broad spectrum of immune cells by secreting immunomodulatory secretomes, that modulate the immune system towards regenerative phenotype. Therefore, the immunomodulatory secrete behavior makes MSCs, especially their secretion product, a potential candidate in immune-mediated regeneration.

1.3.1 MSCs secretome in regenerative medicine

Mesenchymal stromal cells (MSCs) are multipotent adult stem cells capable of differentiating into multiple lineages, including osteoblasts, adipocytes, chondrocytes and myoblasts, under different stimuli and culture conditions. In recent decades, MSCs are one of the most widely investigated cell types in regenerative medicine and have achieved promising therapeutic results in treating graft-versus-host disease, myocardial infarction, cerebral stroke and wound healing etc.[19, 20] However, studies have shown that the multi-lineage potential of MSCs may contribute little to their therapeutic effects. Instead, the paracrine products and extracellular vesicles (EVs) of MSCs, exhibiting multifaceted functions including immunomodulation, angiogenesis, anti-apoptosis, anti-scarring,

chemoatrraction and modulating local stem and progenitor cells are the main contributor to tissue repair/regeneration.[21]

1.3.2 Immunomodulatory paracrine function of MSCs

One of the most important function of MSC secretome is their immunomodulatory properties. In particular, the anti-inflammatory molecules secreted by MSCs under certain priming conditions, such as by being exposed to pro-inflammatory molecules (e.g. TNF-α and IFN-γ) would modulate both innate and adaptive immune response towards pro-regenerative directions.[22] To be specific, MSCs secrete indoleamine-2, 3- dioxygenase (IDO), prostaglandin E2 (PGE2) and tumor necrosis factor α (TNF-α)-stimulated gene 6 (TSG-6), TGF-β, IL10, IL-6 etc., that are able to modulate macrophage towards M2 phenotype, inhibit dendritic cell (DC) maturation, increase regulatory T cell population, induce Th2 immune response, suppress differentiation of B cells and T cells and suppress NK cell activity. These modulatory effects are highly consistent with the immune environment needed for a benign regenerative outcome mentioned above, therefore making MSCs secretome potential candidates in immune-mediated tissue repair/regeneration [23]

Worth mentioning, the anti-inflammatory properties of MSCs also achieved by cell-cell contact. The PD-L1 and PD-L2 expressed on the MSCs cell membrane wound interact with the PD-1/PD-2 molecules on the immune cell membranes and hinder their inflammatory behavior. Studies have shown that trans-well culture of MSCs and immune cells will diminish the MSCs immunomodulatory properties compared to co-culture system due to the avoidance of cell-cell contact.

1.3.3 Immunomodulatory properties of MSC EVs

EVs are small phospholipid vesicles released from a wide variety of cell types including MSCs, aiming at cell-cell and cell-environment communication. Based on the size and intracellular origin, they can be divided into: exosomes, microvesicles (MVs) and apoptotic bodies. EVs with a diameter ranging from 30 to 100 nm are exosomes with the surface marker of CD9, CD63 and CD81. They are formed inside multivesicular bodies that fuse with the plasma membrane resulting in their release into the extracellular space. EVs with diameter ranging from 100–1000 nm are categorized as MVs, which are formed by budding from the plasma membrane in response to a wide variety of stimuli. The largest EVs, which range from 1 to 5 μm in diameter are the apoptotic bodies. And from here on, this dissertation will focus on MVs and exosomes, which will be collectively referred to as EVs.

MSC-EVs assemble similar properties of MSCs due to their retaining surface proteins, enzymes, RNA and miRNA from their cell of origin. Moreover, EVs have been shown to have equivalent therapeutic effects in many disease, including cardiovascular disease, neurological disorder, kidney damage, wound healing and immunological disease.[24-26] The immunomodulatory factors, such as Gal-1, PD-L1, TGF-β, IL10, miRNAs either anchored on the phospholipid bi-layer or trapped inside the EVs as cargoes endowed EVs the ability to modulate the immune system with equivalent capacity as their origin cells. Similar to the MSCs, EVs could modulate macrophage towards M2 phenotype, increase regulatory T cell population and induce Th2 immune response, inhibit T cell proliferation as reported in other studies.

Taken together, MSC paracrine factors and secreted EVs contains a cohort of immunomodulatory components that could targeting broad types of immune cells. During

tissue injury, MSCs could shape the immune response to favor the regenerative process through their secretome. This makes MSCs secretomes a promising candidate in the development of immunomodulatory regenerative medicine as a substitute of cells.

1.4 Biomaterial-based strategies for immunomodulation in regenerative medicine

The immune response towards biomaterials are inevitable and thus can be used to modulate the immune system to favor regeneration. Many aspects of biomaterials are editable to generate desired immune response, including their chemical/physical/biological properties. Therefore, biomaterial design provides a multi-functional tool-box for us to modulate the immune system towards regeneration.

One strategy of biomaterials design is to avoid or minimize the interaction with the immune system. Therefore, the biomaterials were designed to be inert to minimize the possible foreign body reaction without adding inflammatory burden to tissue regeneration. Later on, the biomaterials were designed to actively absorb danger signals or chemokines from the injured sites to mitigate the inflammation caused by tissue damage in the early phase. With the discovery of immune system's multiple impact on regenerative process, the immunomodulatory properties of regenerative biomaterials should be added to the criteria of the material design. Many biomaterials were then designed as carriers for the delivery of immunomodulatory molecules, genes or cells. However, these strategies seemed to have limited outcome for promoting tissue regeneration as single cytokine or gene delivery may have limited potency to impact the overall immune system. Moreover, the aboving material design are mostly designed to target macrophage and manipulate their phenotype. To better interfere with the immune system in terms how, where and when to

be activated is crucial for the building of a pro-regenerative immune environment. Therefore, introducing immunoactive components to material design to directly modulate and qualitatively shape multiple arms of the immune system, not only macrophage but also adaptive T cells, is a new direction for biomaterial design in regeneration medicine in the future. By optimizing the surface chemical/physical and topological properties of materials, or utilizing the inherent ability of nature-derived biomaterials to cross talk with immune system, materials could be designed to be immunoactive and achieve more potent and broader impact on immune system to favor tissue repair/regeneration.

1.4.1 Biomaterials design to mitigate inflammatory immune response

Inert biomaterials to avoid immune response

In the early time, biomaterials are designed to be inert and invisible to avoid the interaction with the immune system. Based on the knowledge back then, the biomaterials that cause immune response, were recognized as foreign body response, is detrimental to tissue regeneration. Therefore, the materials should be designed to be inert in order to reduce immune cell recruitment. Synthetic materials, such as poly(lactide coglycolide) (PLG), poly(ethylene glycol) (PEG) , and poly(vinyl alcohol) (PVA) have relatively low protein absorption level and can be modified to the biomaterials in order to mitigate the immune response.[27]

Biomaterials for pro-inflammatory signal scavenging

Another biomaterial-based strategy to mitigate the immune response in the injured sites is to design scavenging materials to remove pro-inflammatory signals in the body.

The injured sites will produce pro-inflammatory signals post injury, prepared to fight against possible pathogen invasion. These signals could lead to acute inflammation and harm the local tissue. They could also result in long-term chronic inflammation that hindered the healing process. In recent years, biomaterials are therefore designed to scavenge these pro-inflammatory signals and thus dampen the inflammation post injury and promote wound healing.

These pro-inflammatory signals include damage associated molecular patterns (DAMPs), pathogen associated molecular patterns (PAMPs) and inflammatory chemokines etc. The DAMPs and PAMPs could trigger strong intercellular signal cascades through binding to pattern recognition receptors (PRRs) or (toll-like receptors) TLRs of the immune cells and result in strong inflammatory response that may hinder the regeneration. Pathogenic nucleic acids (e.g., viral RNAs, bacterial DNAs) as well as nucleic acids released by necrotic cells are origin of DAMPs and PRRs. Therefore, materials were designed to have the ability to immobilize the nucleic acid and resolve the inflammation. For example, some nucleic acid-binding polymers such as PAMAM could be immobilized to scaffolds or particles for nucleic acid scavenging in the injury sites.[28-30]

Chemokines are class of signaling molecules that could selectively recruit and activate cells during inflammation. During the wound healing process, chemokines are released by tissue-specific cells and resident immune cells at the site of injury to establish a chemo-attractive gradient that promote the invasion of blood-derived immune cells, which are essential for the initial inflammatory phase of acute wound healing. In chronic inflammation also related to high concentration of chemokines released to the injury sites.

Because the chemokines could bind to extracellular matrix glycosaminoglycans (GAGs), material based on GAGs were designed to remove the chemokines from the wound site and resolve the inflammation.

1.4.2 Biomaterials as delivery tool for immunomodulation.

To modulate the immune system towards regeneration, components with immunomodulatory properties could be administrated to the injured sites, such as anti-inflammatory cytokines and cytokines, miRNA, immune cell chemokines, and even primed immune cells. Therefore, the biomaterials could be used as a delivery tool to efficiently delivery theses immunomodulatory components to the target tissue.[31]

Deliver cytokines

Based on the delivery cargoes and the target cells, the biomaterials could be special design to meet the delivery criteria.[32] For example, soluble anti-inflammatory proteins such as IL4 and IL10, typically have an inherently short half-life when administrated in vivo. Encapsulate these cytokines with hydrogels could be more appropriate for the resolution of acute inflammation.[33, 34] On contrast, when dealing with chronic inflammation, it may be better to encapsulate the cytokines in synthetic polymer materials or immobilization to the scaffold surface for sustained release and prolonged bioactivity in vivo.[35]

Deliver nucleic acids

Biomaterials could also be designed to deliver DNA or RNA through packaging with proteins, polymers or lipids to create particles to overcome the extracellular and

intracellular barriers to efficiently delivery the gene to the target cells. The delivery of a gene can be employed to increase the expression of a target gene and the delivery of siRNA or miRNA could specifically decrease the expression of certain gene. Both strategies are potentially useful in increasing or decreasing the expression of immune-related factors. For example, delivery of miR-146a using PEI nanoparticles was able to inhibit renal fibrosis through suppression of the infiltration of macrophages.[36]

Deliver cells

Deliver cells by materials, especially those have been identified as key mediators in the immune-mediated regeneration, is another direct strategy for regenerative immune modulation. As have mentioned, the MSCs are sensors of inflammation and could switch pro-inflammatory environment to anti-inflammatory environment by secreting immunomodulatory molecules, therefore can be delivered by scaffolds to mitigate inflammation conditions.[37] Proper delivery of M2 macrophage and Tregs to the inflammation sites could help resolving the inflammation.[38] In some circumstance, delivery of M1 macrophage could also be pro-regenerative as pro-inflammatory cytokines are related to debris clearance and progenitor cell proliferation. However, it has to be kept in mind that the timing and the specificity of injured tissue needs to be seriously considered when delivering certain immune modulators. As the immune signals and network are time and tissue, even species specific, and inappropriate delivery may be detrimental and induce opposite effects.

1.4.3 Immunoactive biomaterial design

Immunoactive biomaterials could have direct interaction with the immune systems and broadly activate the regenerative immune response. Synthetic materials with optimized chemical/physical/topological properties are mainly designed to modulate macrophage behavior to favor regeneration. The most recent explored nature-derived extracellular matrix are more potent to interact with the immune system by generating new adaptive immune response other than innate immune response.

Chemical and physical properties

The types and the pattern of surface chemistry of biomaterials could drive different immune responses. For example, tuning the surface amine or acrylic acid group and their density on the surface significantly modulated the osteoimmune environment, such as the expression of inflammatory cytokines.[39] The hydrophilicity, and surface charge could interfere with material-immune cell interaction, with the observation that hydrophilic and anionic surfaces promote an anti-inflammatory type of response by dictating selective cytokine production by biomaterial adherent monocytes and macrophages, whereas the hydrophobic surfaces increased monocytes and macrophages adhesion density and foreign body giant cell (FBGC) formation.[40] FBGC formation can also be limited by the size of the biomaterials.[41, 42] Spheres with increasing diameter (1.5– 2.5 mm) reduce the foreign body response compared to smaller diameter (<1 mm), and electrospun fibers (EF) with diameter of 5 μm could induce M2-macorphage commitment and tissue resident stem cell migration compared to nano-EFs.

Topographic properties

Topographic property is another aspect worth considering when design immunoactive biomaterials. Porous materials promote vascularization and less fibrous tissue encapsulation relative to non-porous biomaterials.[43] Porosity on the scale of 30–40 μm also increased the ratio of anti-inflammatory M2 to pro-inflammatory M1 macrophages, leading to fewer FBGC and enhanced tissue repair.[41] Similarly, aligned electrospun nanofibers minimize the host immune reaction, enhance tissue-scaffold integration, and generate a thinner fibrous capsule compared to random fibers and films.[44] Materials with varied micro-groove pattern could also modulate macrophage phenotype.

Extracellular matrix (ECM) materials

By separating of cells from excised tissues, the decellularized ECM scaffolds could be harvested from many tissues. ECM scaffolds have bio-functional components and unique structures that are used to create a pro-generative environment. Worth mentioning, the ECM scaffolds showed potent immunomodulatory properties in vivo. ECM has shown to modulate the wound immune microenvironment through macrophage polarization. They could manipulate the macrophage phenotype towards M2 phenotype. Although the underlying mechanism is still not fully elucidated, studies have shown the matrix-bound micro-vesicles embedded in the ECM and the digested peptide fragments showed strong immunomodulatory function, which could be the reason for immunomodulatory properties of ECM materials. Other than regulate macrophage phenotype, ECM scaffolds were also proved to induce Th2 immune response that is dispensable for their regenerative role in large volume muscle disease.[45, 46] Therefore, The ECM material is a natural scaffold that could modulate both innate immune response and adaptive immune response to favor the process of tissue repair/regeneration.

In short summary, the immune system could be manipulated by varied biomaterial-based strategies to favor tissue repair/regeneration. Most studies focus on minimizing inflammation or manipulating macrophage phenotype post injury and success has been achieved in many tissues. With the accumulated knowledge that the immune system participates in many stages of tissue repair/regeneration more broadly than we imagine, the immunoactive biomaterials with the criteria to generate new immune events to interact with both innate and adaptive immune system is promising future direction. The immunoactive biomaterials design is at least as potent as stem cell based biomaterial design in biomaterials-based regenerative medicine.

1.5 Biomaterial-based strategies for cancer immunotherapy

To fully eradicate cancer utilizing immune system is a promising therapeutic strategies to cure cancer. Cancer vaccine is one of the most efficient strategies of cancer immunotherapy aims to adequately active innate and adaptive immune system to specifically kill cancer cells. The biomaterials in cancer vaccine are designed to facilitate the immune system activation meanwhile providing tumor-specific antigens to the antigen presenting cells.

1.5.1 Concept of cancer vaccine

Cancer immunotherapy aims to generate specific anti-tumor immunity that could suppress or eradicate the tumor without harming the healthy cells. Three key factors need to be considered during cancer vaccine design: a) the antigen source that provide specificity against tumor for immune system; b) the adjuvants that assist immune system activation; c) a delivery method to efficiently deliver the antigen and adjuvants to the immune

system.[47] Source of antigens could be originating from identification of certain idiotype, irradiated tumor cells, tumor cell lysate, tumor-derived exosomes. To identify certain idiotype for each cancer and patient could be time and money consuming. The other antigen source however provides the whole range and personalized tumor antigens, might more practical for providing antigen source. The adjuvant includes bacterial derived nucleic acid/lipids, chemical substance, heat-shock protein etc. One of the most common used adjuvants wound toll-like receptor (TLR) ligands, which could bind to the TLR on the immune cells and non-specifically activate the immune system.[48] To achieve better delivery efficiency of antigen and adjuvants to the immune cells, biomaterials could be used in many ways, which will be discussed later.

To achieve the goal of cancer eradication, a systemic adaptive T and B cell-mediated anti-cancer immunity need to be driven. The immature DCs migrates to the location of antigen/adjuvants, uptake the antigens and sense the adjuvants via TLR, finally become matured with the expression of surface co-stimulatory molecules. Once the DCs were matured they have the ability to present the antigens to the T cells either at the site of vaccination if the ongoing reaction attracts T cells, or in the draining lymph node where the antigen presented by dendritic cells activates Th cells. The activated Th cells will release IFNγ and contribute to both cell-mediated lysis through cytotoxic T lymphocytes (CTL) activation and the differentiation of B cells into plasma cells, which produce anti-tumor antibodies. The CTL will then migrate from the lymph node and infiltrate to the cancer lesion, recruit and activate innate immune cells to secrete more TNFα and IFNγ that lead to inhibited tumor invasion. CTL will also release Granzyme B to direct lysis the tumor cells. When the antigen is expressed on the cell membrane, antibodies secreted by

plasma cells might activate complement-mediated lysis, or antibody-dependent cellular cytotoxicity, cause killing of tumor cells. The long-term maintenance of a protective immune response guarantees surveillance and the continuing elimination of tumor cells as soon as they emerge to prevent tumor recurrence.

1.5.2 Materials in cancer vaccine

Biomaterials based cancer vaccine has longer research history than immunomodulatory biomaterial for regeneration. To eradicate cancer utilizing immune system, emphasis is placed on dendritic cell maturation to present antigen to the adaptive immune system in the lymph nodes. Therefore, biomaterials were designed to facilitate the antigen presentation to innate immune system as well as efficiently generate anti-cancer adaptive immunity.[49-51]

Particulate delivery system

As mentioned earlier, to design a therapeutic cancer vaccine, how to deliver the antigens and adjuvants to the immune cells efficiently is a great challenge. Micro- and-nano-particles made of polymers, liposomes or natural derived vesicles are promising tool for antigen and adjuvant delivery to induce potent cellular and humoral immunity.[52] The encapsulate or surface coating antigens and adjuvants to the particles could increase the availability of the antigens and adjuvants, as direct injected of antigens and adjuvants will diffuse very quickly in the body and achieve limited immunogenicity.[51] Moreover, loading both antigens and adjuvants to one particle also enable one APC to uptake the two key components at the same time, which has been proved to enhance the magnitude of immune activation.[53, 54] Similarly, it has been proved that using of multiple adjuvants

at the same time may cause synergistic effect to activate immune system compared to one alone, thus particles loading multiple adjuvants allow the co-delivery of adjuvants to one APC.[55]

Scaffolds for building "immune-active center"

The materials design focused on the passive delivery of antigens and adjuvants to the immune cells. However, materials could be designed to create an in situ "immune priming center" and thus to promote the attraction of antigen presenting cells (APCs), APC differentiation and activation, and loading with antigen to promote the immune response. Many material design have successfully achieved better vaccine efficacy based on this strategy. [49]

Hydrogels are three-dimensional, hydrated networks of crosslinked polymers. Injectable hydrogels could realize the sustained release of antigens and adjuvants to the surrounding environment.[56] Moreover, they could recruit DCs to the injection site and deliver the antigens and adjuvants to the DCs. Similar strategy has been realized by design of injectable spontaneously assembling scaffolds consisting of mesoporous silica rods (MSRs). When loaded with OVA, GM-CSF and CpG-oligonucleotides, this scaffold-based vaccine elicited potent immune serum antibody responses and cytotoxic T cell responses that enhanced protection against OVA-expressing tumors.[57]

1.6 Motivation and research objectives

1.6.1 Motivation

The immune system is a highly organized network that have a central role to modulate many critical biological events. The most well-known function of immune system is as the first line to provide protection against pathogen invasion. It is also commonly known that the abnormality of the immune system will lead to allergies and autoimmune diseases. However, in recent decades, the biologists have broadened our knowledge about the role of immune system, especially in the cancer immunotherapy and regenerative immunomodulation field.

The concept of cancer immunotherapy is to generative specific anti-tumor immunity that could suppress or eradicate the tumor without harming the healthy cells. With Sipuleucel-T becomes the first cancer vaccine proved by US Food and Drug Administration (FDA), the cancer vaccine showed promising clinical application potential and may eventually become the cure for cancer. However, it is much more difficult to develop a cancer vaccine with therapeutic efficacy, compared to pathogen vaccine, due to the complicated immunosuppressive environment brought by cancer. Three challenges need to be overcome for a successful cancer vaccine development: the identification of tumor specific antigen, the immune stimulator that facilitate the activation of the immune system and the efficient delivery tool to deliver the antigen and the immune stimulator to the immune cells. Biomaterials based strategies is a powerful tool box that could provide possible solutions to these challenge. Therefore, how to design materials to provide solutions to these challenge and enhance the therapeutic efficacy of cancer vaccine is worth exploring.

With the identification of M2 macrophage one decade ago, the role of macrophage and their versatile of phenotypes in tissue regeneration has been largely studied and since

then the immune system is closely connected with regeneration. In recent year, the adaptive immune cells, especially T helper 2 cells and Tregs were identified as pro-regenerative in many tissues such as muscle, heart, skin and neuron. As of today, with new findings that keep involving other types of immune cells to the regenerative process such as innate lymphoid cells (ILC)[58] and gamma delta T cells[59] etc., the immune-mediated regeneration is a brand new and promising direction to head for in the future regenerative medicine realm. Actually, very limited achievements were made from traditional tissue engineering strategies, which emphasis the utilize of stem cells, scaffolds and growth factors to replace the injured tissue. The broadened knowledge of immune-mediated regeneration provide us an alternative and may be effective strategy to modulate the immune system by materials and induce endogenous regenerative process. Therefore, to achieve the goal of designing a biomaterial that have the ability to intentionally manipulate the immune cell behavior and generate a pro-regenerative immune environment in vivo is highly motivated.

1.6.2 Research objectives

The overall objectives for this dissertation is to design biomaterials to qualitatively shape the immune response for biomedical application of cancer immunotherapy and regenerative medicine.

A competent cancer vaccine should provide solutions for the three challenges mentioned before: the identification of tumor specific antigen, the immune stimulator that active the immune system and the efficient delivery tool to deliver the antigen and the immune stimulator to the immune cells. The biomaterials could be designed as delivery

tool that allow co-delivery of antigens and immune stimulators. Bioaterials could also be designed to form an active center that attracts immune cells to the injection sites and activate them. Though many promising results have been achieved to increase anti-cancer immunity by involving biomaterials in cancer vaccine design, to design a material that solve the three challenge simultaneously is still challengeable. Tumor derived exosomes are nano-vesicles secreted by tumor cells with endogenous antigens and immune stimulators. As exosomes are vesicles that aims to transfer the cargoes for cell-cell and cell-environment communications, they are natural nano-particles for delivery. Therefore, in the chapter 2 of this dissertation, the tumor derived exosomes based cancer vaccine were designed to solve these challenges. The mechanistic immune response driven by tumor-derived exosomes were carefully studied in vivo and the therapeutic efficacy to fight against the B lymphoma were evaluated.

The exosomes secreted by cancer cells hold the potential to activate the immune system to fight against cancer. On the other side, the secretome of mesenchymal stromal cells (MSCs) showed strong immunomodulatory properties that could favor tissue repair/regeneration. In fact, MSCs are one of the most widely used stem cells in tissue regeneration. Their therapeutic role is proved to be contributed by the secretome with the function of immunomodulation, pro-angiogenesis, anti-scar, chemo-attraction for progenitor cells etc. Therefore, manipulating the secretome of MSCs by materials, especially the immunomodulatory and pro-angiogenic properties, is a promising strategy for MSC based regenerative medicine design. Moreover, the scaffolds were usually used as a delivery tool for MSCs in regenerative medicine, however, their intrinsic interaction with MSC in terms of paracrine function is very much neglected. In chapter 3 of this

dissertation, a fibrous scaffold with varied topological properties was investigated for the objective of enhancing MSCs paracrine function. The immunomodulatory and pro-angiogenic secretion were studied in the scaffolds-MSCs interaction system. The ability to modulate the macrophage phenotype in vitro and in wound healing model in vivo and the final therapeutic effects by scaffold-MSC secretome were studied.

Immunomodulatory material design for cancer vaccine have a longer history and have achieved many successful examples, compared to regeneration field. Even though the overall direction of immunomodulation of cancer vaccine and regeneration is different, the biomaterial based strategies for immunomodulation could be borrowed from cancer vaccine for regenerative immunomodulatory material design. One of the successful strategy in cancer vaccine design is to utilize the immune response towards materials to attract immune cells to the place of materials and send the anti-cancer signals carried by the materials to the recruited immune cells. Inspired by this strategy, meanwhile on the basis of the previous two objectives, in the chapter 4 of this dissertation, a MSC exosomes-loaded scaffolds were designed for direct regenerative immunomodulation in vivo. The ability of immune cell recruitment and their regenerative behavior change by the exosome-scaffold materials were carefully studied. Even though the adaptive immune cells are identified as key mediator in regeneration, many regenerative immunomodulatory design focused on the immune response of innate immune cells especially macrophage. Therefore, the adaptive immune response driven by exosome-scaffold in the reomote lymphatic organs will also be evaluated to bring new angels for regenerative immunomodulatory material design.

1.7 Specific aims

Specific aim 1: Development of cancer vaccine based on tumor-derived exosomes to generate anti-cancer immunity against B lymphoma

We hypothesized that tumor derived exosomes harboring the endogenous tumor antigens and immune stimulating molecules, meanwhile structured as a natural nano-particle aiming for delivery, could be used in cancer vaccine development against B lymphoma. Furthermore, co-administration of the tumor-derived exosomes with toll like receptor agonists could further enhance the dendritic maturation and antigen presentation efficiency, thus generating a stronger anti-tumor immunity. The potential cellular and humoral immune responses and long term survival efficacy that could be driven by immunization of tumor-derived exosomes were studied in a one week pre-established metastatic lethal B lymphoma model.

Specific aim 2: Investigate the function of fibrous scaffolds to potentiate the immunomodulatory paracrine action of mesenchymal stromal cells (MSCs)

We hypothesized that the fibrous scaffolds and the varied topological cues could potentiate the immunomodulatory and angiogenic paracrine function of MSCs and promote wound healing in vivo. Fibrous scaffolds with different topological cues were fabricated by electrospinning technique. The effects of the fibers on MSCs to produce pro-angiogenic and anti-inflammatory paracrine factors were investigated. The function of these paracrine factors were further studied through collecting conditioned-medium from different culture systems and applying it to cultures of endothelial cells and macrophages in vitro and a skin wound-healing model in vivo.

Specific aim 3: Design of immunoactive exosome-loaded scaffolds with the immune cell recruitment and education properties for regeneration

We hypothesized that the MSC exosome loaded scaffolds would drive regenerative immunomodulation in the wound healing model. The possible mechanism could be: the fibrous scaffolds would recruit immune cells to the transplant site due to foreign body reaction in vivo; the recruited immune cells will then receive the immunomodulatory signals from the MSC exosomes and generate immune environment that favor the tissue repair/regeneration. Through series of chemical modification, electrospun fibrous scaffolds were covalently conjugated with polyethylenimine (PEI) to passively load exosomes through static interaction. The exosome loaded scaffolds were then applied to a wound healing model in vivo and the immunomodulatory properties of the innate and adaptive immune response were evaluated in both local sites and remote lymphatic organs.

CHAPTER 2. DEVELOPMENT OF CANCER VACCINE BASED ON TUMOR-DERIVED EXOSOMES FOR B LYMPHOMA IMMUNOTHERAPY

Tumor derived exosomes (Texo) are potential antigen source for cancer immunotherapy to solve the challenge of identifying particular tumor antigen. However, the therapeutic role of Texo in established diffuse large B cell lymphoma (DLBCL) model and the fundamental immune response driven by Texo in vivo remains elusive. In this study, we developed a Texo-based therapeutic vaccine that could generate long-term protection against aggressive metastatic B lymphoma. The anti-tumor immunity driven by immunization of Texo was carefully studied. The result showed Texo vaccine enhanced both Th1 and Th2 immune response in spleen, meanwhile induced germinal center formation in the draining lymph nodes. The population of regulatory T cells and myeloid-derived suppresser cells were also down regulated by administration of Texo, compared to untreated mice. We proved that the memory B cells secreting anti-tumor IgG1, IgG2a antibodies existed in the bone marrow in Texo immunized mice that may be responsible for the long-term protection against the second lethal tumor challenge. Co-administration of dual toll like receptor (TLR) agonist CpG and MPL with Texo further enhanced dendritic cell activation and CD4+/CD8+ T cell immune response, as well as the survival outcome against B lymphoma. Our study proved the therapeutic role of Texos and unraveled the underlying mechanisms of Texo based vaccine in the established DLBCL model, which paved the way for the possible future clinical application of Texo in B lymphoma treatment.

2.1 Introduction

Tumor immunotherapy aims to generative specify anti-tumor immunity that could suppress or eradicate the tumor without harming the healthy cells. To generate efficient anti-tumor immunity, three criteria needs to be fulfilled.[60] The first is to identify tumor-specific antigens. The second challenge is to properly activate the immune system with stimulator. The last challenge is to deliver the antigens and immune stimulators to the APCs efficiently.[61] Especially, identify specific antigens for individual patient could be time and money consuming. In addition, even if the certain antigens are identified, whether they have potent immunogenicity or if they could induce long term protection is still unknown.

Tumor derived exosomes (Texo) are nano-vesicles secreted by the tumor cells. Due to their cancer cell biogenesis, Texo have full spectrum of unidentified antigens, including proteins and nuclei acids, assembling the tumor cells.[62] Therefore, Texo provides endogenous antigens that allow the immune system to recognized even unidentified tumor antigens.[63] Moreover, Texo carry MHC class I/II molecules, co-stimulatory molecules and heat shock proteins that may potentially stimulate the immune system when encountering the immune cells. As exosomes are vesicles generated by cells to transfer cargoes for cell-cell and cell-environment communications, Texo are natural-derived delivery nano-particles and have been utilized as carriers of drugs for cancer treatment. [64]

Based on the above characteristics, Texo showed great potential in cancer immunotherapy as tumor antigen source, immune-stimulatory molecules presenters and delivery vehicles, which could fulfill the three most challenging criteria of cancer vaccine design. [65] Studies have shown that Texo are a source of shared tumor rejection antigens

that can cross priming cytotoxic T lymphocytes (CTLs). A phase I clinical trial showed the ascites-derived exosomes from cancer-beard patients in combination with the granulocyte–macrophage colony-stimulating factor (GM-CSF) in the immunotherapy can induce beneficial tumor-specific CTL response. [66] However, Texo are also reported to favor the cancer development by supporting tumor proliferation, motility, invasion, angiogenesis, and pre-metastatic niche preparation. In addition, recent research implies that cancer cell–derived exosomes may play a suppressive role in cancer-directed immune response. Therefore, the role of Texo in cancer vaccine is still debatable and the therapeutic effects as well as the fundamental immune responses driven by administration of Texo remain to be fully elucidated.

Non-Hodgkin lymphomas (NHL) is a lethal disease that consists 4.2% of all the cancer cases, and 85% of which are B lymphoma, among which the majority are diffuse large B cell lymphoma (DLBCL). The most common immunotherapy for B lymphoma in clinic is the use of anti-B cell monoclonal antibody, such as rituximab that can specifically target CD20 expressed tumor cells. However, many patients may show no response to rituximab treatment or may develop resistance response and result in recurrence. The overall therapeutic effects that have achieved by monoclonal antibody treatment is to prolong the survival rate by 5 years. Therefore, new immunotherapy strategies remain to be developed for better therapeutic outcomes and Texo is a promising immunotherapeutic methods with the possibility for clinical transfer. However, the therapeutic effects of Texo in a clinical relevant aggressive diffuse large B cell lymphoma (DLBCL) model is still unknown, and the fundamental immune responses driven by Texo remains to be explored.

The purpose of this study is to testify the potential therapeutic effects of Texo in the DLBCL model, elucidate the fundamental immune response driven by Texo, including cellular/humoral anti-tumor immune response and the possible immunosuppressive effects, thus providing insights to possible clinic transfer of Texo-based cancer vaccine. Here, we established an aggressive diffuse large B cell lymphoma (DLBCL), in which lethal dose of A20 B lymphoma cells were injected i.p. and allowed for establishment for a week. The Texo, which were collected from *ex vivo* B lymphoma cells to better mimic the clinical scenarios, were then injected to the pre-established DLBCL mice, with or without the co-administration of the TLR agonists. The survival outcome and the immune response driven by Texo administration were carefully studied. Our results showed that improved survival outcome and long-term protection against two lethal challenge of B lymphoma. Many arms of immune system were activated by Texo-administration including both cellular and humoral anti-tumor immune response. Co-administer of TLR4/9 agonists with Texo showed better survival outcome, compared with Texo alone, by further activate the immune system.

2.2 Materials and Methods

2.2.1 Preparation and characterization of tumor exosomes.

A20 cells (ATCC TIB-208) were purchased from ATCC and used for exosome preparation and all the tumor model in this study. Texo were collected from ex vivo tumor cells. To be specific, 10^5 A20 tumor were injected s.c. to Balb/c mice to develop a s.c. A20 tumor. Three weeks later, the developed solid tumor was harvested, digested to single cell suspension and went through magnetic cell isolation using B cell separation kit (Miltenyi

Biotec) to negatively separate B lymphoma from other cells. The ex-vivo A20 cells were cultured in RPMI medium supplemented with 2% exosome-depleted serum for 48 hours and the supernatant were collected for further isolation of Texo by (ultra)centrifugation. To be specific, the supernatant was centrifuged at 1,200 g for 15 min, followed by 10,000 g for 30min to remove cell debris and apoptotic bodies and the supernatants were collected. To precipitated exosomes, the supernatants were ultra-centrifuged at 100,000 g for 1h. The collected Texo were then washed twice with PBS and finally re-suspend in 200 μL PBS, stored in -80 °C until use. The protein content of collected exosomes was measured by micro BCA protein assay kit (Thermo Fisher) and was used to quantify the dose of Texo in the following study.

The Texo were visualized by transmission electron microscopy (TEM) To prepare the samples, the Texo were fixed with 4% paraformaldehyde (PFA), stained with 2% (w/v) uranyl acetate for 5 mins, washed 3 times with DI water and observed by transmission electron microscopy. The size and zeta potential distribution of exosomes were identified by Zetasizer (Brookhaven Instruments). The exosomal markers were identified by flow cytometry. 10 μg exosomes were covalently conjugated onto 4-μm aldehyde/sulphate latex beads for 15min. The excess aldehyde group were blocked by excessive 100 mM glycine for 30 min. The exosome-beads were stained by exosomal markers CD63/CD9 and MHCI, MHCII and according isotypes, analyzed by BD Aria flow cytometer.

2.2.2 Survival studies

All the in vivo experiments with mice were approved by the institutional animal care and use committees at the Georgia Institute of Technology. The DLBCL model was

established by injection lethal dose of A20 i.p. (1×10^5 for the first survival study, 2×10^5 for the second survival study) in Balb/c mice (n=10). The tumor cells were allowed to established for 7 days, followed by three s.c. immunizations with Texo of Texo-agonists (dose of 10 μg Texo with or without 20 μg CpG, 30 μg MPL per injection) at day 8, 10 and 14, respectively. For survived mice, a second lethal challenge with 2×10^5 A20 cells injected i.p. at day 76 or 74 for the first and second survival study, respectively. The survival of mice was monitored up to day 160. The Kaplan-Meier survival curves were generated, and log-rank (Mantel-Cox) tests were performed to compare survival between various groups using GraphPad Prism 6 software.

2.2.3 Mechanistic studies.

Model establishment. Mechanistic studies were performed as the same immunization setting as the survival study with initial i.p. injection of 2×10^5 A20 cells at day 1 to Balb/c mice (n=6), followed by three Texo immunization at day 8, 10 and 14. On day 21, all the mice were sacrificed and the spleen, inguinal lymph nodes, and blood were collected and analyzed further for cellular and humoral immune responses using flow cytometry and ELISA.

Flow cytometry analysis. To get single cell suspension for flow cytometry assay, lymph nodes were minced and flushed with PBS (with 2% FBS) with a 70 μm filter beneath; spleen were cut into pieces, digested in collagenase D (2mg/mL, Roche) for 30 min, minced and flushed with PBS (with 2% FBS) with a 70 μm filter beneath, followed by RBS lysis treatment (Biolegend). The splenocytes and lymph nodes cells were analyzed for various immune cell populations, CD3+CD8+ T cells, CD3+CD4+ T cells, germinal center–

forming B cells (B220+GL7+FAS+), Tfh (CD3+CD4+PD-1+CXCR5+), MDSCs (CD11b+Gr.1+), Tregs (CD4+CD25+FoxP3+), NK cells (CD3–CD49b+) using a BD LSRII flow cytometer following staining with specific anti-mouse antibodies. The antibodies for flow cytometry were purchased from Biolegend or eBioscience.

Splenocyte restimulation studies. To stimulate the splenocytes with tumor antigens, tumor lysates were prepared by 4 freeze-thaw cycles of 2×10^8 to 4×10^8 A20 cells per mL, and the lysate was centrifuged at 12,000 g x for 20 minutes at 4°C. Splenocytes (1×10^6 cells/well of 96-well plates) from immunized mice in the mechanistic study were re-stimulated *ex vivo* with A20 tumor lysate (100 μg in protein content/well of 96-well plates) for 3 days, then stained and analyzed for IFN-γ+/IL4+, CD3+CD8+, and CD3+CD4+ T cells using a BD LSRII flow cytometer. Furthermore, the culture media were analyzed for IFN-γ and IL4 cytokines using ELISA Ready-Set-Go! Kits (eBioscience, San Diego, CA).

Measurement of antibody levels in blood. Blood were drawn from the mice and the serum were collected by centrifugation. Serum antibody levels of IgG1, IgG2a and IgG2b were measured by ELISA using plates precoated with A20 tumor lysate (100 μg/ml). Optical density for various serum dilutions was measured at 450 nm.

2.2.4 ELISPOT assay for antibody-secreting bone marrow cells.

The bone marrow cells were separated from survived mice and seeded in MultiScreenHTS-IP Filter Plate (Millipore) coated with A20 tumor lysate (10 μg per well). After cultivation in the incubator overnight, the plates were washed with PBS and stained by alkaline phosphatase-conjugated secondary antibodies against mice IgG1 and IgG2a.

The spots were visualized by adding alkaline phosphatase substrate (Vector). The plates were scanned and counted on a CTL reader.

2.2.5 ADCC assay of mice serum

The target cells A20 were labeled with CFSE and mixed with RAW 264.7 at the ratio of 1:8. The serum from the survival study were added to the mixture of target/effector cells at 5% concentration. After 24h culture, the target/effector cells were harvested, stained with PI and analyzed by flow cytometry, to determine the dead cells. Target/effector cells without supplement of serum were served as a control.

2.2.6 BMDC activation and MLR reaction.

Bone marrow cells were isolated from femurs and tibias of the mice by flushing the bone marrow, going through the 70μm filter, followed by RBS lysis. The bone marrow cells were cultured in RPMI 1640 Glutamax medium (Invitrogen, Carlsbad, CA), supplemented with 0.25mM beta-mercaptoethanol, 1 × non-essential amino acid, 10% heat inactive FBS (FBS incubated at 56℃ in water bath for 30mins), 1% penicillin & streptomycin and 25 ng/ml mouse granulocyte macrophage colony-stimulating factor (GM-CSF) and 25 ng/ml IL-4 (Peprotech, Rocky Hill, NJ) for 6 days. Medium was changed every other day. On day 7, the cells were stained by CD11c antibody and analyzed by flow cytometry to determine the differentiation of DCs. The DCs acquired were incubated with 5 μg Texos with or without 2 μg CpG and 2 μg MPL for 48 hours. The BMDCs activation was evaluated by analyzing surface expression of co-stimulatory

molecules CD86, MHCII, and CD40 using BD Accuri flow cytometer. The flow cytometer data was further analyzed with Flowjo software.

To carry out the MLR study, the BMDCs were isolated and differentiated as described above. CD4+ or CD8+ naïve T cells isolated from the spleen of naïve mice using CD4 or CD8 MicroBeads with MACS columns and MACS separators (Miltenyi Bioetch, Germany) The BMDC were first activated with Texo/Texo-agonists for 48 h as described above and then co-cultured with CD4+ or CD8+ naïve T cells at a ratio of 1:2. After 96 h, the culture medium was collected and analyzed for IFN- γ and IL4 cytokines using ELISA Ready-Set-Go! Kits (eBioscience, San Diego, CA).

2.2.7 Statistical analysis

Quantitative results were presented as means±standard deviation (SD). Statistical comparisons were performed by unpaired, 2-tailed t test to compare pairs of groups, and one-way analysis of variance (ANOVA) followed by Tukey tests to compare multiple experimental groups. Log- rank (Mantel-Cox) test was done to define significant difference in survival between two groups in the therapeutic studies. Values of $P < 0.05$ were considered statistically significant. *P<0.05, **P<0.01, ***P<0.001, ****P<0.0001.

2.3 Results

2.3.1 Preparation of tumor-derived exosomes

As shown in figure 2.1, the A20 tumor cells were first injected subcutaneously and allowed to develop into solid tumor. The tumor mass was then digested to single cell

suspension and B cells were specifically isolated by magnetic cell isolation in vitro. The exosomes were collected from the ex-vivo B lymphoma to better mimic the clinical scenarios. The tumor-derived exosomes (Texo) or Texo coupling with TLR 4/9 agonists were injected to a pre-established metastatic B lymphoma model to evaluate the possible anti-tumor immune response and the therapeutic efficacy.

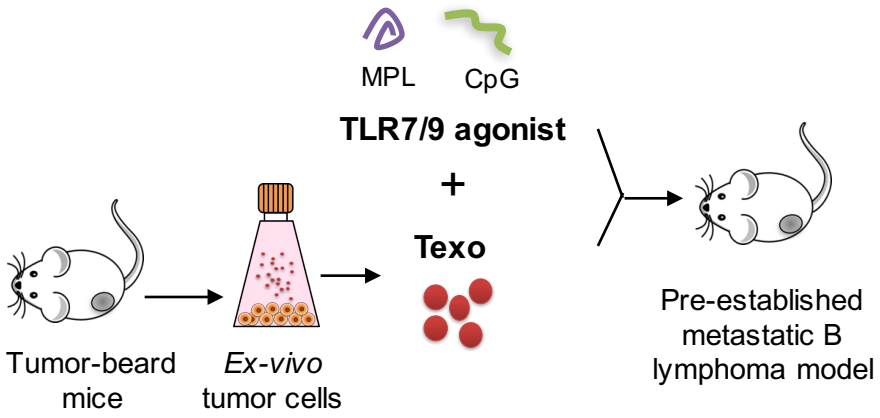

Figure 2.1 Tumor cells were harvested from mice bearing subcutaneous tumor, went through magnetic separation for B lymphoma cells. The ex-vivo tumor cells were cultured and Texo were isolated from the supernatant. Texo or Texo-agonist vaccine were injected to mice bearing pre-established metastatic B lymphoma. The in vivo immune response and survival outcome were examined.

The TEM imaging showed the phenotype of Texo was nano-scaled vesicles. (Fig. 2.2 A) By DLS measurement, the Texo were identified with a diameter ranging from 50 nm to 100 nm and a negatively charged zeta potential. (Fig. 2.2 B) The Texo showed the expression of exosomal markers CD9 and CD63. MHCI and MHCII molecules were also identified on the Texo, indicating the potential immunogenicity of Texo. (Fig. 2.2 C)

A

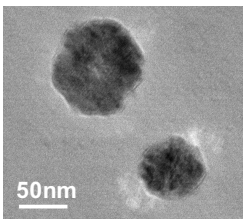

B

	Exosome
Size (nm)	76.67±25.35
Zeta potential (mV)	-30.80±9.82

C

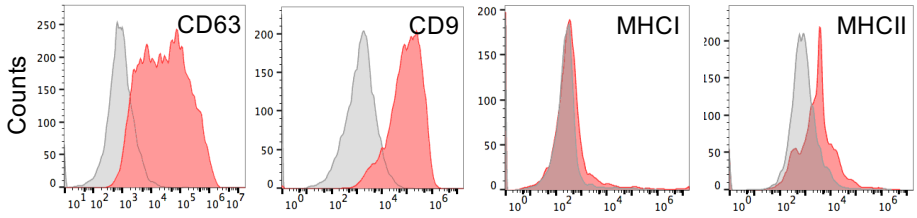

Figure 2.2 Characterization of tumor-derived exosomes. (A) TEM photograph of exosomes collected from supernatants of ex vivo A20 cells. Scale bar: 50nm. (B) Size and zeta potential of exosomes measured by DLS. Mean ± STD. (C) Histogram of exosomal markers (CD63/CD9) and MHC family (MHCI/MHCII) detected by flow cytometry. Grey and red peaks indicate isotype and antibody staining of exosome-conjugated latex beads, respectively.

2.3.2 Therapeutic effects of Texo in pre-established DLBCL model.

Texo harbored tumor specific antigens and immunostimulatory components such as heat shock proteins, therefore holding great therapeutic potentials as cancer vaccine. However, their therapeutic effects have not been testified in the pre-established DLBCL model. In an attempt to elucidate the anti-cancer effect of Texo alone in the DLBCL model, 1×105 lethal dose of A20 cells were injected i.p. and were allowed to establish for one week, followed by the Texo injection at day 8, 10 and 14 subcutaneously as therapeutic vaccines. (Fig. 2.3 A) First of all, the survival curve showed that, without interference, total 10 mice in PBS group showed 0 survival rate with a median survival of 39.5 days. For the group of Texo, four mice were dead at first but the survival curve showed a platform around day 50 with 60% survival rate. To evaluate the long-term protection of Texo vaccine, the survived mice were then re-challenged with a second lethal dose of 2×105 of tumor cells

i.p. at day 76. Astonishingly, the mice in Texo group that had survived the first tumor challenge achieved 100% survival rate in the second tumor re-challenge study. (Fig. 2.3 B) To make fair control, another PBS group challenged with 2×105 of tumor cells were made accordingly at day 76, the result showed 0 overall survival rate and the medium survival of 28 days. (data not shown) Compared to untreated PBS group, immunization with Texo has significantly prolonged the medium survival of the cancer beard mice from 38.5 days to more than 160 days, even under the circumstance of a second lethal tumor re-challenge. (Fig. 2.3 C) These results indicate that Texo alone have anti-tumor therapeutic effects on the established DLBCL model in this study and the long term memory of the immune system towards B lymphoma could be generated post the immunizations of Texo.

2.3.3 Anti-cancer cellular immune response driven by immunization of Texo.

With the proof that the Texo could generate anti-cancer therapeutic effects in the established DLBCL mice, we then move to explore the exact immune response driven by Texo administration and elucidate the mechanism for the therapeutic effects of Texo vaccine. The mechanistic study has the same cancer model set up and Texo vaccination pattern as the survival study, in which 1×105 lethal dose of A20 cells were injected i.p., followed by three immunizations of Texo at day 8, 10 and 14 subcutaneously. At day 21, all mice were sacrificed and the immune response in the spleen and inguinal lymph nodes were evaluated. (Fig. 2.4 A) Here, the healthy naïve mice without tumor or Texo injection and PBS group with tumor and PBS injected were served as controls.

To evaluate the immune response driven by Texo, we first examined the possible suppressive immune response, due to the debatable role of Texo in facilitating tumor

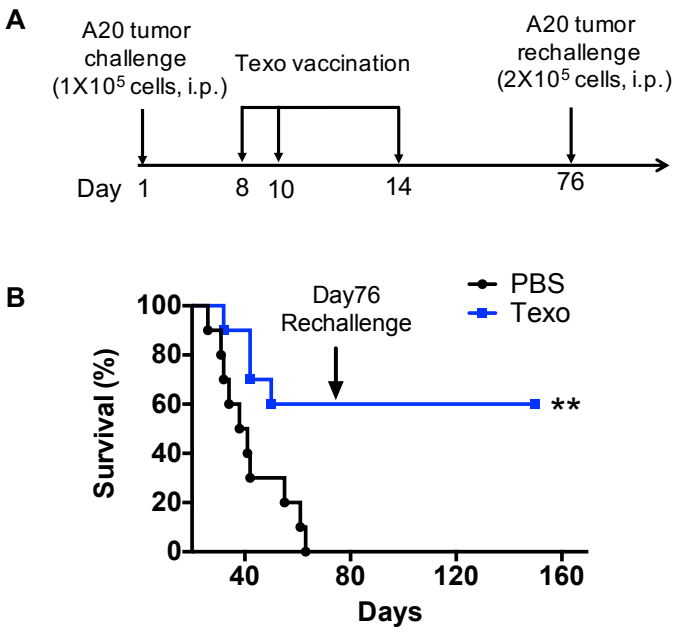

C

	P Value (log rank)	Median survival (days)	Hazard ratio (log rank) and 95% CI of ratio
PBS	-	39.5	-
Texo	0.0037	>160	0.2227 (0.06185 to 0.5503)

Figure 2.3 Therapeutic anti-tumor immunity of Texo vaccine. (A) Lethal dose of tumor cells were injected in Balb/c mice and allowed to establish for 7 days before three immunizations of Texo (10 µg Texo per injection). Survived mice were re-challenged with lethal dose of A20 tumor cells at day 76. (B)Survival of the mice (n=10) were measured daily. (C) Table showing median survival, log Rank P values, Hazard ratios for Texo compared to PBS. ** indicates P<0.01.

growth through suppressing the immune system. To be exact, the population of myeloid derived suppresser cells and regulatory T cells (Tregs), which were considered being hijacked by the tumor cells to mitigate the immune response against tumor. The result showed that the granulocytic and monocytic MDSC population were not elevated in the spleen compared to the naïve and PBS group. (Fig. 2.4 B) As for the Tregs, the Treg population in PBS group showed significant up-regulation compared to naïve mice, indicating the suppressive immune environment in the tumor beard mice. However, when

immunized with Texo, Treg population were significantly decreased compared to PBS group, assembling the level of Treg numbers in the healthy naïve mice in both spleen and lymph nodes, which indicates the tumor-associated suppressive immune response were reversed by Texo immunization in both spleen and lymph nodes. (Fig. 2.4 C) Therefore, the subcutaneous administration of Texo in our study did not lead to suppressive immune response but even decreased the population of Tregs that were supposed to be increased by tumor invasion.

The anti-tumor cellular immune responses were then examined by re-stimulating the splenocytes from the mechanistic study with A20 tumor cell lysates. When re-encountering the antigens in vitro, the immune response of splenocytes were supposed to be magnified, meanwhile resembling their behavior in vivo. The result of tumor lysate re-stimulation study showed that Texo could induce elevated population of both IL4 secreting and IFNγ CD4+ T cells, compared to the other two control groups, indicating both Th1 and Th2 immune response were activated by immunization of Texo. (Fig. 2.4 D-E) The population of IL4 secreting CD8+ T cells did not have significant differences between the groups, however, the population of IFNγ secreting CD8+ T cells were elevated in the spleen. (Fig. 2.4 F-G) The ELISA measurements of IL4 and IFNγ concentration in the supernatants of the re-stimulation splenocytes were consistent with flow cytometry results: The Texo group has significant higher concentration of IL4 and IFNγ cytokines compared to PBS and Naïve group (Fig. 2.4 H-I), indicating the activated CTL immune response may be responsible for the therapeutic effects against B lymphoma. No significant change in NK cell population in the spleen were identified. (Fig. 2.4 J)

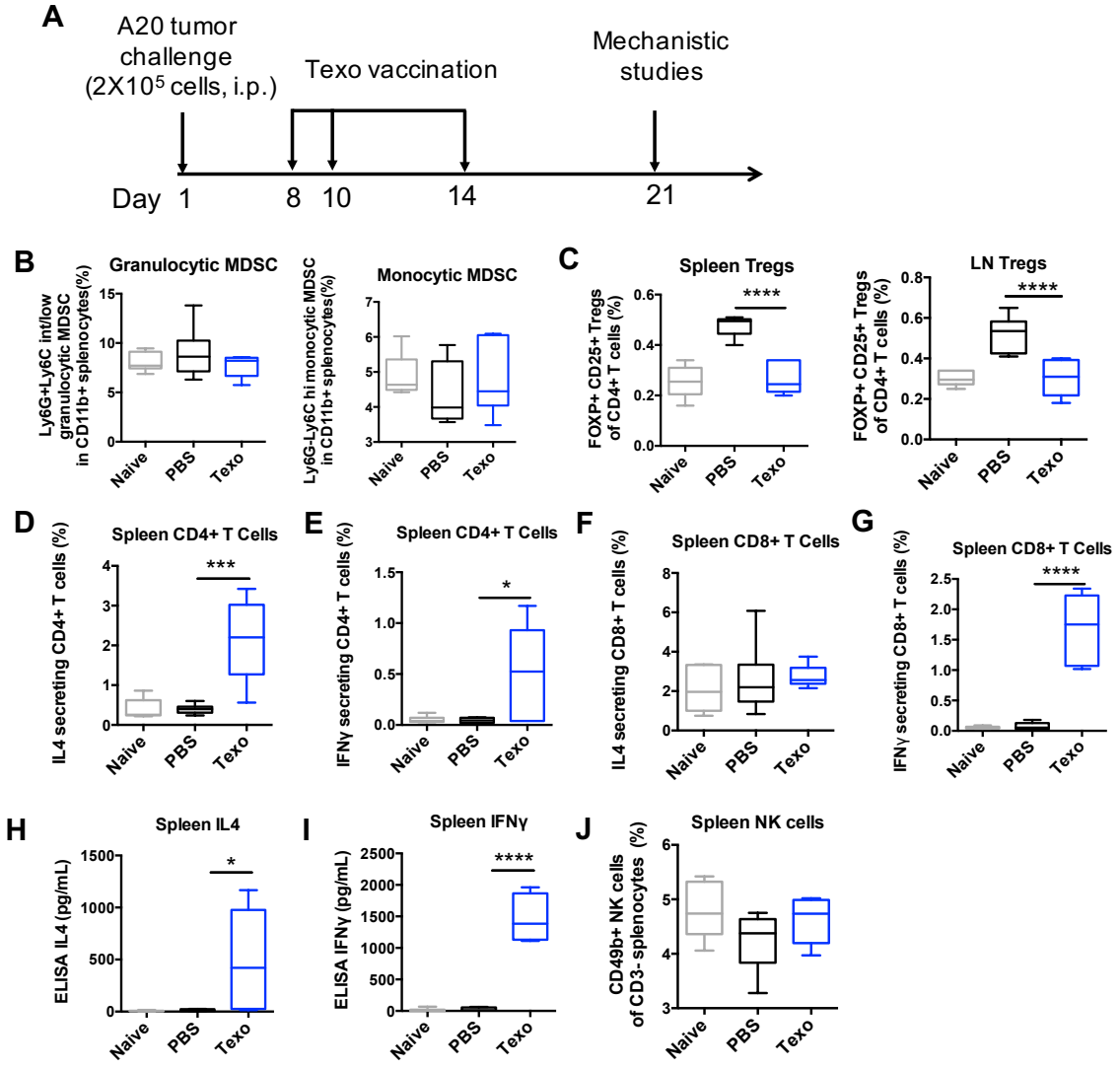

Figure 2.4 Cellular immune responses driven by Texo vaccine. (A) Time line for mechanistic studies. Lethal dose of tumor cells was injected in Balb/c mice and allowed to establish for 7 days before three immunizations of Texo (10 μg Texo per injection). Mice were sacrificed on day 21, then LN and spleen were harvested for immunology analysis. (B) Granulocytic MDSC and monocytic MDSC in spleen. (C) Treg percentage of CD4+ T cells in spleen and LN. Splenocytes were restimulated with A20 cell lysate for 72 hours in vitro, then IL4 and IFNγ secreting CD4+ T cells (D-E) and CD8+ T cells (F-G) were analyzed by flow cytometry, and the culture medium were measured for IL4 and IFNγ concentration (H-I) by ELISA. (J) Natural killer cells percentage in spleen. *P<0.05, **P<0.01, ***P<0.001, ****P<0.0001

2.3.4 Anti-cancer humoral immune response and long term protective memory B cells driven by immunization of Texo.

Other than cellular immune response, the humoral response, especially the secretion of antibody against the tumor cell are identified as an efficient way to eradicate tumor. However, in the exosome vaccine study, the consequence of therapeutic outcome emphasis the CLT immune response but neglected the possible therapeutic humoral immune response. To this end, the humoral immune response including germinal center formation and antibody secretion driven by Texo treatment were carefully studied in the mechanistic study, with the same experimental setting as in figure 2.5 A. Firstly, the inguinal LNs were harvested and the germinal center reaction were examined by flow cytometry. Here, strong germinal center reactions were observed in the Texo group. Texo immunized mice showed significantly increased population of B200+GL7+ B cells. (Fig. 2.5A) Of those B220+ B cells, the GL7 and FAS double positive population was also significantly increased in Texo group, compared to untreated PBS group and naïve mice. (Fig. 2.5B) The population of follicular T cells that function as facilitating germinal center formation were also seen to be elevated in Texo groups, compared to untreated PBS group and naïve mice. (Fig. 2.5C)

To evaluate the humoral immune response driven by Texo vaccination, the tumor specific IgG1, IgG2a and IgG2b in the blood from both mechanistic study and survival study were tested by IgG titter. At early time point as day 21 post tumor injection, only increased anti-A20 IgG1 secretion were observed in the mice serum. (Fig. 2.5D) However, no differences were observed in anti-A20 IgG2a and IgG2b secretion in the serum among the three groups at day 21 post tumor injection. (Fig. 2.5E-F) Interestingly, the elevated anti-A20 IgG1, IgG2a and IgG2b level in the serum was detected at a later time point at

day 160 post tumor injection, when compare the serum from those survived mice in the Texo group with the healthy naïve group and PBS groups from the first survival study. (Fig. 2.5G-I)

As shown that the tumor specific antibodies are highly detectable for relatively long periods (Fig. 2.5G-I), thus it is speculated that the observed antibody titer might be maintained by antibody-secreting plasma B cells. The bone marrow cells of the survived mice in the Texo group were analyzed by ELISPOT for A20 specific IgG1 and IgG2a. The three mice of PBS mice were served as control. The result showed the existence of A20-speicific IgG1 and IgG2a antibody secreting memory B cells in the bone marrow for Texo groups, while none spots were observed in the control PBS mice. (Fig. 2.5J-K) To further confirm that the antibodies had cytotoxic effects against tumor cells, the blood serum were added to the co-culture of A20 cells and macrophage/splenocytes and the antibody-driven cell cytotoxicity (ADCC) of the serum against A20 cells were evaluated by PI staining. It was found that only the serum from survived mice in Texo group showed significant promoted ADCC effects against A20 cells, compared with serum from PBS group. (Fig. 2.5L) On the contrary, the serum from dead mice in Texo group showed no significant differences with PBS serum. Based on the above data, it could be concluded that the Texo could induce the generation plasma B cells that secrete anti-tumor antibodies. Therefore, the observed memory B cells in the bone marrow generated post Texo immunization might be responsible for the long-term protection of the mice against dual tumor challenge.

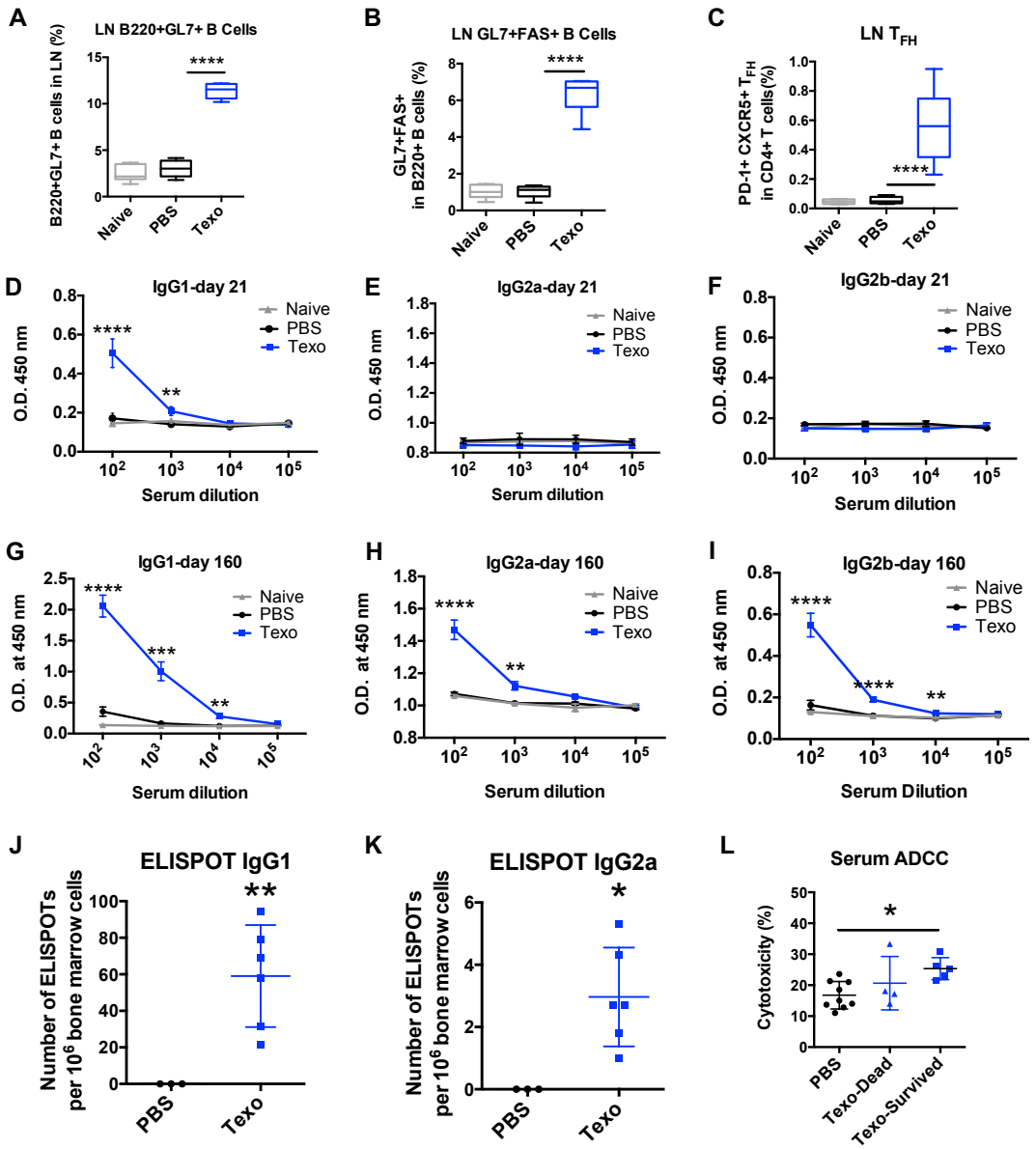

Figure 2.5 Humoral responses for Texo vaccine. Graphs showing frequencies of germinal center (A, B) and TFH cells (C) in the draining LN. The antibody level of IgG1, IgG2a, IgG2b against A20 tumor lysate in the serum at day 21 in the mechanistic study (D-F) (time line is the same as in figure 3) and at day 160 of survived mice in Texo group in survival study (G-I) (PBS mice serum were harvested at the day they were dead). The plot showing bone marrow cells that secreting IgG1 (J) and IgG2a (K) antibodies against tumor lysates using ELISPOT at day 160 of survived mice in Texo group in survival study (PBS mice were from rechallenge survival study at day 53 post tumor injection). (L) Graph showing cytotoxicity of serum against A20 cells in the survival study. 1% serum were applied to the co-culture of A20 cells and macrophages at the ratio of 1:8. *P<0.05, **P<0.01, ***P<0.001, ****P<0.0001

2.3.5 Co-administration of TLR4/9 agonists with Texo enhanced anti-tumor immunity.

TLR agonist could facilitate non-specific immune activation by binding to the TLR on the immune cells. It has been reported that co-administration of two TLR agonists may generate synergistic activation effects on the immune system compared to one alone. In order to further activate the observed Th1 and Th2 immune response driven by Texo immunization (Fig. 2.6D-I), the MPL and CpG were co-administer with the Texo to further improve the therapeutic effects against the DLBCL. In the second survival study, a more aggressive DLBCL model were adopted with 2×105 tumor cells injected i.p., doubled the initial tumor cell number in the first survival study. Still, the injected tumor cells were allowed to establish for a week without any interference. (Fig. 2.6A) In the more aggressive model, Texo alone showed limited therapeutic effects. The median survival is day 30 for Texo group, which had no significant differences with PBS group with a median survival of day 29. However, the Texo-agonists showed significant improvement on mice survival with a median survival of day 43.5 compared with PBS group. The Texo-agonists group showed 30% survival rate at the end of the study, whereas the Texo group 10% and PBS 0. (Fig. 2.6 B, C) Worth mentioning, the all survived mice in Texo-agonist group and Texo group had survived the second lethal challenge of tumor cells at day 74, indicating again the immunization of Texo could generate long term protection against the B lymphoma.

To elucidate the effects on the immune activation and the improved therapeutic effects of Texo-agonists, the bone marrow derived dendritic cell (BMDC) maturation and the T cell immune response in the mixed lymphatic reaction (MLR) were evaluated in vitro. The results showed that the Texo could enhance BMDC maturation by increasing the

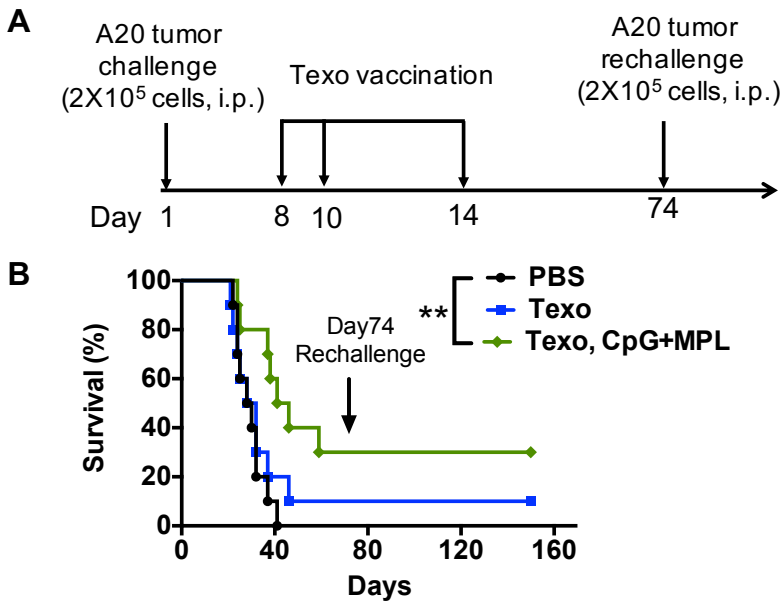

C

	P Value (log rank, c/w PBS)	Median survival (days)	Hazard ratio (log rank, c/w PBS) and 95% CI of ratio
PBS	-	29	-
Texo	0.4540	30	0.7367 (0.2750 to 1.676)
Texo, CpG+MPL	0.0037	43.5	0.2989 (0.6345 to 0.5060)

Figure 2.6 Therapeutic efficacy of Texo-adjuvant vaccine. (A) Lethal dose of tumor cells were injected in Balb/c mice and allowed to establish for 7 days before three immunization of Texo-adjuvant vaccine (10 µg Texo/20 µg CpG/30 µg MPL/1 mg Alum per injection). Survived mice were re-challenged with lethal dose of A20 tumor cells at day 74. (B)Survival of the mice (n=10) were measured daily. (C) Table showing median survival, log Rank P values, Hazard ratios for Texo-adjuvant groups compared with PBS. ** indicates P<0.01.

population of MHCII+CD86+ and MHCII+CD40+ BMDC. The co-administration of MPL and CpG further enhanced the BMDC maturation maker expression. (Fig. 2.7 A, B) The IL12p70 secretion in the supernatant of BMDC culture showed the similar trends. (Fig. 2.7 C) The primed DCs by Texo or Texo-agonists were then co-cultured with CD4+ T cells or

CD8+ T cells isolated from spleen and the supernatant of the MLR were measured for IL4, IFNγ concentration. The IL4 concentration was significantly elevated in the CD4+ T cell MLR and CD8+ T cell MLR for Texo-agonists group compared to Texo alone and PBS group. (Fig. 2.7 D, F) Significant increase of IFNγ was observed in both Texo and Texo+agonists group compared with PBS group in the CD4+ T cell MLR and CD8+ T cell MLR. (Fig. 2.7 E, G)

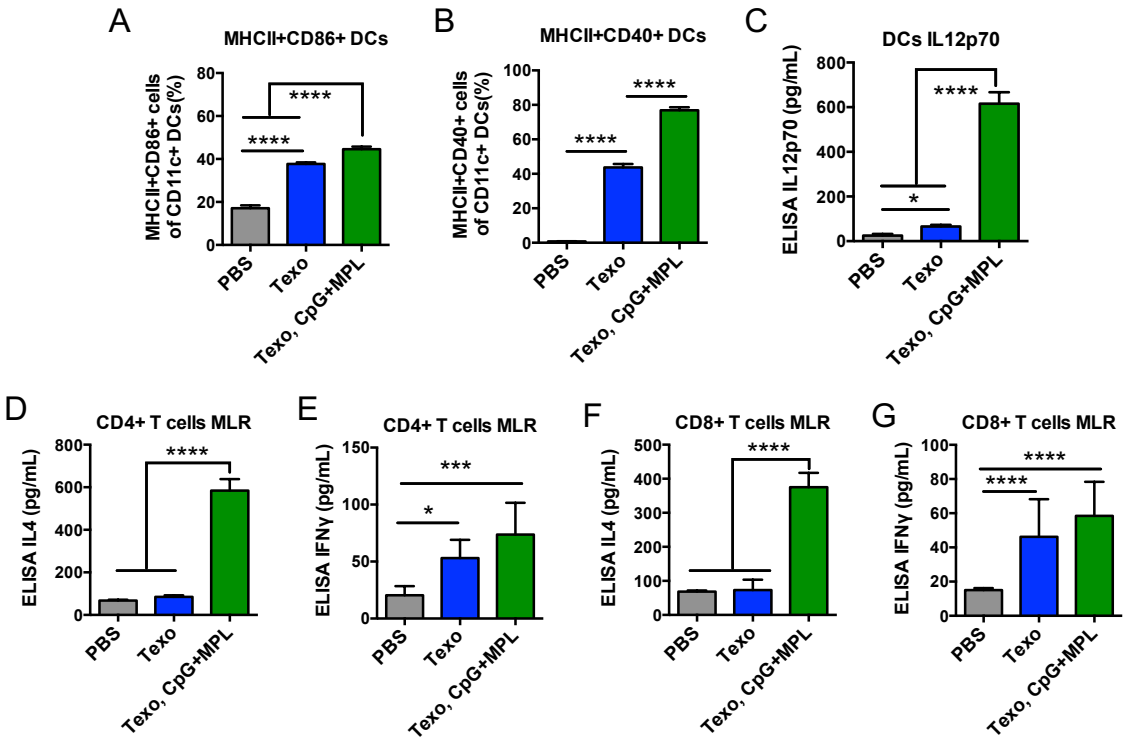

Figure 2.7 Texo-adjuvant vaccine enhanced BMDC maturation and T cell immune response. Graph showing percentage of CD11c+ BMDC expressing both MHCII and CD86 (A), both MHCII and CD40 (B), and the IL12p70 (C) concentration in the supernatant measure by ELISA. The IL4 (D, F) and IFNγ (E, G) secretion in the supernatant of isogenic MLR study between BMDCS and CD4+ T cells, or between BMDCS and CD8+ T cells. *P<0.05, ***P<0.001, ****P<0.0001.

2.4 Discussion

Cancer immune therapy is a modern treatment method with the promising potential to completely cure the cancer. Especially, the tumor-antigen specific therapeutic vaccines allow the generation of tumor-specific anti-cancer immunity while without endangering healthy tissues. However, the tumor-antigen specific therapeutic vaccines often require the identification of certain antigens, which is time and money consuming, thus largely limited their clinical applications. Texo have inherited similar spectrum of tumor specific antigens, allowing the immune system to identify multiple antigens for an individual patient. Their components of immune-active molecules and the structure of nano-vesicles meant for cargo delivery contribute to the possibilities for Texo to be used as cancer vaccine. [67-69]However, the role of Texo in cancer treatment is still debatable as some studies claim the Texo have the properties to support cancer growth. Therefore, the purpose of this study is to testify the therapeutic effects of Texo immunization and comprehensively elucidate the immune response driven by Texo administration, ultimately paving the way for Texo-based cancer vaccine for B lymphoma.

In the survival study, three experimental designs were adjusted in order to better mimic the scenario in the clinical settings for B lymphoma. First, the Texo were collected from *ex vivo* A20 B lymphoma cells that had been established in vivo, instead of A20 cell lines. Second, a pre-established aggressive DLBCL model was adopted, in which the lethal dose of A20 cells were injected i.p., and allowed to establish for 7 days in vivo, followed by immunizations of Texo. Compared to s.c. injection of B lymphoma cells or vaccine immunization even before tumor establishment, our experimental setting is more clinical relevant. Third, in a very later time point post the first tumor challenge, the survived mice

were re-challenged with a second lethal dose of tumor cells and the survival curves were monitored for upto 160 days. This experimental setting focused on the long-term protection against tumors, which is needed by clinical treatment in case of possible tumor recurrence. By three s.c. injections, the Texo alone with very low dose (10 μg per injection) showed impressive long-term immune protection against two lethal tumor challenges and achieved as high as 60% survival rate and >160-day median survival in the lethal B lymphoma model, compared to untreated PBS group with 0 survival rate and 39.5-day median survival. (Fig. 2.3) Though many exosome-based cancer vaccines in research or clinic focused on dendritic cell derived exosomes (Dexo), the process of pulsing antigens to patients' autologous DCs is time and money consuming, also complicated the clinical operating process. Since the immunogenicity of Texo has been proved here and in many other studies, direct injection of Texo to defeat cancer might be an alternative option for Dexo-based cancer vaccine and worth being pushed forward in clinic.

The following mechanistic study has shown the activation of both cellular and humoral immune response that may underlie the therapeutic effect of Texo against B lymphoma. It has been reported that both CD8+ and CD4+ T cells are required for the therapeutic effect of Texo in the established lymphoma model. And our study has further implicated the Texo driven T cell immune response. First of all, it is very interesting to see that the Texo immunization leads to the simultaneous induction of IFN-γ mediated Th1 and IL4 mediated Th2 immune response. (Fig. 2.4 D, E) The Texo could also activate IFN-γ secreting CD8+ T cells, indicating the potential antigen-specific CTL responses driven by Texo. The strong humoral immune responses were also observed by activation of germinal center reaction in the lymph nodes, inducement of the anti-tumor antibody secretion in the blood and

generation of anti-tumor plasma B cells in the bone marrow. (Fig. 2.5) Especially, high level of anti-tumor IgG2a, IgG2b and IgG1 were found at day 160 in the blood immunized with Texo. Since the IgG1 antibody secretion is related to Th1 immune response, while the IgG2a and IgG2b secretion is mediated by Th2 immune response, the antibody secretion pattern is consistent with our previous results showing activation of both Th1 and Th2 immune response. The existence of plasma cells secreting anti-tumor antibodies in the bone marrow as well as the ADCC effects of blood serum further proved the close relationship between humoral immune response and long-term protection against tumor induced by Texo injections. Our study has revealed the potential therapeutic role of humoral immune response driven by Texo in B lymphoma treatment for the very first time. As many studies focused CTL immune response to clear the tumor cells, our study emphasizes the equivalent importance of anti-tumor humoral immune response in B lymphoma treatment.

TLR agonists could specifically bind to the TLR on the immune cells and active full spectrum of immune responses based on the signaling mechanisms of certain TLR agonist. CpG and MPL are TLR9 and TLR4 agonists, respectively. They are potent adjuvants with low toxicity and are widely used in clinical trials in cancer immunotherapy. It has been reported that CpG could induce strong type 1 immune responses, while MPL can induce both tumor-specific humoral and cellular immune responses. Moreover, co-administration of dual or multiple adjuvants are proved to be even more potent compared to one in cancer immunotherapy. Therefore, the TLR agonists were added to the formulation of the Texo based cancer vaccine in our study to further prompt the observed cellular and humoral anti-cancer immune responses. In a more aggressive DLBCL model, in which the initial injected tumor cell number were doubled, when Texo alone showed limited therapeutic effects, the

co-administration of Texo and TLR4/9 agonists showed supreme effects on improving the cancer mice survival. Other adjuvants, including the Alum and PLGA micro-particles that could absorb exosomes by static interaction, were also tested in the survival study, however achieved no therapeutic effects. (data not shown) Therefore, the adoption of TLR agonists as adjuvant in Texo-based adjuvants are recommended to treat B lymphoma in the future research and clinic study. Administration of TLR4/9 agonists has further activated multiple effector arms of immune system, including bone marrow dendritic cell maturation, CD4+ and CD8+ T cell immune response *in vitro*. (Fig. 2.7) Surprisingly, Texo alone did not induce Th2 immune response in MLR in vitro though showed strong Th2 immune response in mechanistic study in vivo. The possible reason could be the Texo may activate the T cell immune cells by not only APC-T cell pathway but direct interrelation with T cells. However, the addition of TLR4/9 agonists has tremendously activated the Th2 immune response in the MLR. Regardless of the deeper mechanism of Texo-TLR4/9 driven immune response, which needs further examination in vivo, the co-administration of TLR4/9 with Texo holds the potential to further activate the immune system and achieve improved therapeutic effects in aggressive B lymphoma model compared to Texo alone.

To conclude, our study confirmed the promising therapeutic potential of Texo-based cancer vaccine in the DLBCL model and comprehensively evaluated the mechanism of the anti-cancer immunity driven by Texo. The Texo vaccine provides long-term immune protection against pre-established DLBCL model. The immunization of Texo activate many effective arms in the immune system, including cellular immune responses and anti-cancer humoral immune response. Especially, the plasma B cells with the capacity of secreting anti-tumor antibodies may be responsible for the long-term protection effects

caused by Texo. The formulation of Texo plus TLR4/9 agonists showed enhanced therapeutic outcome and provide options for adjuvant selection in the Texo-based cancer vaccine. Our study elucidated the mechanism and proved the therapeutic effects of Texo-based cancer vaccine that paved the way for the possible translate of Texo in the clinical treatment for B lymphoma.

CHAPTER 3. FUNCTIONAL FIBROUS SCAFFOLDS FOR POTENTIATING IMMUNOMODULATORY PARACRINE ACTION OF MESENCHYMAL STROMAL CELLS

While the studies on the material interaction with mesenchymal stromal cells (MSCs) have been mainly focused on the ability of materials to provide environment to regulate cell viability, proliferation or differentiation, the therapeutic effects of MSC-material constructs may result from the secretion of immunomodulatory and angiogenic cytokines from MSCs. Here, electrospun scaffolds composed of fibers in random, aligned and mesh-like patterns were fabricated, and the paracrine behavior of adipose-derived MSCs (Ad-MSCs) on the scaffolds were investigated in comparison to the cell culture via conventional microplates. It was found that the Ad-MSCs on the electrospun fibers produced significantly higher levels of anti-inflammatory and pro-angiogenic cytokines compared to those cultured on microplates. The enhanced modulatory effects of the secreted products of Ad-MSCs on fibrous electrospun scaffolds were also proven in the cultures of endothelial cells and the LPS-stimulated macrophages, with three types of scaffolds showing distinct influences on the paracrine function of Ad-MSCs. In a skin excisional wound-healing model in rat, the conditioned medium collected from the MSC-scaffold system accelerated the wound closure, promoted the macrophage recruitment and enhanced the polarization of macrophages toward the pro-healing phenotype in the wound bed. Our study demonstrates that the fibrous topography of scaffolds is a key material property that modulates the paracrine function of cells. The discovery elucidates a new aspect of material

functions, laying the foundation for developing scaffold materials to promote tissue regeneration/repair through guiding the paracrine signaling network.

3.1 Introduction

Mesenchymal stromal Interestingly, both Th1 and Th2 immune response were activated simultaneously. As many study emphases the Th1 biased immune response is the key to drive specific tumor cell killing effects, the observed Th2 immune response provide new angels to re-evaluate the function of T helper cell activation. cells (MSCs) are multipotent adult stem cells capable of differentiating into multiple lineages, including osteoblasts, adipocytes, chondrocytes and myoblasts, under different stimuli and culture conditions.[21] In recent decades, MSCs are one of the most widely investigated cell types in regenerative medicine and have achieved promising therapeutic results in treating graft-versus-host disease, myocardial infarction, cerebral stroke and wound healing etc.[19, 20, 22] However, studies have shown that the multi-lineage potential of MSCs may contribute little to their therapeutic effects. Instead, the paracrine products of MSCs could exhibit multifaceted functions including immunomodulation, angiogenesis, anti-apoptosis, anti-scarring, chemoattraction and modulating local stem and progenitor cells.[21, 70] In particular, the trophic factors, such as vascular endothelial growth factor (VEGF), hepatocyte growth factors (HGF) and basic fibroblast growth factor (bFGF), secreted by MSCs could promote vascularization in the wound area.[71, 72] The anti-inflammatory molecules, including indoleamine-2, 3-dioxygenase (IDO), prostaglandin E2 (PGE2) and tumor necrosis factor α (TNF-α)-stimulated gene 6 (TSG-6), would modulate both innate and adaptive immune responses away from scarring but towards regeneration.[23, 70, 73] Taken together, MSCs

hold promise to serve as a vital cellular modulator by sensing the environment and creating an orchestrated network of molecules to promote the tissue repair/regeneration process.

Scaffold is a key component in the concept of tissue engineering, which works as a substrate for cells to attach and grow.[74] With the microstructures, surface morphology/chemistry and mechanical properties, the intriguing function of a scaffold lies in its ability to generate tailored microenvironment that may guide the cell behavior through specific cell-material interactions. Under the assumption that scaffolds may be designed to promote the differentiation of MSCs during cell transplantation to supplement the injured tissue with functional cells, numerous studies have been carried out in this aspect to understand/engineer the bioactivity of scaffolds.[75-79] Yet little is known about how scaffolds and the material topographical properties might affect the paracrine function of MSCs, despite the pivotal role of the secretory products of MSCs in mediating the local signaling processes *in vivo*. In this study, we thereby are interested in designing experiments to probe two fundamental questions: 1) how the secretory behavior of MSCs would be altered upon the contact with a fibrous scaffold and 2) whether this new aspect of cell-material interaction has implication for tissue repair/regeneration settings. In particular, we intend to investigate the profile of the pro-angiogenesis and anti-inflammatory factors secreted by MSCs, as these two categories of cytokines may participate in key tissue repair/healing processes and are potent factors that may improve the therapeutic effects of MSCs *in vivo*.

To this end, we here selected electrospun fibers (EFs) to probe the relationship between fibrous microenvironment and the MSC paracrine activity. Because of the advantages such

as the convenient fabrication process, the wide choice of materials and precision control over fiber parameters, EFs constitute an important category of scaffold materials that haven been intensively studied in tissue engineering. [80-82] In particular, by mimicking the natural extracellular matrix, the micro-/nano-fibers have been found to provide distinct contact cues to modulate cell activities, including supporting cell proliferation, promoting the stemness and maintaining pluripotency of stem cells.[83, 84] In addition, the orientation/alignment of fibers has also been shown to generate topography-induced cues to promote Schwann cell maturation, vascular endothelial cell growth, myotube formation and MSC differentiation. [77-79, 85, 86]

Here, polycaprolactone (PCL) EFs with three different alignment characteristics were fabricated as model scaffold materials. The effects of the fibers on rat adipose-derived MSCs (Ad-MSCs) to produce pro-angiogenic and anti-inflammatory paracrine factors were investigated. The function of these paracrine factors was further studied through collecting conditioned-medium (CM) from different culture systems and applying it to cultures of endothelial cells and macrophages *in vitro* and a skin wound-healing model *in vivo*. Our study suggests that the fibrous topographical structure has profound effects on the secretory behavior of Ad-MSCs and the cells tend to produce cytokines that are capable of promoting angiogenesis, immunomodulation and tissue healing processes. The discovery on the relationship between cell paracrine function and materials reveals a new aspect of material properties that has not been systematically studied before. The study also suggests the potential approach to modulating of the paracrine signaling network through design of functional scaffolds to improve cell-based regenerative therapy.

3.2 Materials and Methods

3.2.1 Materials and reagents

Ultrapure water ⩾18 MΩ was derived from deionized water though a Milli-Q system (Millipore, Billerica, MA). Polycaprolactone (PCL) and lipopolysaccharide (LPS) were obtained from Sigma-Aldrich (Milwaukee, WI). QuantiT™ PicoGreen® dsDNA Assay Kit, TRIzol kit, Dulbecco's phosphate buffered saline (DPBS) and cell culture reagents were purchased from Invitrogen (Carlsbad, CA, USA) unless otherwise specified. Solution Cell Activity Assay (MTS) systems were from Promega (Madison, WI). Matrigel was from BD Biosciences (San Jose, CA, USA). 4',6-diamidino-2-phenylindole (DAPI) and Rhodamine Phalloidin was obtained from the ThermoFisher (MA, USA). Human umbilical vein endothelial cells (HUVECs), Endothelial cell medium (ECM), endothelial cell growth supplement (ECGS) were purchased from ScienCell (Carlsbad, CA). Rat adipose-derived mesenchymal stromal cells (Ad-MSCs) were purchased from Cyagen Biosciences Inc (Santa Clara, CA, USA). The murine-macrophage cell-line RAW 264.7 were obtained from the Cell Culture Center of the Institute of Basic Medical Sciences (Beijing, China). Suppliers of other chemicals, biological reagents, and equipment were specified below.

3.2.2 Cell culture

All cells were cultured at 37°C under humidified atmosphere with 5% CO2. The Ad-MSCs were cultured in minimum essential medium α (MEM-α) supplemented with 10% fetal bovine serum (FBS), 0.4% penicillin/streptomycin (P/S), without further supplement

of growth factors. For the collection of conditioned media, the MSCs were cultured in FBS-free MEM-α for a prescribed period of time. The Ad-MSCs between passage 3 and 5 were used for the following experiments. The human umbilical vein endothelial cells (HUVECs) were maintained in endothelial cell medium (ECM) supplemented with 5% FBS, 1% (P/S) solution and 1% ECGS. RAW264.7 macrophages (MΦ) were cultured in DMEM supplemented with 10% FBS and 1% P/S. To detach cells from the culture plates, Ad-MSCs and HUVECs were treated with trypsin/EDTA solutions, while macrophages were pipetted repeatedly to induce the detachment.

3.2.3 Fabrication of fibrous scaffolds

Electrospun fibrous scaffolds were prepared from polycaprolactone (PCL) solution. 15% w/v PCL was dissolved in a mixture of CHCl3 and dimethylformamide at the volume ratio of 9:1. After stirring for 3 h until PCL was completely dissolved, 1 mL of the solution was loaded into a syringe with a blunt-ended stainless steel needle. The feeding rate and the applied voltage were controlled at 0.5 mL/h, 12kV, respectively. The collection distance for random EF (REF) and mesh-like EF (MEF) was 14 cm and for aligned EF (AEF) 10 cm. The REF was collected on a flat plate, the MEF on a copper mesh, and AEF through a rotating cylinder at speed ~3000r/min. The EF membranes were cut into predefined sizes and shapes manually. For sterilization, EF membranes were rinsed with 75% ethanol solution for 30 mins and then washed with sterilized DI water for three times and air dried in bio-safety cabinet (Thermo, Germany). The EF scaffolds were exposed under ultraviolet radiation for 30 min on each side in the bio-safety cabinet for further sterilization and were kept in sterile dishes at 4°C until being used.

3.2.4 SEM and confocal imaging

Topographical features of the scaffolds were examined by scanning electron microscopy (SEM) (S-4800, Hitachi, Japan). For the measurement of fiber diameter, 300 fibers were randomly selected in the SEM pictures and the diameter was calculated by ImageJ software. To examine the cell morphology on the scaffolds, 2×104 Ad-MSCs were seeded on the scaffolds for 24 h. The scaffolds were washed with PBS, and the attached cells were fixed in 2% glutaraldehyde overnight at 4°C. Samples were then dehydrated by rinsing in ethanol solution with series of concentration (from 30% to 100%, v/v) for 15 min at each step. Once dried, the samples were examined via SEM. For fluorescent confocal imaging, scaffolds seeded with Ad-MSCs were fixed overnight by 2% paraformaldehyde (PFA), and the cells were stained with Rhodamine Phalloidin for 1 h and then DAPI for 5 min. The stained cells were pictured by A1R-si confocal microscope (Nikon, Japan)

3.2.5 Real time PCR assay

All gene expression assays, including the expression of paracrine products and cell differentiation and stemness markers were performed through the same protocol. 1×105 Ad-MSCs were seeded on polystyrene 24-well plates or on circular scaffolds trimmed with the same size as the microwell and supplied with MEM-α medium supplemented with 2% FBS and 1% P/S. For the nuclear factor-κB (NFκB) inhibition study, the medium was additionally supplemented with 1 mM NFκB inhibitor, pyrrolidinedithiocarbamic acid, ammonium salt (PDTC) (Sigma-Aldrich, Milwaukee, WI). After cultivation for 24 h (or 7 d), the total RNA of these samples was extracted using the TRIzol kit according to the manufacturer's instructions. The total isolated RNA was reverse transcribed with

TransScript First-Strand cDNA Synthesis SuperMix (Transgene, Beijing, China). The gene expression levels were analyzed using the SYBR Green real-time PCR method and were quantified using the Bio-Rad CFX connect real time PCR system (Bio-Rad, Hercules, CA). Primers were ordered from Sangon (Shanghai, China). The sequences of primers for qRT-PCR were listed in Table 1 in the supplementary information (SI). All gene expression values in one sample were normalized to the GAPDH level. Relative expression was calculated using the comparative Ct method. The mean minimal cycle threshold values were calculated from triplicate reactions.

3.2.6 Cell proliferation and metabolic assays

Ad-MSCs cultured on different substrates for 1-5 day were examined for metabolic activities and DNA contents through the MTS assay and picogreen staining, respectively. For the MTS assay, the supernatants in each cell culture well were removed, and 20 μl CellTiter96 aqueous one solution, diluted 5 times with fresh medium, were added. The plates were kept at 37 ºC in the dark for 2 h. The absorbance of the supernatant was measured at 490 nm using the SpectraMax M2 microplate reader. To determine the DNA contents in each sample, the cells cultured on the EF scaffolds were lysed using 0.1% Triton X-100 solution at 4 ºC overnight to obtain the DNA sample solutions. 100 μl of DNA sample solutions were mixed with an equal volume of PicoGreen reagent according to the manufacturer's protocol. After 5 min, the fluorescence was measured using the microplate reader (excitation: 480 nm; emission: 520 nm) to determine the DNA contents of the samples and the cell numbers were then calculated based on the standard curve. To determine the metabolic activity on the single cell level, the value of MTS assay was normalized to the cell number determined by the DNA content assay.

3.2.7 Assay of paracrine products

1×105 Ad-MSCs were seeded on 24 well plates or 1.9 cm2 scaffolds and supplemented with 1 mL culture medium. To collect the CM, cells were first cultured in complete MEM-α medium for 12 h, then washed three times with PBS and supplemented with FBS free MEM-α medium to exclude the influence of serum in the culture. After 24 h cultivation, the supernatant was collected and centrifuged at 5000 rpm to remove the dead cells and cell debris. (When the cells were maintained under the serum-free conditions, the culture was conducted for a maximum of 24 h to ensure that the CM was collected from healthy cells.) The cells remained in the MP or scaffolds were fixed with 2% PFA and stained with 0.5 μg/mL DAPI for 10 min. Fluorescence images fully covering the microwell were captured by an IX71 fluorescence microscope (Olympus, Japan), and the number of cells in each well was counted based on DAPI staining without repetition by ImageJ software. The concentration of all the CM samples was then adjusted with MEM-α to make sure the secretory products measured in different samples were generated by the same number of cells. Enzyme-Linked ImmunoSorbent Assay (ELISA) analyses for PGE2, TGF-β, VEGF, bFGF and HGF (R&D) in CM were then performed following the manufacturer's instructions. The nitric oxide in conditioned medium was measured by colorimetric Griess reaction kit (Beyotime, China).

3.2.8 Expression profiling of LPS-induced macrophages

The macrophage cell line raw264.7 were seeded in 24-well culture plates at 2×105 per well for 24 h, followed by adding 500 ng/ml LPS to stimulate macrophages. After 1 h, the LPS-containing supernatants were removed and cells were gently washed with DPBS

for three times. The macrophages were then treated with 50% complete DMEM and 50% CM. The concentration of CM samples was adjusted according to the Ad-MSCs number as described above. After 8 h treatment, the total RNA of macrophage was extracted from each sample and the relevant gene expression was measured by real time qPCR assay. Samples supplemented with or without LPS, both without CM treatment, were served as the positive or negative controls, respectively.

3.2.9 HUVEC proliferation and tube formation assay

For the HUVEC proliferation assay, the HUVECs were cultured in complete ECM medium for 6 h for cells to fully adhere to the microplates. The medium was then changed to a serum-free ECM containing 1% P/S and 1% ECGS to starve the cells for 12 h. The media were then replaced with the ECM (containing 2% FBS and 1% P/S) and CM at 1:1 volume ratio. The CM were prepared and adjusted according to the Ad-MSCs number as described above. Before each step of changing the medium, cells were washed with sterile DPBS gently for three times. After 24 h, the cells fixed in 2% PFA and stained with 0.5 μg/mL DAPI for 10 min. The cell number was counted based on the DAPI staining as described above. For the HUVEC tube formation assay, 1×104 HUVECs were seeded onto the Matrigel films in 96-well plates, treated with 50% CM and 50% ECM supplemented with 2% FBS and 1% P/S. Cells were incubated for 6 h and imaged under bright-field microscopy. Tube length was quantified by ImageJ software. The HUVECs cultured in the ECM supplemented with 2%FBS, 1% PS and 1% ECGS, and the ECM with 2% FBS and 1% P/S lacking ECGS, served as the positive and negative control, respectively, in both HUVEC proliferation and tube formation assay.

3.2.10 Rat skin excisional wound healing model

All procedures were performed in accordance with the regulations approved by the Institutional Animal Care and Use Committee (IACUC) of Peking University. Sprague–Dawley male rats (Vitalriver, Beijing, PR China) weighing 290–320g were anesthetized; two 7-mm diameter round full-thickness excisional skin wounds were created on each side of the midline using a biopsy puncher following the hair removal from the dorsal skin. A donut-shaped silicone splint was glued to the skin using the superglue with the wound centered in the splint. The splint was used to stabilize the wound and avoid contraction, making wound area comparable. For in vivo experiments, each CM sample was collected as described above and further concentrated (nearly 30 times) by ultrafiltration with a 3 kDa molecular weight cut-off filter (Millipore, America) following the manufacturer's instructions. Each wound then received 200 μL solutions of the CM collected from MSC-MEF or MSC-MP, or just blank MEM-α in a randomized order. In the application of the solutions, 150 μL CM was injected subcutaneously around the wound and 50 μl CM was topically smeared onto the wound bed. Finally, a Tegaderm (3M, MN, USA) was placed over the wounds to keep the wounds clean and avoid contamination. Digital photographs of the wounds were taken at day 0, 4, 7, and the wound area was measured by the ImageJ software. The wound area was not calculated after day 7 because of the fall-off of the splint. The percentage of the wound closure was calculated as: (area of original wound - area of actual wound)/area of original wound × 100%.

3.2.11 Histology and immunostaining

Rats were sacrificed at day 7 or day 14. The skin tissues including the wound and the surrounding skin were harvested, and was cut into two parts from the middle line for histology observation. The dermal specimens were then fixed with 10% formaldehyde, embedded in paraffin and cut into sections with thickness of 5 μm. The sections were stained with hematoxylin and eosin (H&E) or Masson's trichrome (MT) before imaged by a light microscope (Olympus, Japan). For the immunohistochemical staining, the tissue slides were deparaffinized followed by antigen retrieval in boiling citrate buffer (10 mM citrate, pH 6.0) for 24 min. Non-specific binding was blocked by incubation with 5% donkey serum (Jackson, 017-000-121) for 30 min at room temperature. The sections were decanted and incubated with primary antibodies overnight at 4°C. The primary antibodies against the pan-macrophage marker CD68 (mouse anti-rat CD68, Abd Serotec, MCA341GA), and the M2 macrophage marker CD206 (goat anti-human CD206, Santa Cruz, sc-34577) were applied to the specimen. The sections were then washed and incubated with the two fluorescently conjugated secondary antibodies, donkey anti-mouse Alex Fluor-555 (Invitrogen, A31570) and donkey anti-goat Alex Fluor-488 (Jackson, 705-545-147), for 1 h at room temperature. The nuclei were labeled with DAPI, and the slides were covered with the fluorescent mounting medium (Boster， AR1109) for confocal microscopy imaging. The macrophage cell number of different types was counted by ImageJ software based on the color of fluorescent dye.

3.2.12 Statistical analysis

Quantitative results were presented as means±standard deviation (SD). Statistical comparisons were performed by one-way analysis of variance (ANOVA) followed by

Holm-Sidak tests to compare selected data pairs. Values of $P < 0.05$ were considered statistically significant.

3.3 Results

3.3.1 Preparation of electrospun fibrous matrices and culture of Ad-MSCs

As shown in figure 3.1, three types of EF materials, showing random, aligned and a mesh pattern, were first prepared, which were designated as REF, AEF and MEF, respectively. The materials were seeded with Ad-MSCs and the paracrine products from different culture system were analyzed through profiling the gene expression and protein secretion from the cells. The function of the paracrine products was investigated by collecting the CM and applying them to the in vitro cultures of endothelial cells/macrophages and an in vivo skin wound healing model. In all the experiments, the cells cultured on the polystyrene microplate (MP) were used as a control for comparison to understand how the materials with fibrous topological characteristics may affect the paracrine secretion of MSCs.

In Figure 3.2, it is shown that the EF scaffolds fabricated through electrospinning processes using different collectors had distinct morphologies. (Fig. 3.2 A-C) While the REF and AEF contained random and aligned fibers, respectively, the MEF collected using the copper mesh as a collector was made of bundled fibers oriented vertically in lattice patterns with the grid length at 830 μm. It is noted that the loose fibers deposited inside the grid were also vertically crossed. By tuning the electrospinning parameters, the fiber diameters in the three types of EFs were controlled at the scale of 1 micrometer in three materials (Fig. A1) to minimize the influence of the fiber size.

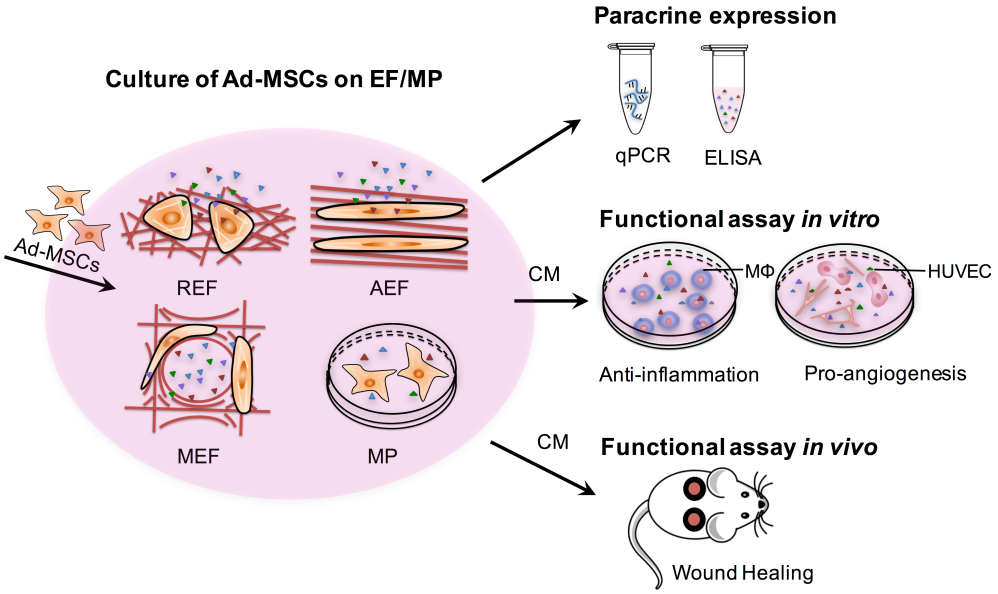

Figure 3.1 The experimental design to investigate the influence of the fiber morphology and fiber orientation on the paracrine secretion and function of Ad-MSCs. The scaffolds for cell culture included electrospun fibers in random, aligned and a mesh organization, which were designated as REF, AEF and MEF, and the cultures on EFs were compared to the Ad-MSCs cultured on polystyrene microplate (MP).

When the Ad-MSCs were cultured on the three EF scaffolds, the cells could all adhere and grow. Both the SEM and confocal microscopic studies show that the cytoskeletons of the Ad-MSCs following 24h h culture were random or oriented depending on the topology of the underlying scaffold. (Fig. 3.2 D-I) On the REF, the cells were basically round with protruding edges, likely resulting from the cytoskeletons stretched in different directions (Fig. 3.2 D, G). On both AEF and MEF the cells were relatively elongated and oriented on top of the aligned or bundled fibers (Fig. 3.2 E-F, H-I), respectively. In particular, the majority of the Ad-MSCs adopted two vertical directions on

MEF, both on the grid lines on the fiber bundles and inside the grids on the loose fibers. (Fig. 3.2, F1-3 and A2)

When the metabolic levels were examined through the MTS assay, it was shown that the cells seeded on the EF scaffolds were metabolically more active than the cells on 2-D MP on day 1, and the metabolic levels then dropped and became similar to the cells cultured on microplates. In studying the cell proliferation levels, there was no statistical difference among the cells on the three types of EFs (Fig. 3.2 J). Quantification of the cell number indicates that the cells proliferated at a similar rate as those grown on the MP. (Fig. A3) As the Ad-MSCs are multipotent with differentiation capabilities toward connective tissues, the gene expression of the adipogenic, chondrogenic and osteogenic markers were analyzed. Compared to the gene expression at day 0, no genes were found to express at elevated levels up to day 7, suggesting the Ad-MSCs basically remained undifferentiated. Interestingly, the stemness marker, OCT4, was found upregulated by 3.0~3.5 fold ($P<0.0001$) when the cells were on the fibrous scaffolds. (Fig. 3.2 K)

3.3.2 Gene expression and protein secretion of paracrine factors by Ad-MSCs

To investigate the paracrine products of Ad-MSCs and the topological cues that the scaffolds may generate, the gene expression and molecular secretion levels were assayed through quantitative RT-PCR and ELISA, respectively, on a set of factors that are relevant in the inflammation and angiogenesis. In general, the secretion of all the factors examined

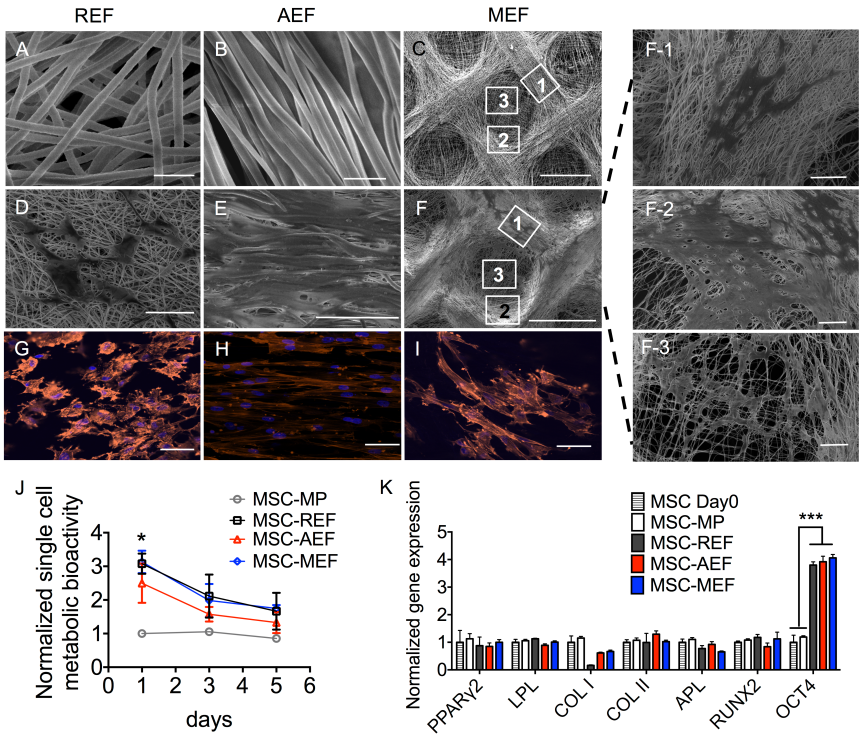

Figure 3.2 A-C, SEM images of the EF scaffolds, REF, AEF and MEF used for cell culture. D-F and G-I, SEM and fluorescent confocal images of the Ad-MSCs adhered on different EF scaffolds; the boxed areas in F were enlarged in F-1, F-2 and F-3, showing the morphology of cells adhering to the bundled fibers, cornered region and central loose fibers inside the grid on the MEF, respectively. (Scale bars: A and B, 5 µm; C and F, 500 µm; D, E, F1-3 and G-I, 50 µm). (G-I, red: cytoskeleton stained with rhodamine phalloidin; purple: nuclei stained with DAPI) J, MTS assay of the metabolic activities of single Ad-MSC on different substrates. * indicates the significant differences between MP and three EF groups on day 1. K, the gene expression of MSC differentiation and stemness markers at day 7. All ddCt values were normalized to the expression at day 0. (J and K, mean±STD, n=4~6, * P <0.05, **P<0.01, ***P<0.001)

was promoted by varied degrees compared to the control group and the trends found in the RT-PCR and ELISA experiments were basically consistent. In particular, Cyclooxygenase 2 (COX-2) is an essential enzyme in the synthesis of PGE2, an important anti-inflammatory mediator and wound-healing inducer secreted by MSCs.[8, 9, 23] Quantitatively, the elevation of COX-2 and PGE2 were the most pronounced among the selected factors that were examined: while the COX-2 mRNA levels expressed by the cells

on EFs were about 5.4-, 6.3-, 10.8-fold ($P<0.0001$) higher on REF, AEF and MEF compared to the MP, respectively, the actual elevation of PGE2 enzymes were ranging from 70- to over 300-fold ($P=0.007$ (MSC-REF), 0.005 (MSC-AEF) and 0.004 (MSC-MEF)) (Fig. 3.3 A, B). iNOS is another factor whose expression was promoted significantly, with the actual secretion increased by 7-,17-and 12-fold on REF, AEF and MEF ($P=0.005$, 0.003 and 0.006), respectively. Among other protein factors, the mRNA of the anti-inflammatory TGS-6 was found to increase by around 5-fold ($P<0.0001$); the secretion levels of reparative TGF-β ($P=0.028$ (MSC-AEF)) and angiogenic VEGF by around 3-fold ($P=0.006$ (MSC-REF), 0.003 (MSC-AEF) and 0.005 (MSC-MEF)). To rule out the effects of possible side-products released from scaffolds, the medium conditioned by the blank scaffolds was also used to culture MSCs and no influence from the blank scaffolds was observed. (Fig. A4)

When the three different scaffolds were compared, it is noted that the materials containing oriented fibers showed more potent effects on promoting the expression of PGE2 ($P=0.0004$ (MSC-AEF) and 0.0125 (MSC-MEF)), iNOS ($P=0.0008$ (MSC-AEF) and 0.0369 (MSC-MEF)), VEGF ($P=0.0006$ (MSC-MEF)) and HGF ($P=0.0016$ (MSC-MEF)) compared to REF, according to the secretion measurements. In effecting the production of other molecules, the influences of the three materials were not significantly different. To further understand the possible molecular signaling mechanisms involved in the elevation of the paracrine secretion by Ad-MSCs, the gene expression of Ad-MSCs treated with an NFκB inhibitor, PDTC, was analyzed. NFκB is a key transcriptional regulator that is known to mediate cellular responses to external stimuli and the MSC priming by TNF-α, LPS or hypoxia.[24, 25] As PDTC was added prior to seeding the Ad-

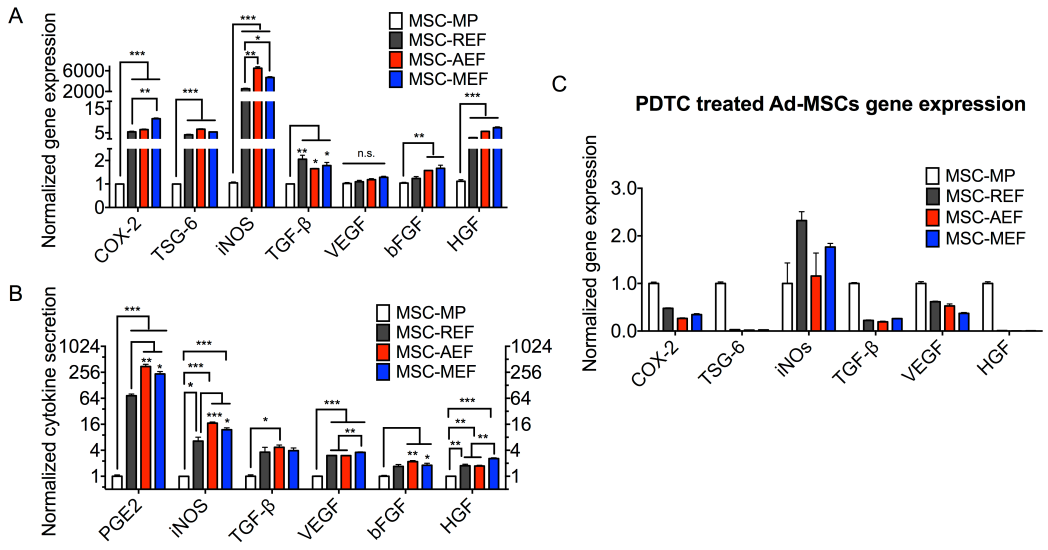

Figure 3.3 A, the mRNA analysis of the selected anti-inflammatory and pro-angiogenic factors expressed by Ad-MSCs. B, the analysis of the paracrine products secreted by Ad-MSCs. C, the reversal of the enhanced expression of the anti-inflammatory and pro-angiogenic factors by Ad-MSCs via the supplementation of PDTC, an inhibitor of the NFκB signaling pathway. All values were normalized over the microplate (MP) group. (Mean±STD, n=4~6, *P <0.05, **P<0.01, ***P<0.001)

MSCs, it was shown through the mRNA analysis that the paracrine responses of MSCs toward fibrous materials were all significantly reversed (P<0.001). (Fig. 3.3 C)

3.3.3 In vitro anti-inflammatory and pro-angiogenic function of the Ad-MSC paracrine products

To probe the function of the secretory products of Ad-MSCs, the serum-free media conditioned by the Ad-MSCs cultured on different scaffolds and microplates were separately collected and applied to the cultures of macrophage and endothelial cells. Specifically, the murine RAW 264.7 macrophages were pre-treated with LPS and the inflammatory response induced which manifested in the drastically elevated secretion of tumor necrosis factor α (TNF-α) and interleukin 1β (IL-1β). When the CM containing the

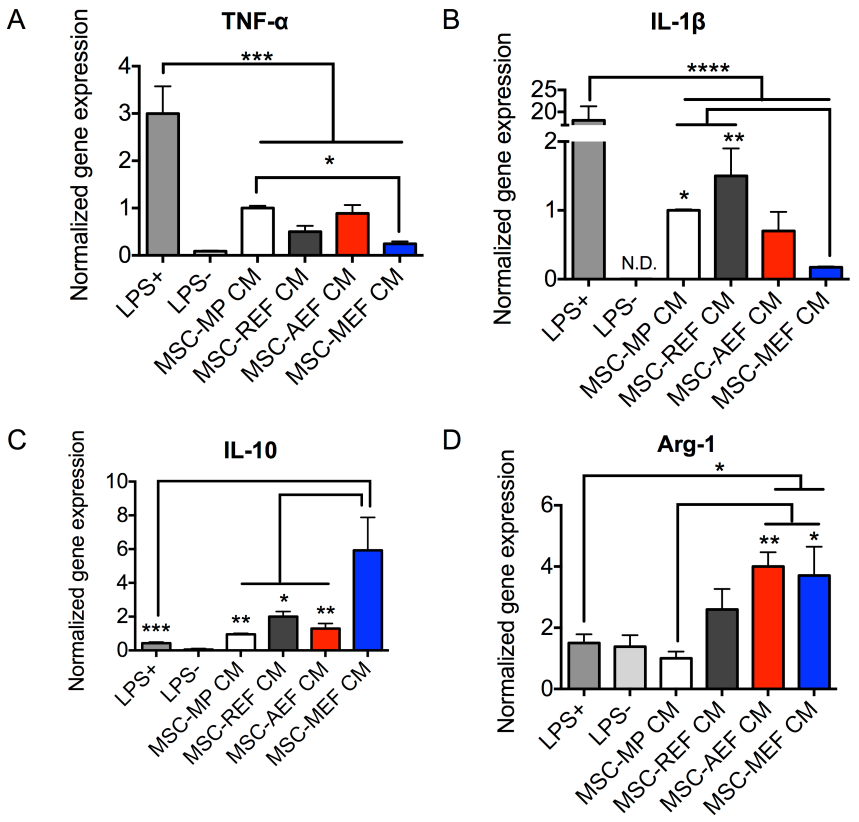

Figure 3.4 The effects of the conditioned medium (CM) derived from Ad-MSC cultures on the pro-/anti-inflammatory expression of LPS-stimulated RAW 264.7 macrophages: A, TNF-α; B, IL-1β; C, IL-10; D: Arg-1. The LPS (+) and LPS (-) RAW 264.7 macrophages free of CM treatment were positive and negative controls, respectively. All data were normalized over the LPS (+) macrophages treated with the MSC-MP CM. (Mean ± STD, n=4~6, *P <0.05, **P<0.01, ***P<0.001)

secreted products from a normalized number of Ad-MSCs were added, the elevation of these inflammatory factors was reversed, including the CM collected from cells on the MP. Interestingly, this effect was only most significant from the CM obtained from the MSC-MEF system. (Fig. 3.4 A, B) With respect to the beneficial anti-inflammatory factors produced by macrophages, IL-10 and Arg-1, they only increased in the groups treated with the CM derived from the MSC-AEF and MSC-MEF systems but not MSC-MP and MSC-REF compared to the LPS (+) group. Among the MSC-EF groups, the effects of the CM

collected from the cells cultured on oriented fibers were more potent compared to the MSC-REF CM, and the MSC-MEF CM showed the most potent effect on promoting the expression of IL-10, reaching over 5-fold of the function of the MSC-MP CM. (Fig. 3.4 C, D) In the group of MSC-AEF, the upregulated level of IL-10 expression in macrophage cells was lower than that of Arg-1. It could be due to other components in the culture which enhanced the expression of Arg-1 (such as PGE2/TGF-β/IL-4) or downregulated IL-10 (such as IFN γ/IL-1β). When the medium conditioned by blank scaffolds was tested on macrophages, no effects from the scaffolds were observed. (Fig. 3.4)

In analyzing the pro-angiogenic function of the CM of Ad-MSCs, the endothelial cells treated with or without 1% ECGS were performed as negative and positive controls, respectively. It is shown that when the CM samples were applied to the culture, the proliferation level of endothelial cells and the total length of the vessel-like tubes formed by cells both increased compared to the negative control, suggesting the trophic effects of the collected CM. (Fig. 3.5) Among the four groups of CM samples, the effects of the CMs collected from the MSC-EF culture were all significantly more potent compared to the MSC-MP CM. There is also a trend that the oriented fibers facilitated more production of the pro-angiogenic factors from Ad-MSCs in comparison to the random fibers. As is shown in Fig. 4, the HUVEC number normalized over the group of the MSC-MP CM was 1.5, 1.8, 2.0 and the accumulative tube length 1.3, 1.4, 1.5, for the groups treated by the CM collected from the MSC-REF, MSC-AEF and MSC-MEF culture, respectively.

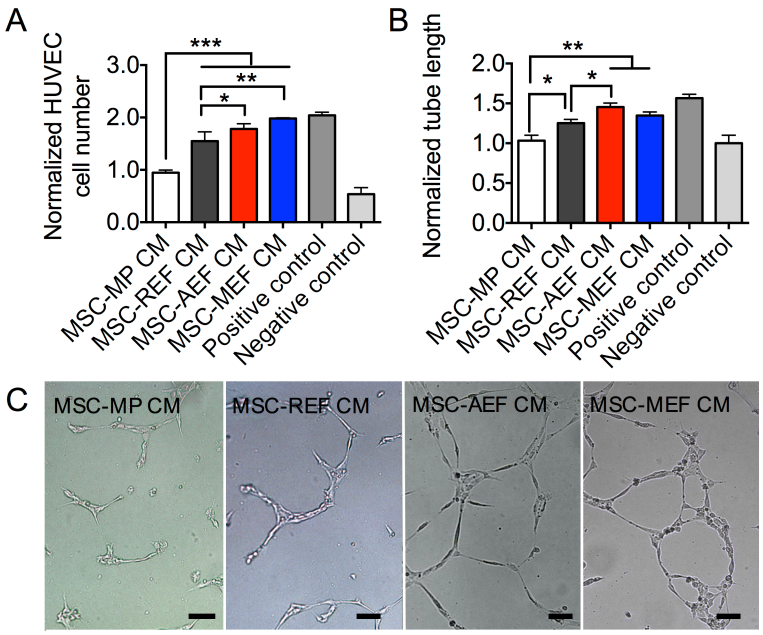

Figure 3.5 The effects of the conditioned medium (CM) derived from Ad-MSC cultures on the HUVECs proliferation (A) and tube formation (B). The blank MEM-α supplemented with or without 1% ECGS were used as the positive and negative control, respectively. The tube length was calculated by 5 repeated wells of 96-well plates for each group. All data were normalized over the endothelial cells treated with the MSC-MP CM. (Mean±STD, n=4~6, *P <0.05, **P<0.01, ***P<0.001) C, epresentative images of the endothelial cells forming tubes when treated with different CMs. (Scale bar: 200 μm)

3.3.4 In vivo wound healing effects of the Ad-MSC paracrine products

To further investigate the function of the paracrine products of the Ad-MSCs and the effects of the fiber topography, the CM samples were harvested, concentrated and used for treating a skin excisional wound in rats. In these in vivo experiments, the CM from the MSC-MEF culture, which showed the optimal effects in the in vitro analysis, was studied and compared to the CM samples collected from the MSC-MP culture. In all three groups including the negative control of the blank medium, the skin wounds all visually prompted healing processes, with the wound closure rate found highest in the group treated by the MSC-MEF CM. In particular, the percentage of the healed region reached 76.5 ± 10.7 %

(Mean±STD, n=8) at day 7 when the MSC-MEF CM was applied to the skin wounds; in contrast, the wound closure was around 38.8% ± 16.3 and 53.3% ± 4.6% in the control and the MSC-MP CM groups, respectively. (Fig. 3.6 A, B)

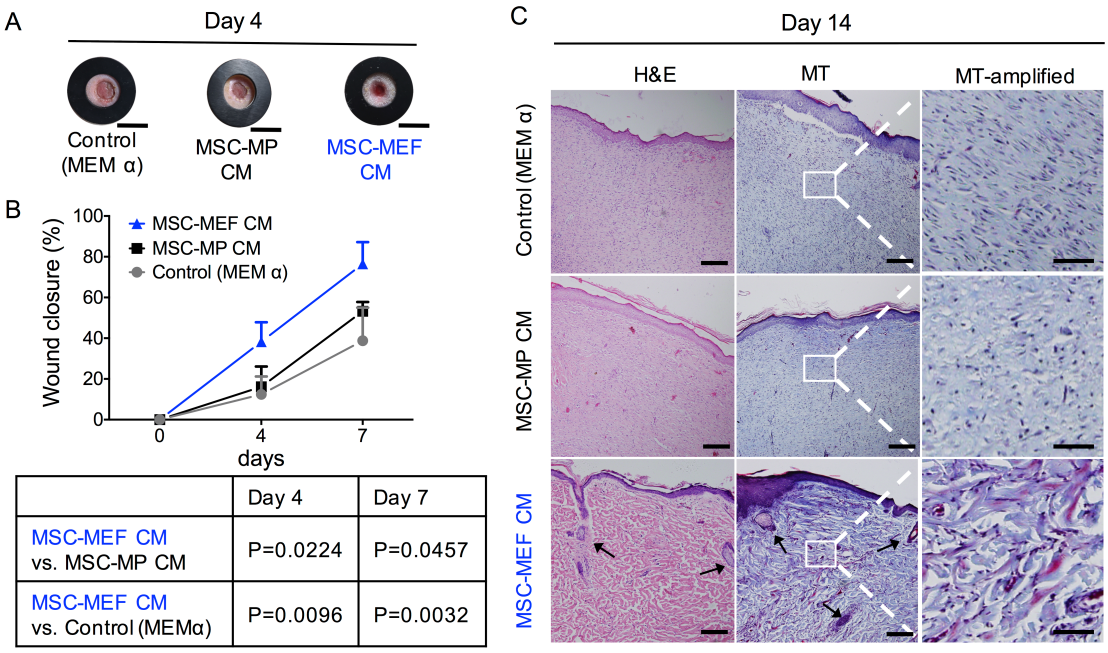

	Day 4	Day 7
MSC-MEF CM vs. MSC-MP CM	P=0.0224	P=0.0457
MSC-MEF CM vs. Control (MEMα)	P=0.0096	P=0.0032

Figure 3.6 The healing effects of the conditioned medium (CM) derived from Ad-MSC cultures on the rat skin excisional wounds. A, representative photographs of the wounds treated by MEM-α or MSC CM at day 4. (Scale bar: 10 mm) B, the measurements of the wound closure within 7 days post the CM or MEM-α treatment; the table lists the P values for comparing the treatments with MSC-MEF CM to those with MSC-MP CM or MEM-α. (Mean±STD, n=8, one-way ANOVA) C, the micrographs of the H&E- and Masson's trichrome (MT)-stained wounds at day 14. The arrows in the MEF-MSC CM group in bottom left and bottom middle images indicate appendage-like structures. (Scale bars: images in the left (H&E) and middle (MT) columns, 200 µm; images in the right (MT-amplified) column, 50 µm)

In the histological analysis, it is shown through H&E-staining that full epithelialization were attained in the excisional regions in all three groups (Fig. 3.6C) at day 14. The Masson's trichrome staining revealed the dermal layer in the group of MSC-MEF CM contained collagen deposition in a fine reticular pattern, in resemblance with the

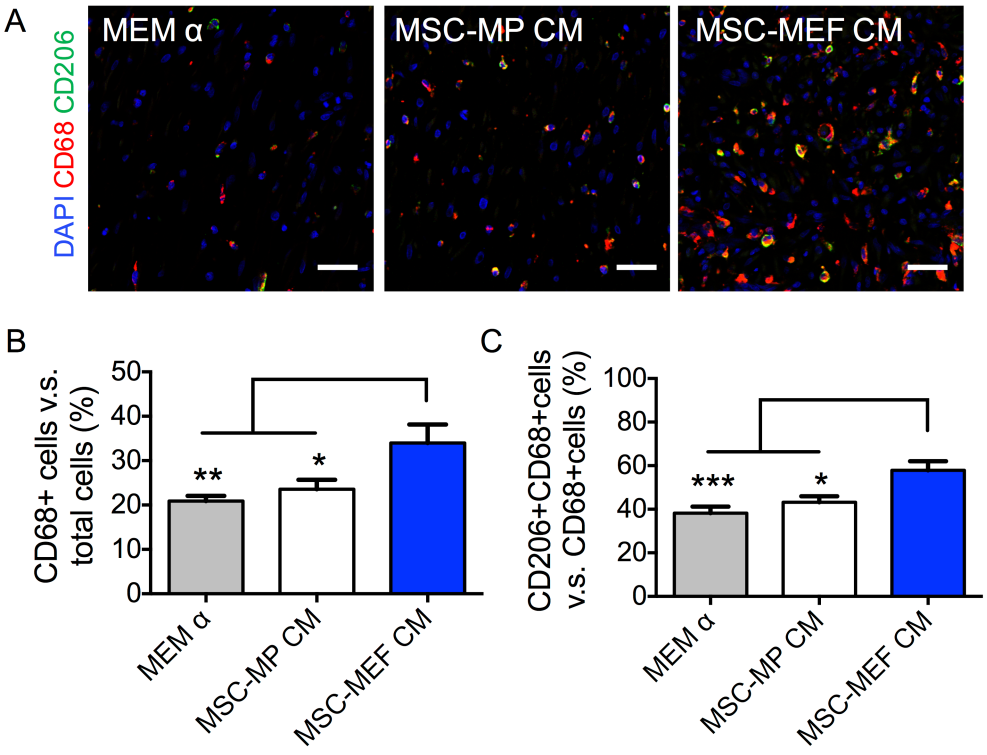

Figure 3.7 A, Fluorescence confocal microscopic analysis of the wound sections stained with the microphage pan-maker, CD68 (red), the M2 phenotype marker, CD206 (green), and nucleus marker, DAPI (blue). (yellow: co-staining of CD68 and CD206 markers) B, the percent population of CD 68+ macrophages over the total number of cells. C, the percent CD206+CD68+ cells over the CD 68+ cells in the wound bed under MEM-α, MSC-MP CM or MSC-MEF CM treatment at day 7. (Mean±STD, n=20; scale bars: 200 μm)

normal dermal tissue. Moreover, appendage-like structures were also visible. In contrast, the collagen in the MEM-α and microplate CM groups appeared to be haphazardly arranged and thick, showing the traits of fibrotic deposition. (Fig. 3.6 C)

In wound healing, macrophage cells play a key role in intercellular communications to modulate the inflammatory and reparative processes. The tissue slides of the wound beds at day 7 were immunostained for CD68 and CD 206, a pan-macrophage and a M2 macrophage maker, respectively, to probe the macrophage phenotype. As is shown in Fig 6, in all three groups, macrophage cells and M2 macrophages were stained positively to

various degrees. In particular, the density of the macrophage cells (Fig. 3.7A) in the wound beds were highest in the MSC-MEF CM group: The percentages of the CD68+ macrophages over the total cells and the dually stained CD206+CD68+ cells over the total CD68+ cells were about 34.0% and 57.8%, respectively.

3.4 Discussion

The combinatorial use of cells and materials has become an important approach in cell-based therapies, in which understanding the interaction between cells and materials and the associated mechanisms is essential to developing functional materials for future regenerative medicine. It is desirable that biomaterials could be generated to provide microenvironment for controlling different cell behavior. The influence of materials on cells, however, is intricate, and much is unknown on how cells should be manipulated to achieve the optimal cell function and thereby therapeutic outcome in vivo. In the settings where the stem cells need to replenish the cell loss caused by injury, the function of materials to enhance cell differentiation and prolong the residence time is key and has been intensively investigated. Evidences obtained through many years of in vivo studies, however, have shown that the transplanted cells would only exist for a relatively short period of time in the host due to the complex host reactions, and the paracrine activity of cells may provide a new effective approach in mediating molecular network within the environment towards tissue regeneration.

In fact, animal studies have shown that the paracrine signals produced by MSCs were able to evoke responses from local cells in the tissue to initiate regeneration [72, 87], and the

paracrine process might also be responsible for the therapeutic effects of MSCs in clinical trials in treating heart ischemia, skin wounds and bone/cartilage injuries.[20, 88-90] On the other hand, it is noticed that in the practices involving the injection of MSCs, the cells usually need to be activated/stimulated [91] through pro-inflammatory factors (e.g. TNF-α, LPS and toll-like receptor (TLR) ligands) or hypoxia condition (i.e. reduced oxygen concentration or 3D spheroid culture). The rational is based on the fact that MSCs can respond to inflammation or hypoxia through producing elevated levels of modulatory paracrine factors including pro-angiogenesis or anti-inflammatory cytokines. [23, 91-93] Recently, a few studies showed that nanoparticles conjugated with extracellular matrix-derived peptide, collagen or hyaluronic porous scaffolds had the potency to promote MSCs paracrine function in vitro.[83, 94-97] However, there was no direct in vivo study that investigated the therapeutic effects of the paracrine products derived from MSCs cultured on biomaterials. Also, little is known regarding how fibrous scaffolds, especially the topologic characteristics, would affect MSCs paracrine function.

Through profiling the important cytokines that are relevant to the pro-angiogenic and anti-inflammatory function of MSCs, our study unambiguously indicates that the fibrous topography provided unique microenvironment that could enhance the paracrine secretion of Ad-MSCs. The in vitro functional assay of the conditioned-media was correlated with the quantitative analysis of the cytokines. The Ad-MSCs anti-inflammatory cytokine secretion on scaffolds was capable of promoting macrophages to demonstrate M2-like phenotype in vivo (Fig.6A, 6C). Similarly, the effect of the CM on the tube formation and endothelial proliferation may be related to the TGF-β, bFGF and VEGF factors observed in the cytokine assay. Compared to other methodologies, the upregulation of PGE2

secretion level which was 233.9±56.3 fold of the MSC-MP group in our study could be significantly higher than the systems involving inflammatory stimuli and 3D culture in the literatures.[73] [95, 98] Another interesting aspect is that the secretion of anti-inflammatory and pro-angiogenic factors were both upregulated by the fibrous scaffolds, whereas the results in favor of only one category of factors were reported. For example, the MSCs cultured on porous scaffolds showed a lowered level of VEGF secretion despite the elevation in the production of PGE2 [98]; the hypoxia condition could only induce angiogenic molecule secretion but not any anti-inflammatory molecule secretion.[99]

Our study showed that the mechanism associated with the topographical effects of scaffolds on MSCs could share a similar down streaming signaling molecules, NFκB, with other methodologies. NFκB signaling pathway but not the JNK-dependent mechanism, has been indicated in the stimulation of MSCs through TNF-α, hypoxia and LPS; it is also a rapid acting factor to regulate of the expression of many genes involved in inflammatory processes. [100, 101] It is therefore reasonable to speculate that the fibrous scaffolds might trigger cellular responses similar to an external inflammatory stimulus. In Fig. 1J, it was observed that the metabolic activity of MSCs was much higher on the EF scaffolds in the first few days and reduced to levels close to the cells on the microplates. The result might be indicative of the dynamic effects of the scaffolds on cells: Upon the contact with fibers, cells responded through adhesion and cytoskeletal reorganization, and the enhanced activity diminished with time. As seen in Fig. 1K, the Oct4 gene in MSCs was upregulated under the influence of the EF scaffolds. The observation suggests that the fibrous topography may also be beneficial for maintaining the stemness of MSCs as well as the relevant cytokine repertoire, as the cells were not committed to a specific cell/tissue type.

More advanced methodologies need to be established to capture the compositional and kinetical characteristics of cytokine release from cells to obtain in-depth understanding of the cell-scaffold interactions.

In our study, it was shown that the fibrous topography not only exhibited the effects on enhancing the paracrine function of MSCs, the cells also exhibited differential responses on three types of scaffolds containing fibers of different orientation characteristics. Among the cytokines examined, the oriented fibers seemed to enhance the expression of PGE2, iNOS and HGF. In the functional assay, the CM derived from the MSC-MEF culture showed potent effects on promoting the anti-inflammatory responses of macrophage cells, showing significant differences compared to the random fibers. On the other hand, the anti-inflammatory function of CM of the MSC-MEF culture was also more significant compared to its pro-angiogenesis function in the assay of endothelial cells. The underlying mechanisms responsible for the function of MEF need to be further understood, given the complicated microenvironment on the MEF scaffold, which induced cell shapes between the round cell shape on REF and the fully stretched cell on AEF. Our results are also comparable to previous studies which showed that the Ad-MSC phenotype, e.g. multipotency and osteogenenic/adipogenic differentiation, may be alterable by substrates affecting cell orientation and shape.[76, 79]

Studying the paracrine function of cells has profound implication for understanding how the cells transplanted in vivo can facilitate the tissue repair/regeneration processes [89, 102], which thereby can shed light on the design principle for scaffold materials. Once transplanted, the exogenous cells may be exposed to a myriad of molecules and cells generating signals to mount reactions that determine the fate of the graft. [103] The cells

may also suffer from hypoxia condition if transplanted at an extra-vascular site with insufficient blood supply.[104, 105] A third complexity may come from the pathological environment involved acute or chronic inflammatory factors in injury. [106] These complex conditions can lead to minimal or transient therapeutic effects of transplanted cells. By applying the CM to the skin wound, it is clearly shown that the repertoire of Ad-MSCs paracrine products derived from the MSC-MEF system did contain therapeutic substances that may benefit tissue regeneration. This result matches the in vitro functional assays in which the pro-angiogenic and anti-inflammatory potency of the conditioned media were observed. Based on our study, the paracrine products of Ad-MSC may have played roles in promoting the skin repair/regeneration through the various pro-angiogenic and anti-inflammatory factors.

One mechanism might be linked to the ability of the CM to modulate the activities of macrophages (Figure 6A, C) in the wound bed toward the resolution of inflammation and repair of tissues.[107, 108] It is known that the wound in the skin of vertebrates can contain the pro-inflammatory macrophages which through cytokine signals (e.g. TNF-α and IL-1β) instruct fibroblasts to produce unorganized collagen, leading to the formation of scar tissue and inadequate regeneration of dermal appendages. [109, 110] It is possible that in our study the MSC-derived PGE2, which was shown increased significantly in vitro, promoted the secretion of IL-10 in macrophages and reduced the secretion of TNF-α and IL-1β, through the activation of the EP4 receptor on macrophages.[23] Also, the TSG-6 secreted by Ad-MSCs, may also attenuate inflammation by decreasing TLR2/NF-κB signaling in resident macrophages.[111] Other beneficial effects of modulating cell-cell communication network through macrophages might include promoting the activity of

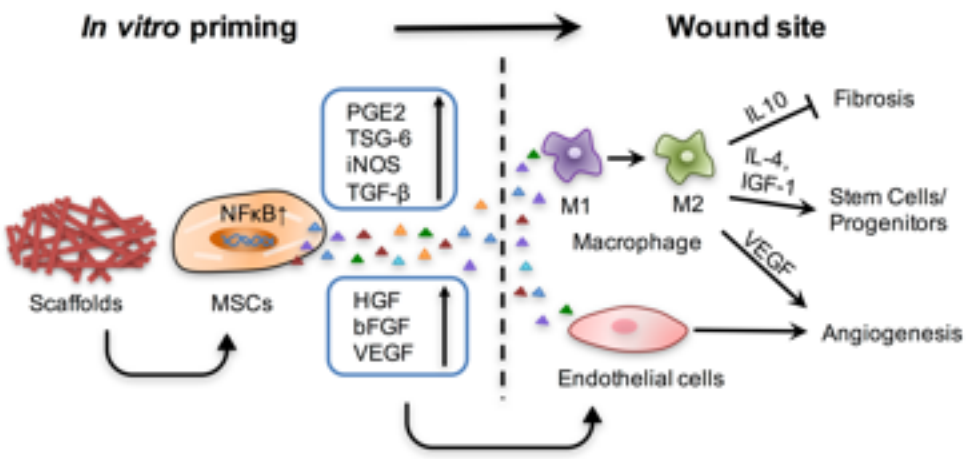

Figure 3.8 Schematic of the MSCs under the influence of scaffolds to generate paracrine products to modulate the cell communication network toward tissue repair/regeneration.

progenitors in the skin wounds, as shown in the studies which suggested the role of macrophages in the differentiation of myoblasts and oligodendrocyte progenitor cells in respective regeneration of smooth muscle and in central nervous tissue.[112]

A summary of the involvement of the scaffold-MSC construct in the cellular communications is depicted in Fig. 7. More studies will be needed to further elucidate relationships in the interplay of scaffolds, transplanted cells and host tissue so that the beneficial effects of the paracrine factors can be controlled and maximized. In particular, extracellular vesicles (EVs) are membrane-surrounded structures released by cells and play important roles in the intercellular transmission of biological signals to regulate immunomodulatory and tissue repair processes. Recent studies have shown that the EVs released by MSCs, including microvesicles and exosomes, have therapeutic effects on tissue injuries, which could be attributed to the protein and microRNA cargoes contained in EVs.[113-116] It was possible that the cytokines examined in this study was also relevant to the EV structures. It will be of great interest to further explore the release of

EVs on scaffolds to gain a mechanistic understanding of how materials may be used to potentiate the function of MSCs.

Lastly, as shown in our study, MSC-derived conditioned medium may be directly developed into therapeutics as regenerative medicine.[117] Compared to cell infusion/transplantation, harvesting secreted products from cells would avoid introducing live cells into the body, and allow for more convenient control of the dosage and storage of the therapeutic substance. The studies on the use of CM of MSCs for treating various diseases increased rapidly in recent years [117-119], including the development Ad-MSC CM for hair follicle regeneration [120] and wound healing in human [121]. On the other hand, it is a great challenge to establish the regulatory policies to address the quality, safety and efficacy of this new category of therapeutics containing mixed components. As mentioned above, isolating the EVs in the CM is a promising direction; however, the markers and components of EVs should be profiled and the reproducibility and consistency of the products be established to ensure the quality.[122-124] With the regulatory consensus, the design of the in vitro culture condition and exploration of the function of fibrous scaffolds would then provide approaches to improve the therapeutic efficacy of CM-derived products.

CHAPTER 4. DESIGN OF EXOSOME-LOADED SCAFFOLDS FOR REGENERATIVE IMMUNOMODULATION

The immune system has been identified as a key mediator in tissue regeneration by playing critical roles in angiogenesis, fibrosis and tissue remodeling. Implantation of designer scaffold materials can involve both innate and adaptive immunity which could potentially be manipulated to generate pro-regenerative tissue responses. Mesenchymal stromal cells (MSCs) provide promising repair/regenerative modalities in many diseases through their paracrine products, and the exosomal secretion by MSCs in particular exhibits the immunomodulatory properties by targeting a broad spectrum of immune cells. Here, we developed a method to create electrospun fibrous scaffolds bound with MSC exosomes and investigated the immunomodulatory function of the new biological materials as cell-free constructs for tissue regeneration. The fibrous scaffolds were fabricated with morphological features to attract immune cells and the MSC exosomes were utilized to further educate the recruited cells towards pro-regenerative immune reactions. The results showed that exosomes were efficiently loaded onto the poly(ethylamine)-modified electrospun fibers and the electrostatic binding between exosomes and the scaffold allowed the uptake of exosomes by macrophages which were induced with M2-like phenotypes in vitro. In the immunological analyses post-implantation, local M2-biased responses at the implantation site and remote Th2 immune responses and increased population of regulatory T cells in the lymphatic tissue or spleen were observed in a wound healing model. The results suggested the immunomodulatory function of MSC exosome-loaded scaffolds and

the design of functional synergy between exosomes and materials presented a new paradigm to promote tissue regeneration.

4.1 Introduction

Immune systems are best known for the role of first line against pathogens. They were also responsible for tissue development, homeostasis, and tissue repair/regeneration. Varieties of immune cell types are proved to be involved in the process of tissue repair.[112] Through their behavior of phagocytosis, timing of present and retreat, shifting of cytokine secretion, the immune cells construct an integrated environment to impact the key events of tissue repair/regeneration, including stem/progenitor cell proliferation/differentiation, angiogenesis, tissue remodeling.[125-128] Macrophages are most well studied immune cells that could mediate different stages of tissue repair post injury due to their highly programing possibilities.[3, 129] The pro-inflammatory M1 macrophage are responsible for debris clearance, but long-lasting M1 response will lead to chronic inflammation and impair healing. Macrophage shift towards reparative M2 macrophage has been identified as a signature event presenting a benign tissue repair in heart, muscle, neuron etc. post injury.[1, 130-132] Recent studies showed the adaptive immune cells also participates in tissue repair, especially the T cells.[133] Regulatory T cells (Tregs) are able to secreting immunomodulatory cytokines, such as IL-10 and TGF-β, that skew macrophage towards M2 phenotype as well as growth factors, such as amphiregulin, that directly induce the proliferation and differentiation of tissue resident progenitor cells thus favor tissue regeneration.[8, 11, 14] CD4+ T helper 2 (Th2) secrete IL4 and IL10 to cross talking with innate immune cells such as macrophage and favor tissue repair.[16, 17] Whereas CD8+ T

cells and CD4+ T helper cells are considered to promote inflammation and negatively influence reparative process.[18]

Mesenchymal stromal cells (MSCs) is the most widely-used stem cell type in clinical applications aimed at tissue repair and immunomodulation, achieved by their strong secretion capacities.[134] Due to the versertile bio-functional components harbored in the MSC secretome, MSCs have the ability to target and modulate the behavior of many immune cell types, such as convert macrophage towards M2 phenotype, inhibit DC maturation, suppress differentiation of B cells and effector T cells, increase Treg population, induce Th2 immune response and suppress NK cell activity etc.[135, 136] Exosomes are membrane-surrounded nano-vesicles released from MSCs shuttling cargos of proteins and RNA as important intercellular messenger, assembling similar immunomodulation properties of MSCs.[137-142] MSC exosomes have been used as substitute of live cells and showed equivalent immunomodulatory functions and therapeutic effects as cell transplantation in many tissues.[113, 116, 143] Moreover, exosomes relieve the safety risk brought by live cell transplantation, meanwhile could be easily stored and transported. Therefore, MSCs exosomes are potent candidate for regenerative immunomodulatory material design.

With the knowledge how the immune system greatly influences the process of tissue repair/regeneration, tuning immune system towards pro-regenerative state based on the criteria of immune response for specific tissue to heal properly is a new realm for regenerative medicine. Many studies have tried to manipulate the behavior of macrophage by utilizing the physicochemical properties of the biomaterials or using biomaterials as a delivery tool for immune modulators. As the adaptive immune response, especially the T

cells, were identified as key participants in tissue regeneration other than innate immune cells, immunoactive biomaterial design to crosstalk with broader spectrum of immune cells and generate new pro-regenerative immune events are of great promises that has hardly been explored. Recently, the extracellular matrix (ECM) bio-scaffolds were shown to drive reparative microenvironment in the traumatic tissue injury and this process is dispensable of T helper 2 cells participation. This study has exhibited the power of nature-derived biomaterials to generate adaptive immune response for promoting tissue regeneration.[144] Therefore, to further design the immunomodulatory biomaterials, especially synthetic materials, and explore their role in both innate and adaptive immune response in vivo for tissue regeneration is of great interest and importance.

Electrospinning has the advantages of the convenient fabrication process, the wide choice of materials and the precision control over fiber parameters and architectures, thus provide an easy and quick tool box for regenerative immunomodulatory material design. The architectural and topographical cues of scaffolds influence immune cell activities, such as adhesion, proliferation, or secretion profiles. In particular, the fiber orientation, diameter of EFs and the pore size of the EF membranes have been found to regulate macrophage recruitment and phenotype commitment differently. [145, 146] Physiochemical properties, such as surface charge and hydrophilicity or bio-functional molecule introduced by blend electrospinning or surface modification are also modalities of EFs to modulate immune system both in vitro and in vivo. Moreover, EF scaffolds have the structure assembling the natural ECM and have been assessed as useful platforms for designing functional wound-dressing materials. However, the studies mainly focused on EF scaffolds as a delivery tool and substrate for cell infiltration but neglect their intrinsic immunomodulatory properties

when aiding wound healing.[147-150] Indeed, the immune response towards implanted EF scaffolds are inevitable and the involved subsets of immune cells can thus be targeted and manipulated for immune-mediated tissue regeneration through materials design.

Here we developed a MSC exosome loaded EF scaffolds for regenerative immunomodulation in the wound healing model. We hypothesized that the EF scaffolds would recruit immune cells to the transplant site due to foreign body reaction in vivo; the recruited immune cells will then receive the immunomodulatory signals from the MSC exosomes and generate immune environment that favor the tissue repair/regeneration. Through series of chemical modification, micro- polycaprolactone (PCL) EFs were covalently conjugated with polyethylenimine (PEI) to passively load exosomes through static interaction. The exosome loaded PEF (Exo-PEF) were then applied to a wound healing model in vivo and the immunomodulatory properties of the innate and adaptive immune response were evaluated in both local sites and remote lymphatic organs. Our study suggests the designed exosome loaded EF biomaterial system have active immunomodulatory properties in vivo and resulted in adequate immune cell subtypes with phenotype that have been identified as positive role in immune-mediated regeneration. By exploring the adaptive immune response in the lymphatic organs, this study also brings new angles, that worth considering for regenerative immunomodulatory material design in the future.

4.2 Materials and Methods

4.2.1 Materials and reagents

Ultrapure water ⩾18 MΩ was derived from deionized water though a Milli-Q system (Millipore, Billerica, MA). Polycaprolactone (PCL) and lipopolysaccharide (LPS) were obtained from Sigma-Aldrich (Milwaukee, WI). TRIzol kit, Dulbecco's phosphate buffered saline (DPBS), PRMI mdium, DMDM medium and other cell culture reagents were purchased from Invitrogen (Carlsbad, CA, USA) unless otherwise specified. 4',6-diamidino-2-phenylindole (DAPI) and Rhodamine Phalloidin was obtained from the ThermoFisher (MA, USA). Human umbilical vein endothelial cells (HUVECs), Endothelial cell medium (ECM), endothelial cell growth supplement (ECGS) and were purchased from ScienCell (Carlsbad, CA). Mice bone marrow mesenchymal stromal cells (BM-MSCs) and it's culture medium basal medium were purchased from Cyagen Biosciences Inc (Santa Clara, CA, USA). The murine-macrophage cell line RAW 264.7 were obtained from the Cell Culture Center of the Institute of Basic Medical Sciences (Beijing, China). Tumor necrosis factor-alpha (TNF-α), macrophage colony-stimulating factors (M-CSF), interleukin 4 (IL4) were purchased from Peprotech. (Canada) Suppliers of other chemicals, biological reagents, and equipment are specified below. The flow cytometry antibodies and reagents were purchased from Biolegend (US) uless otherwise specified.

4.2.2 Cell culture

All cells were cultured at 37°C under humidified atmosphere with 5% CO2. The BM-MSCs were cultured in basal medium supplemented with 10% fetal bovine serum (FBS), 0.4% penicillin/streptomycin (P/S). The BM-MSCs between passage 5 and 9 were used for the following experiments. The human umbilical vein endothelial cells (HUVECs) were

maintained in endothelial cell medium (ECM) supplemented with 5% FBS, 1% (P/S) solution and 1% ECGS. RAW264.7 macrophages (MΦ) were cultured in DMEM supplemented with 10% FBS and 1% P/S. Macrophage isolated from bone marrow of Balb/c mice were cultured in PRMI supplemented with 0.25mM beta-mercaptoethanol, 1 × non-essential amino acid, 10% heat inactive FBS (FBS incubated at 56℃ in water bath for 30mins), 1% penicillin & streptomycin and 20ng/mL G-CSF. To detach cells from the culture plates, BM-MSCs and HUVECs were treated with trypsin/EDTA solutions, while macrophages were pipetted repeatedly to induce the detachment.

4.2.3 Isolation and identification of BM-MSC exosome

BM-MSCs at 80% confluent in cell culture flask were cultured in serum-free medium for 24 hours to collect the supernatant. The supernatant was centrifuged at 1,200 g for 15 min, followed by 10,000 g for 30min to remove cell debris and apoptotic bodies. The exosomes were precipitated by ultra-centrifuged at 100,000 g for 1h, and was washed twice with PBS. The precipitated exosomes were resuspend in 200 μL PBS, stored in -80 °C until use. The protein content of collected exosomes was measured by micro BCA protein assay kit (Thermo Fisher). The collected exosomes were fixed with 4% paraformaldehyde (PFA), stained with 2% (w/v) uranyl acetate for 5 mins, washed 3 times with DI water and the exosomes morphologies were observed by transmission electron microscopy. (Tecnai G2 T20) The size and zeta potential distribution of exosomes were identified by Zetasizer (Brookhaven Instruments). To identify exosomes, 10 μg exosomes were covalently conjugated onto 4-μm aldehyde/sulphate latex beads for 15min. The excess aldehyde group were blocked by excessive 100 mM glycine for 30 min. The exosome-beads were stained

by exosomal markers CD63/CD9 and according isotypes and analyzed by BD Aria flow cytometer. For mass spectrum, exosomes were lysed in lysing buffer (6% SDS, 200 mM DTT, 200 mM Tris-HCl, pH 7.6.) at 95°C for 5 min followed by filter aided sample preparation (FASP).

4.2.4 Fabrication and characterization of BM-MSC exosome-loaded PEI modified electrospun fibrous (Exo-PEF) scaffolds

Electrospun fibrous (EF) scaffolds were prepared from polycaprolactone (PCL) solution. 21% w/v PCL was dissolved in a mixture of CHCl3 and dimethylformamide at the volume ratio of 9:1. After stirring for 3 h until PCL was completely dissolved, the solution was loaded into a syringe with a blunt-ended stainless 21G steel needle. The feeding rate and the applied voltage were controlled at 2 mL/h, 10kV, respectively. The EF was collected on a flat steel plate covered with foil paper at a distance of 14cm from the needle tip. Sodium hydroxide treatment was employed to enhance the PCL EF hydrophilicity and induce carboxyl group to the EF for further modification of poly(ethylamine) (PEI). PCL EF scaffolds were immersed in the mixture of 1M aqueous sodium hydroxide solution and 75% ethanol solution (v/v) at the ratio of 1:1 for 30mins with gentle agitation at room temperature. After hydrolysis, the scaffolds were washed with large volume of DI water.

To covalently modify PEI to the EF, sodium hydroxide treated PCL EF was rinsed in 0.1M 2-Morpholinoethanesulfonic acid (MES) buffer, pH 5.1. 1-ethyl-3-(3-dimethylaminopropyl) carbodiimide hydrochloride (EDC) (Pierce Biotechnology Inc.) and water soluble sulfo N-hydroxysuccinimide (Sulfo NHS) (Pierce Biotechnology Inc.) were

dissolved in ice cold 0.1M MES buffer and added dropwise to the EF. EDC activation was done for 2h on the shaker at room temperature. 70 kDa branched PEI (Macklin, Shanghai, China) was diluted in 0.2 M MES buffer, pH 6.5. Activated PCL EF were transferred to the PEI solution incubated for another 2h at room temperature on an up-down rotator. PEI-conjugated EF (PEF) were washed 4 times in excess 1 M NaCl to remove physically adsorbed PEI. To confirm the success of PEI conjugation, 2,4,6-Trinitrobenzene sulfonic acid (sigma) (TNBSA) assay were performed to detect the existence of amine group on the surface PEF by forming of a highly chromogenic (orange) product. The TNBSA assay were also performed in the solution that rinsed PEF overnight to confirm fully removal of unbound PEI.

The water contact angles of the PCL EF scaffolds before and after PEI modification were measured at room temperature and 60% relative humidity, using sessile drop method on a contact angle analyzer (USA Kino Industry Co., Ltd). For sterilization, EF membranes were rinsed with 75% ethanol solution for 30 mins and then washed with sterilized DI water for three times and air dried in bio-safety cabinet (Thermo, Germany). The EF scaffolds were exposed under ultraviolet radiation for 30 min on each side in the bio-safety cabinet for further sterilization and were kept in sterile dishes at 4°C until being used. Up to 30 μg BM-MSC exosomes were dissolved in 1mL PBS, added to manually tailored 12mm diameter PEF, rotating for 30 min at 4°C. The loading capacity of PEF were determined by protein content remained in the PBS after exosome loading. The loaded exosomes were determined by the difference between the protein content before and after loading. The morphology of EF in each step was characterized by scanning electron microscopy (SEM) (Quanta FEG450, FEI, US).

4.2.5 HUVEC proliferation assay

To determine the change of cell adhesion properties of EF after series of chemical and biological modification, HUVECs were seeded on PCL EF, NaOH treated PCL, PEF and Exo-EF (10 μg), with HUVEC cultured in microplates supplemented with or without exosomes (10 μg) as a control. After 24 h, cells were fixed in 2% PFA and stained with 0.5 μg/mL DAPI for 10 min. Fluorescence images fully covering the microwell/EF were captured by an IX71 fluorescence microscope (Olympus), and the number of cells in each well was counted by ImageJ software.

4.2.6 Trans-well system

The exosomes were incubated with 0.1mM DiI, washed with PBS for three times to remove excessive dye. A trans-well microplate with pore size of 0.4 μm that allow substance transfer but avoid cell-material contact between upper and lower chambers was used. The exosomes/Exo-EF were placed on the upper chamber and 2×105 macrophage RAW264.7 was seeded in the plate in the lower chamber. Exosomes that directly added to the macrophage or macrophage seeded on the Exo-EF membrane were used as a control.

4.2.7 Macrophage gene and secretion profile

Bone marrow cells from femurs and tibias from mice were harvested and cultured in RPMI medium, supplemented with 0.25mM beta-mercaptoethanol, 1 × non-essential amino acid, 10% heat inactive FBS (FBS incubated at 56℃ in water bath for 30mins), 1% penicillin & streptomycin and 20ng/mL G-CSF. Medium was changed every other day. On day 7, the bone marrow-derived macrophage (BMDM) was stained by F4/80 antibody and

analyzed by flow cytometry to determine the differentiation of BMDM. BMDM were then detached and seeded onto PCL EF, PEF and Exo-EF (10 μg exosomes) or 48-well microplate supplemented with or without 10 μg exosomes at the density of 2×105 per scaffold/microwell. BMDM were classically activated with LPS (100 ng/ml, Sigma-Aldrich L2880). Supernatant was harvested at 24 hours post-seeding, TNFα and IL10 were in the supernatants were determined by ELISA assay. Cells were treated with TRIzol kit and total RNA was extracted, reverse transcribed with TransScript First-Strand cDNA Synthesis SuperMix (Transgene, Beijing, China) The gene expression levels were analyzed using the SYBR Green real-time PCR method and quantified using the Bio-Rad CFX connect real time PCR system (Bio-Rad, Hercules, CA). Primers were ordered from Sangon (Shanghai, China). The sequences of primers for qRT-PCR were listed in Table 1 in the supplementary information (Supplementary Table 1). All gene expression values in one sample were normalized to the beta-actin level. Relative expression was calculated using the comparative Ct method. The mean minimal cycle threshold values were calculated from triplicate reactions.

4.2.8 In vivo imaging of exosomes

The exosomes were incubated with 10 nM DiI, washed with PBS to remove excessive dye. The DiI labeled exosomes were either directly injected or loaded onto PEF and implanted to the abdomen of mice subcutaneously. The biodistribution of exosomes in live mice under isoflurane anesthesia, was determined using an IVIS 200 Optical Imaging System (Xenogen, Caliper Life Sciences). All mice were imaged with identical instrument settings with excitation wavelength at nm, emission wave length at nm.

4.2.9 Mice wound excisional model

All procedures were performed in accordance with the regulations approved by the Institutional Animal Care and Use Committee (IACUC) of Peking University. Balb/c female mice (Vitalriver, Beijing, PR China) weighing at 10-week old were anesthetized; two 8-mm diameter round full-thickness excisional skin wounds were created using a biopsy puncher following the hair removal from the dorsal skin. The PCL EF, PEF and Exo-EF (30 μg exosomes) with 12mm diameter were implanted subcutaneously at the injury site. For exosome group and PBS wound control group, 200uL exosomes (30 μg) in PBS or blank PBS were injected subcutaneously around the wound. Finally, a Tegaderm (3M, MN, USA) was placed over the wounds to keep the wounds clean and avoid contamination. Digital photographs of the wounds were taken at day 0, 3, 7, and the wound area measured by the ImageJ software. The percentage of the wound closure was calculated as: (area of original wound - area of actual wound) / area of original wound × 100%.

4.2.10 Histology and immunostaining

Mice were sacrificed at day 7 or day 14. The skin tissues including the wound and the surrounding skin were harvested and was cut into two parts from the middle line for histology observation. The dermal specimens were then fixed with 4% PFA, embedded in paraffin and cut into sections with thickness of 5 μm. The sections were stained with hematoxylin and eosin (H&E) or Masson's trichrome (MT), imaged using a light microscope (Olympus, Japan).

4.2.11 Immunomodulation assay of Exo-PEF in vivo

For immunomodulatory properties of Exo-PEF in vivo, The PCL EF, PEF and Exo-EF (30 μg exosomes) with 12mm diameter were first implanted to the naïve mice. A scission and a pocket was made, and materials were subcutaneously implanted at the abdomen of the naïve mice. Exosomes (30 μg) and PBS were injected subcutaneously as control groups. Scission and pocket were in all mice. At day 14, mice were sacrificed, inguinal lymph nodes, spleen and implant sites were harvest. To get single cell suspension for flow cytometry assay, lymph nodes were minced and flushed with PBS (with 2% FBS) with a 70 μm filter beneath; spleen were cut into pieces, digested in collagenase D (2mg/mL, Roche) for 30 min, minced and flushed with PBS (with 2% FBS) with a 70 μm filter beneath, followed by RBS lysis treatment (Biolegend); implant sites were scraped to remove fat tissue, cut into pieces and incubated in digesting buffer (100ug/mL Liberase TM (Roche), 1mg/mL collagenase D (Roche), 1mg/mL hyaluronidase (Sigma) in OptiMEM (invitrogen)) for 1.5h at 37 °C on a shaker, minced and flushed with PBS (with 2% FBS) with a 70 μm filter beneath.

To explore the immunomodulatory function of Exo-PEF in a disease model, wounds were created and materials were implanted as mentioned above. The skin of healthy mice and wounds injected with PBS were used as controls, designated as HC and WC, respectively. Mice were sacrificed and the wound sites, LN and spleen were harvested at Day3, 7 and 14. Single cell suspension were prepared as described above.

For flow cytometry staining, samples first went through FC blocking with anti-mouse CD16/32 for 5mins, then stained with fluorescent antibodies CD3, CD4, CD11c, CD25, F4/80, CD86. After fixation, samples were treated with intracellular staining permeabilization wash buffer, stained intracellularly for Foxp3, CD206. For intracellularly

staining of cytokines IL4, IFN-γ, IL10, TNF-α, samples were incubated with Brefeldin A for 4 h before all staining steps.

4.2.12 Statistical analysis

Quantitative results were presented as means±standard deviation (SD). Statistical comparisons were performed by one-way analysis of variance (ANOVA) followed by Holm-Sidak tests to compare selected data pairs. Values of $P < 0.05$ were considered statistically significant.

4.3 Results

4.3.1 Preparation of exosome loaded electrospun fiber scaffolds

MSCs exosomes were visualized by TEM and the classic "cup-shaped" morphology were observed. (Fig. 4.2 A). The zeta potential and size of the exosomes were measured by DLS. The result showed MSC exosomes we collected has a diameter varied from 50 nm to 100nm approximately. The zeta potential of exosomes was around negative 30mV (Fig. 4.2 B), witch allowed the further coupling of exosomes to the PEF through static interaction. The unmodified EF (UEF) were modified with PEI for two purpose: first is to improve the hydrophilicity of the EF for better cell attachment; second is to introduce positive charge for coupling of exosomes. Newly synthesized PEF were rinsed in the PBS upto 48 hour and no amine groups could be detected in the rinsed PBS by TNBSA assay, which proved the excessive PEI were thoroughly removed. (Supplementary Fig. 2A)

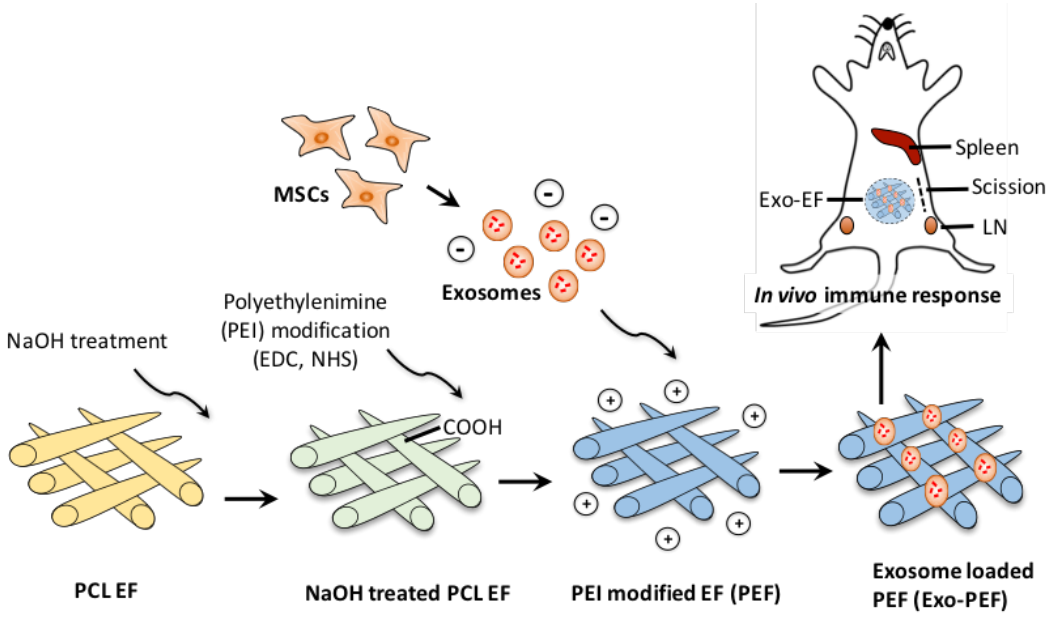

Figure 4.1 Unmodified PCL electrospun fiber (UEF) were first treated with NaOH to generate carboxyl group on the EF surface. The PEI were then covalently conjugated to the EF through reaction between carboxyl group and amine group, designated as PEF. Exosomes isolated from MSCs supernatants were then loaded to the PEF through static interaction, designated as Exo-PEF. The Exo-PEF were transplanted to either healthy mice or in wound healing model of mice to study the regenerative immunomodulation in transplant site/wound site, spleen, and inguinal lymph nodes (LN) driven by Exo-PEF. The UEF and injection of exosomes and PBS were served as controls.

On contrary, the PEF showed the color reaction in TNBSA assay (data not shown), indicating the conjugation of PEI to the EF. The UEF and PEF morphology and diameter were shown in figure 4.3 A, and no significant change in EF morphology were observed before and after PEI modification. However, the hydrophilicity of the EF was significantly improved by modification of PEI. (Fig. 4.3 B) The PEF could load up-to 30 μg exosomes in terms of protein content per cm2, significantly higher compared to the maximal exosome loading capacity of UEF, which is around 0.5 μg per cm2. (Fig. 4.3 D) When rinsing Exo-PEF in the PBS, the loaded exosomes were not released up-to 72 hours determined by microBCA protein content measurement. (data not shown) The exosomes labeled with red

A

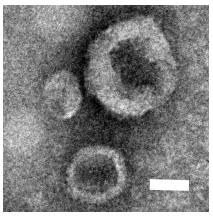

B

	Exosome
Size (nm)	76.67±25.35
Zeta potential (mV)	-30.80±9.82

Figure 4.2 A, SEM imaging of BM-MSC exosomes. Scale bar indicates 50 nm. B, Size and zeta potential of BM-MSC exosomes

fluorescence DiI could be visualized by the confocal imaging, showing exosomes were distributed along the electrospun fibers. (Fig. 4.3 C) The SEM imaging also showed roughness change of the fiber (Fig. 4.3 C) surface compared with UEF and PEF shown in figure 4.3 A. To confirm the series of modification to EF had improved the surface properties for better cell engraftment, human umbilical vascular endothelial cells (HUVEC) were seeded on the EF and showed improvement cell proliferation on Exo-PEF compared to UEF. (Supplementary figure 5)

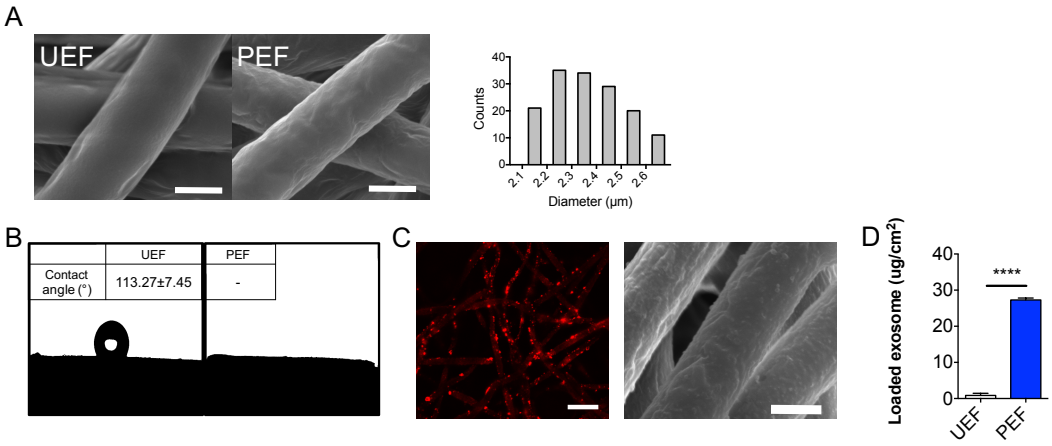

Figure 4.3 A, the SEM morphology of UEF, PEF and the fiber diameter distribution of PEF. Scale bar indicates 2μm. B, Water contact angle of UEF and PEF. C, Confocal imaging of DiI-labeled BM-MSC exosomes (red dots) loaded onto PEF. Scale bar indicates 20μm. SEM imaging of Exo-PEF. Scale bar indicates 2μm. D, Maximum exosome loading capacity of UEF and PEF.

4.3.2 Macrophage up-taking of exosomes and phenotype on Exo-PEF in vitro

To explore the immunomodulatory properties of Exo-PEF, we first studied the interaction between Exo-PEF and macrophage in vitro. To reveal how exosomes loaded to the PEF would be taken-up by macrophage, a transwell system were adopted that allow exosome and medium exchange but not cell infiltration between upper and lower chambers. The result showed that the macrophage taking exosomes on Exo-PEF is contact-dependent, as no fluorescent exosomes could be detected in macrophage once separate the cells with

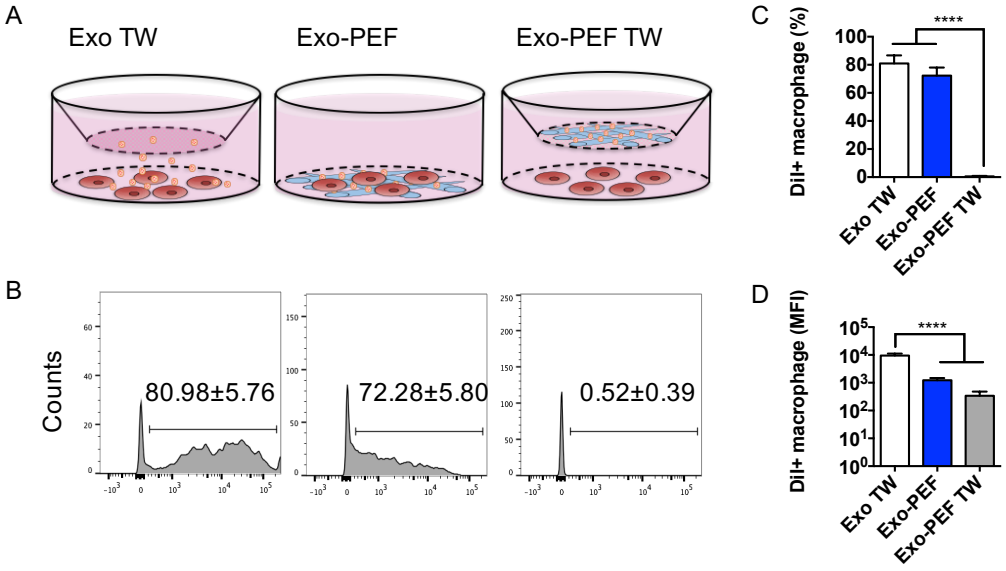

Figure 4.4 Exosome uptake by macrophage on Exo-PEF. A, Schematic of trans-well system. Free exosomes and Exo-PEF were placed in the upper chamber of the trans-well and DiI labeled macrophages were seeded on the lower chamber or directly on the Exo-PEF. B, Representative gating of DiI+ macropahge. C, D, Percentage and MFI of DiI+macrophage. n=6, *P<0.05, **P<0.01, ***P<0.001, ****P<0.0001.

Exo-PEF in different chamber. (Fig. 4.4 A-C) Though the percentage of exosome+ macrophage was equivalent between Exo-TW group and Exo-PEF, the MFI of Exo-PEF group was significantly lower than Exo TW group. It could be explained that the exosomes were distributed all over the surface of the fibers, which has a much larger area compared

to microplate well, and thus decreased the chance for macrophage to encounter the exosomes.

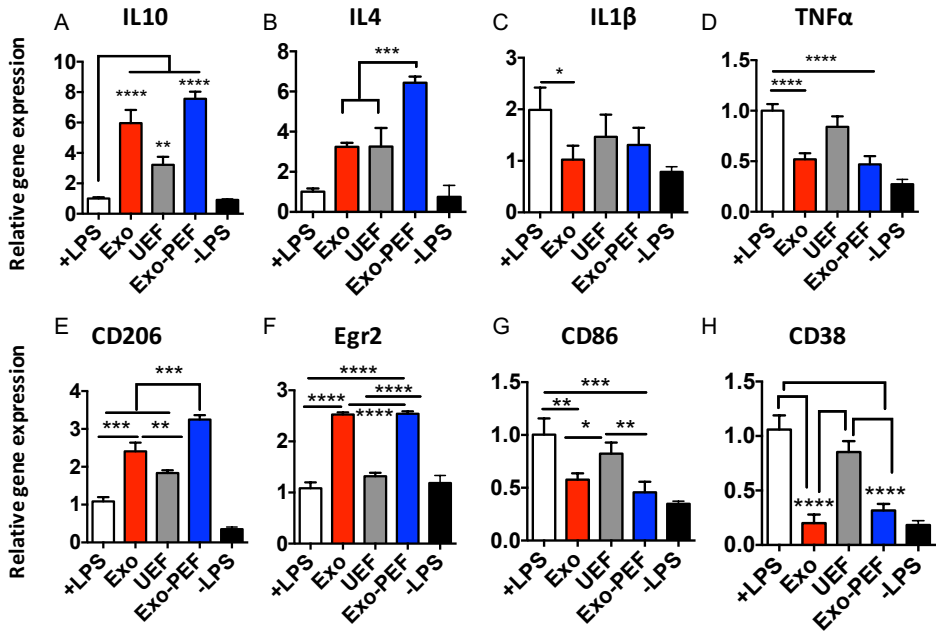

Figure 4.5 Macrophage phenotype on Exo-PEF in vitro. Bone marrow derived macrophage (BMDM) were stimulated with LPS and seeded on the UEF, Exo-PEF or on the microplates supplemented with exosomes. The +LPS and –LPS were served as controls. The graphs showed BMDM gene expression level of anti-inflammatory cytokines IL10 (A) and IL4 (B), pro-inflammatory cytokines IL1β(C) and TNFα (D), macrophage M2 markers CD206 (E) and Egr2 (F), macrophage M1 marker CD86 (G) and CD38 (H). n=4, *P<0.05, **P<0.01, ***P<0.001, ****P<0.0001.

To determine the macrophage phenotype on the Exo-PEF, bone marrow derived macrophage (BMDM) were stimulated with LPS and then seeded on the EF or on microplates supplemented with exosomes. The gene expression of cytokine profile and macrophage surface markers were then examined. The anti-inflammatory cytokine IL10 and IL4 gene expression of BMDM were upregulated by 4~9 fold when treated with exosome or seeded on UEF and Exo-PEF compared to LPS+ control. Especially, Exo-PEF are significantly more potent at upregulating IL4 gene expression compared UEF and

exosome alone. The pro-inflammatory cytokine IL1β and TNFα were downregulated by around 2 folds and only Exo and Exo-PEF group had significant difference compared to LPS+ alone. (Fig. 4.5 A-D) The Exo and Exo-PEF group also upregulated the M2 marker CD206, Egr2 gene expression and downregulate the M1 marker CD86 and CD38 gene expression compared to LPS+ group and UEF group with significance. (Fig. 4.5 E-H)

4.3.3 In vivo immunomodulatory properties of Exo-PEF

As we have shown that the UEF and Exo-PEF were able to modulate macrophage phenotype in vitro, we then move on to in vivo transplantation to study the macrophage recruitment and phenotype commitment in healthy mice without immune background brought by disease. The Exo-PEF were subcutaneously transplanted in the abdomen of mice. The result has proved our hypothesis that more macrophages were recruited to the transplant site due to the presence of EF (Fig. 4.6 A). The Exo-EF has recruit even more macrophages compared to UEF, probably due to the chemokines carried by exosomes. The phenotype of these recruited macrophages were analyzed based on CD86 and CD206. Interestingly, both UEF and Exo-EF has higher numbers of CD206+ M2 macrophage compared to control and Exo group. (Fig. 4.6 C) However, the Exo-PEF has less CD86+ M1 cells compared to UEF (Fig. 5B). By calculating the M2/M1 ratio, the Exo-PEF showed a significant M2 biased immune response, compared with control and UEF, which is similar to Exo group (Fig. 4.6 D).

The crosstalk between adaptive immune response and innate immune response together contribute to the building of the immune environment for tissue regeneration. To this end, the innate and adaptive immune response happened in the lymphatic organs were

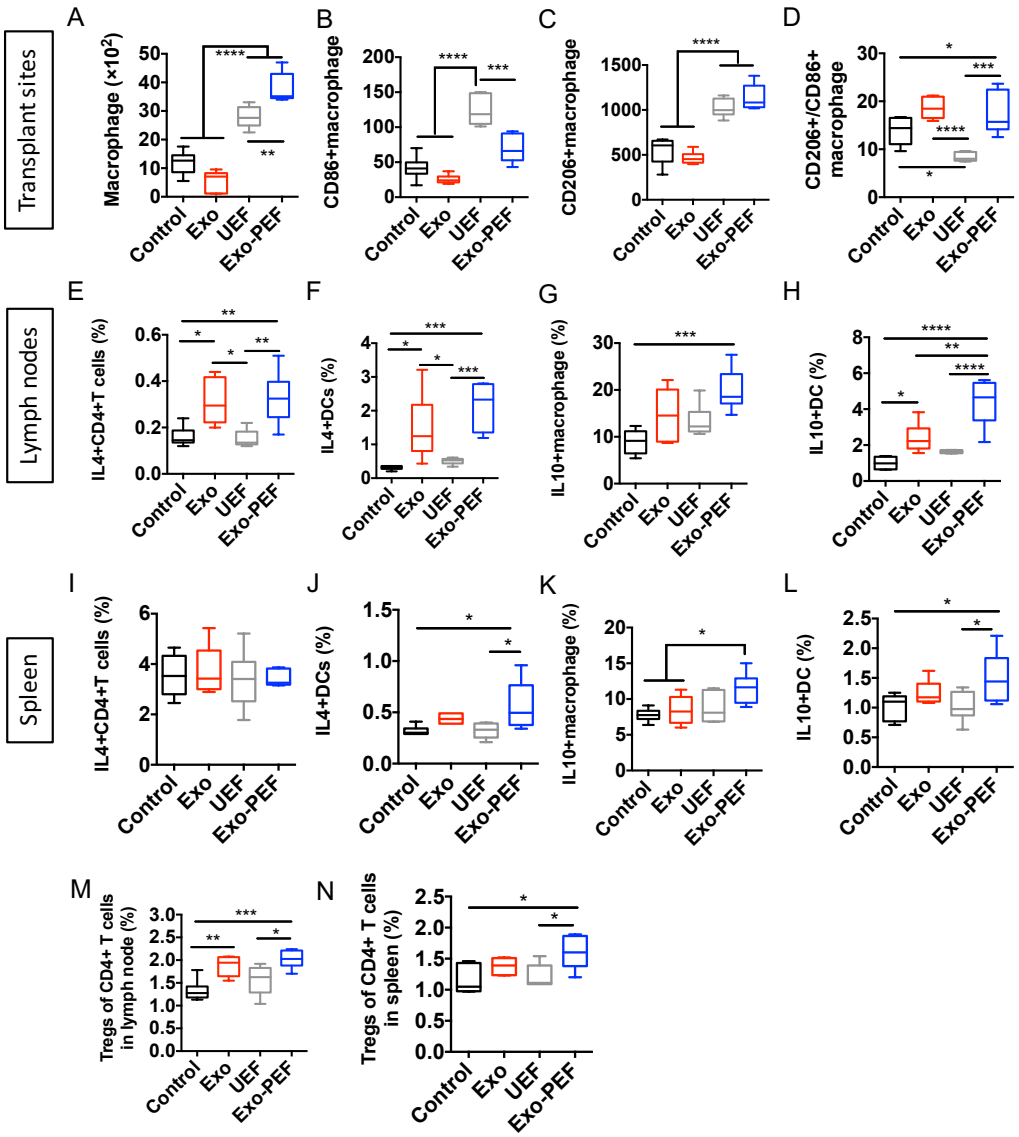

Figure 4.6 Immunomodulatory properties of Exo-PEF in vivo. UEF and Exo-PEF were subcutaneously transplanted to the abdomen of the healthy mice trough a thin scission. Exosomes in PBS or PBS alone were injected subcutaneously as control groups. The scission was made for all groups regardless of EF transplantation. At day 14, mice were sacrificed and immune response in transplant site, inguinal lymph nodes and spleen were analyzed. The graphs showing total macrophage number (A), CD86+M1 macrophage (B), CD206+M2 macrophage (C) per 10^5 cells and the M2/M1 ratio (D) in the transplant sites. In the lymph nodes, IL4 secreting CD4+T cells (E), DCs (F), IL10 secreting macrophage (G) and DCs (H) were analyzed. In the spleen, IL4 secreting CD4+T cells (I), DCs (J), IL10 secreting macrophage (K) and DCs (L) were analyzed. The Tregs population gating based on CD25+Foxp+ CD4 T cells in the lymph nodes (M) and spleen (N) were analyzed. n=6. *P<0.05, **P<0.01, ***P<0.001, ****P<0.0001.

also examined. In the inguinal lymph nodes, a Th2 immune response were observed in Exo and Exo-PEF group, as shown in the figure 4.6 E that population of IL4 secreting CD4+ T helper cells were significantly higher than control and UEF group. We also observed the Exo-PEF could induce higher percentage of IL4 secreting dendritic cells (DCs), L10 secreting DCs and macrophages in the lymph nodes. (Fig. 4.6 F-H) In the spleen, IL4 secreting CD4+ T cells were not significantly different between groups. Only the percentage of IL4 secreting DCs, IL10 secreting DCs and macrophages in Exo-PEF group were higher compared to the other groups. The percentage of regulatory T cells (Tregs) were significantly higher in Exo and Exo-PEF group in the lymph nodes (Fig. 4.6 M), but only Exo-PEF showed significant higher number of Tregs compared to control and UEF (Fig. 4.6 N)

4.3.4 Immunomodulatory properties and therapeutic efficacy of Exo-PEF in wound healing model

With previous results showing that the Exo-PEF have the properties to modulate the macrophage towards regenerative M2 both in vitro and in vivo, meanwhile drove Th2 immune response and more Tregs in the lymphatic organs. The next question we ask is that could the observed immune response brought by Exo-PEF be transferred to the wound healing model and modulate the immune response regardless of the intrinsic immune response driven by the injury. The skin full excisional wound model were established on the Balb/c mice. UEF, Exo-PEF were applied to the wound and exosome or PBS were injected to the wounds as controls. Mice were sacrificed and analyzed for the immune response in transplant site at day 3, 7 and 14 and lymphatic organs at day 7 and 14. First of all, the trend of macrophage migration and retreat on time axis post injury were observed

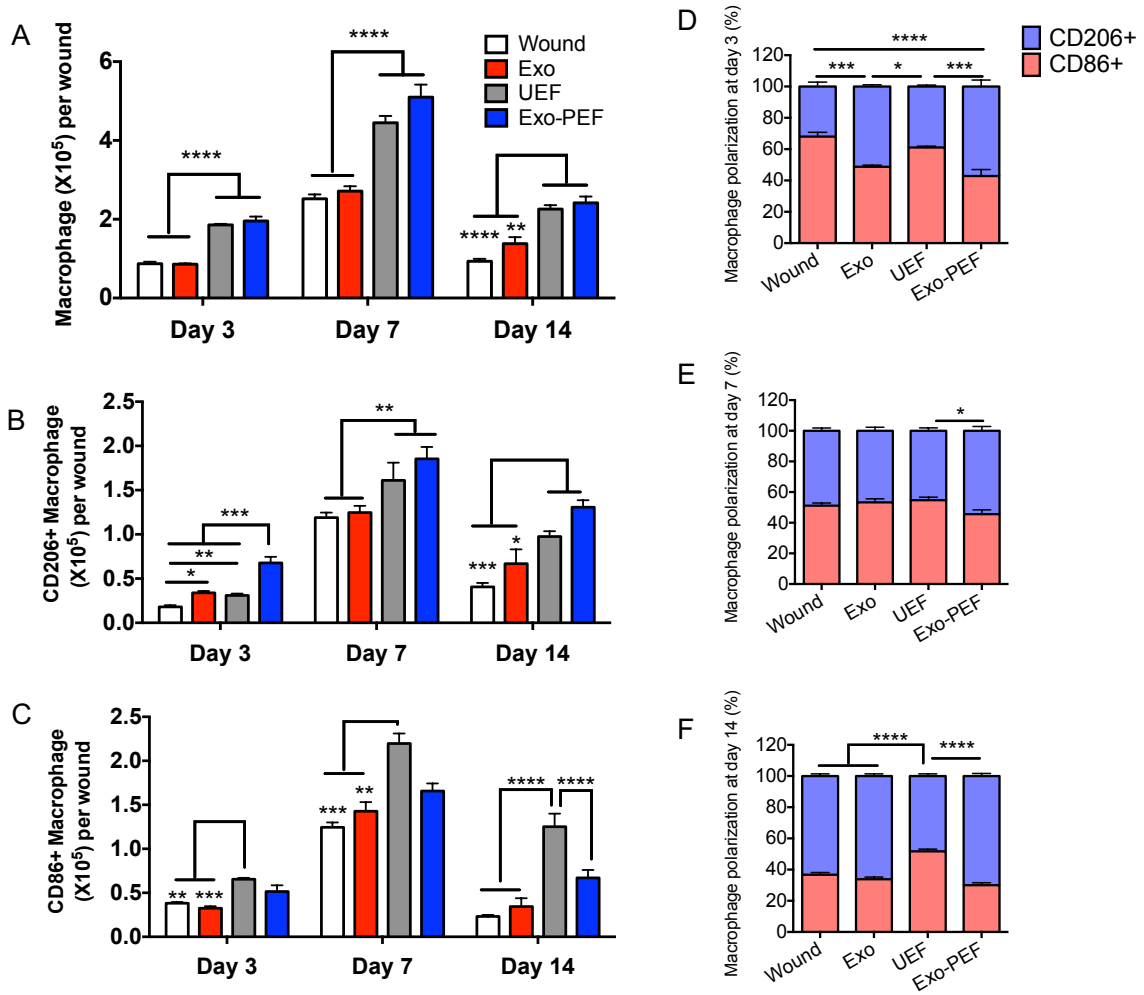

Figure 4.7 Macrophage recruitment and phenotype in wound healing model. Skin full excisional wounds were created on the Balb/c mice, UEF and Exo-PEF were applied to the wound. PBS and exosomes were injected around the wound subcutaneously. Mice were sacrificed at day 3, 7, 14 to study the immune response in wound sties. The graphs showing total macrophage (A), CD206+macrophage (B) and CD86+macropahge (C) in the wound sites on day 3, 7 and 14. Macrophage polarization were calculated based on CD86, CD206 markers at day 3, 7 and 14 (D-F). n=6, *P<0.05, **P<0.01, ***P<0.001, ****P<0.0001.

for all groups. Similar as reported in other research, macrophage number peaked around day 7 and followed by retreatment afterwards.[5] Compared to wound driven macrophage infiltration, the UEF and Exo-PEF recruited significantly more macrophages to the wound sites at all three time points examined. (Fig. 4.7 A) Again, the macrophages phenotype was

further identified based on CD86 and CD206. Similar to the transplantation study, the UEF significantly induced accumulation of CD86+ M1 macrophage compared to wound and Exo group at day 3 and day7 and all other groups at day14. On contrary, the Exo-PEF did not have significant higher number of M1 macrophage compared to control wound and Exo group on three time points. (Fig. 4.7 B) Though both UEF and Exo-PEF showed higher number of CD206+M2 macrophage at day7 and 14, the Exo-PEF showed significant higher number of M2 macrophage compared to other three groups as early as day3. The Exo group only showed higher number of M2 macrophage compared to control wound on day 3. (Fig. 6C) Other than that, no significant changes in total macrophage number or M1, M2 macrophage number were observed. When calculating the M2/M1 ratio, the overall trend of shifting from M1biased immune response to M2 biased immune response was observed on the time axis in control wound, Exo and Exo-PEF group during the two weeks post injury. However, the UEF group showed attenuated M1-biased inflammatory response through the two weeks. (Fig. 4.7 D-F) As early as day 3, The Exo and Exo-PEF had significant M2 biased immune response compared to wound control and UEF. (Fig. 4.7 D) Due to the endogenous immune modulatory mechanisms against injury, all groups exhibited decreased M1/M2 ratio on day 7 compared to day 3. (Fig. 4.7 E) At day 14, except for UEF, all other group established a M2-biased immune homeostasis resembling the healthy tissue. (Fig. 4.7 F)

By interpreting the immune response in the lymph nodes and spleen in the wound healing model, the Th2 immune response and increased Tregs population were observed. Specifically, Exo and Exo-PEF showed significantly more IL4 secreting CD4+ T cells compared to wound control and UEF in the lymph nodes at day 7. (Fig. 4.8 A) In the spleen,

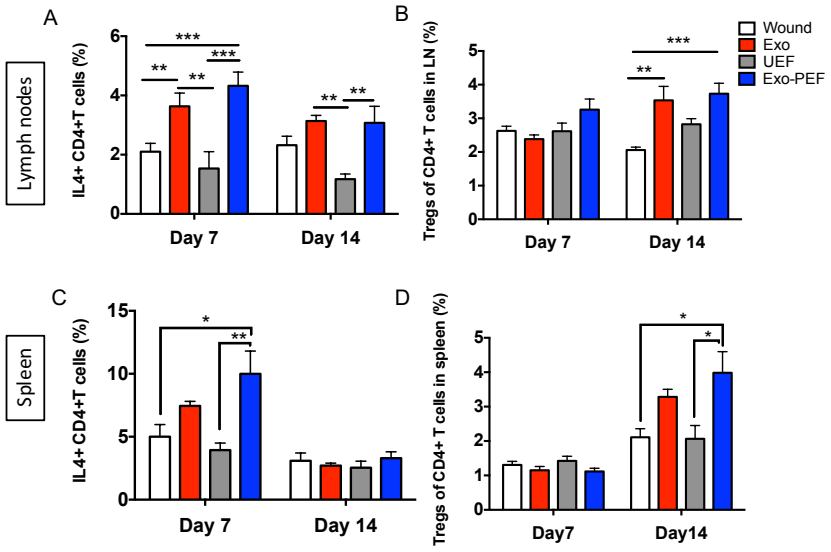

Figure 4.8 Immune response in LN and spleen in the wound healing model. Skin full excisional wound were created on the Balb/c mice, UEF and Exo-PEF were applied to the wound. PBS and exosomes were injected around the wound subcutaneously. Mice were sacrificed at day 7, 14 to study the immune response in the spleen and LN. The graphs showing IL4 secreting T cells, Tregs in LN (A, B) and in spleen (C, D) at day 7 and day 14. n=6, *P<0.05, **P<0.01, ***P<0.001, ****P<0.0001.

only Exo-PEF showed more IL4 secreting CD4+ T cells compared to wound control and UEF at day7, while no differences were found at day 14. (Fig. 4.8 C). The population of Tregs were significantly increased by Exo and Exo-PEF in the lymph nodes at day 14. In the spleen, only Exo-PEF group significantly increased the Treg population compared with wound control and UEF at day 14. No significant changes were observed on Treg population on day7 for both LN and spleen. (Fig. 4.8 B, D)

The ultimate goal of designing regenerative immunomodulatory materials is to enhance the process of tissue repair/regeneration. To this end, we then evaluated the wound healing process under the treatment of exosome, UEF and Exo-PEF. As shown in the figure 8, Exo and Exo-PEF could significantly enhance the skin excisional wound closure, while

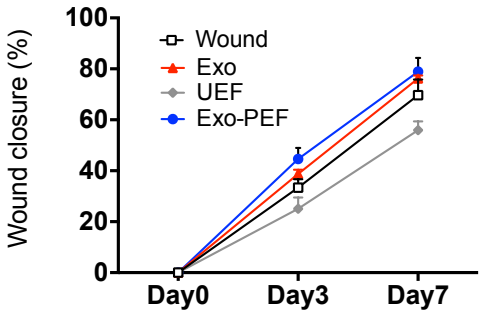

Tukey's multiple comparisons test	Day 3		Day 7	
	Significance	Adjusted P Value	Significance	Adjusted P Value
WC vs. Exo	*	0.0410	*	0.0189
WC vs. Exo-PEF	****	< 0.0001	***	0.0006
Exo vs. Exo-PEF	*	0.0237	ns	0.5952

Figure 4.9 Therapeutic effects of Exo-PEF in wound healing. Skin full excisional wound were created on the Balb/c mice, UEF and Exo-PEF were applied to the wound. PBS and exosomes were injected around the wound subcutaneously. The wound closure percentage were calculated and P values were listed (A). n=14, *P<0.05, **P<0.01, ***P<0.001, ****P<0.0001.

the UEF hindered the process of wound closure, in comparison with control wound. Especially, the Exo-PEF have significantly accelerated wound closure compared to Exo groups at day 3, indicating superior therapeutic function of Exo-PEF. (Fig. 4.9 A)

4.4 Discussion

With the identification of M2 macrophage one decade ago, the role of macrophage and their versatile phenotypes in tissue regeneration has been largely studied and since then the immune system is closely connected with regeneration. In recent year, the adaptive immune cells, especially T helper 2 cells and Tregs were identified as pro-regenerative in many tissues such as muscle, heart, skin and neuron.[15, 16] As of today, with new findings that keep involving other types of immune cells to the regenerative process such as innate lymphoid cells (ILC) and gamma delta T cells etc., the immune-mediated regeneration is a brand new and promising direction to start from in the future regenerative medicine realm. To this end, the overall goal of this study is to design a biomaterial that have the ability to intentionally manipulate the immune cell behavior and generate a pro-regenerative immune

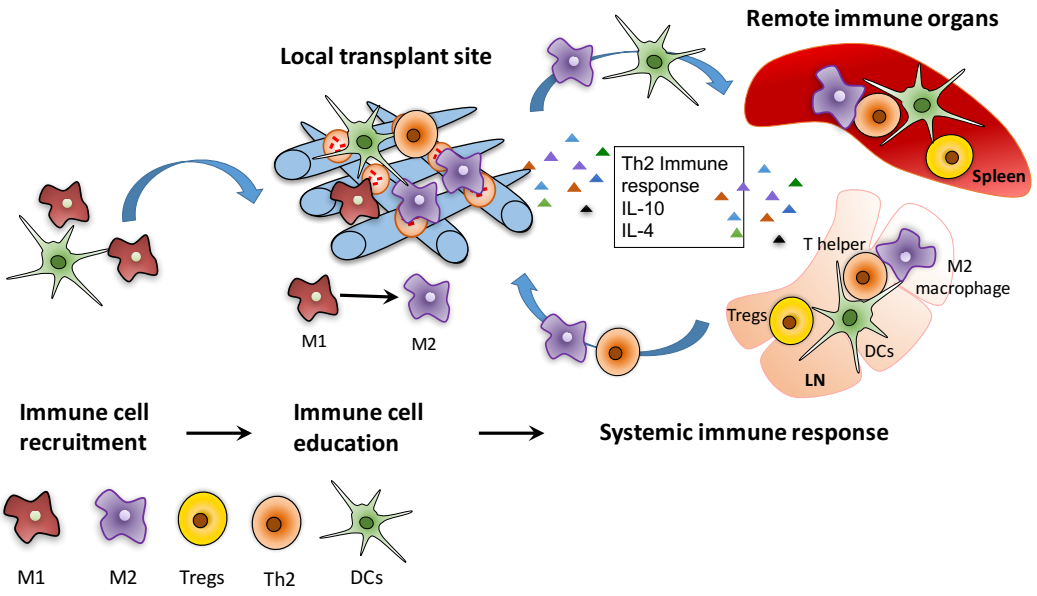

Figure 4.10 Possible mechanism of the regenerative immunomodulatory properties of Exo-PEF. M1: M1 macrophage. M2: M2 macrophage. Tregs: regulatory T cells. Th2: T helper 2 cells. DCs: dendritic cells.

environment in vivo. Speaking of biomaterials modulating immune system, one of the most achieved successful examples should be in the cancer vaccine design. One strategy in cancer vaccine design involving materials is to create an "immunoactive center" in vivo. Through utilizing the immune response towards materials, immune cells would be recruited to the place of injection/transplantation, where the immune cells will receive the anti-cancer signals carried by the materials.[56, 57] Inspired by this concept, comes out our material design in this study: utilize fibrous scaffolds to recruit the immune cells and MSC exosomes to send regenerative signals to the recruited immune cells.

MSC exosomes were selected to be the origin of regenerative signals in our study. Due to the cohort of bio-functional ingredients carried by exosomes, they are supposed to target a broad type of immune cells, which is hard to achieve by a single cytokine administration. In our study, the immunomodulatory property of exosomes was observed

on manipulating macrophage phenotype, T helper cells secretion and Tregs accumulation in vivo, which proved the multi-targeting capacities of exosomes. To combine exosomes with fibrous scaffolds, we designed a PEI modified EF that could actively load exosomes through static interactions, instead of simply applying exosomes to EF scaffolds. This design aims to increase the retention of exosomes in the transplant sites and thus increase the chance of being uptaken by the recruited immune cells. In vitro assay showed that the loaded exosomes will not be released from the scaffolds when rinsing in PBS (data not shown). The macrophage uptake study in the trans-well system indicates a contact-dependent way for macrophage to uptake scaffold bond exosomes (Fig. 4.4). Therefore, it could imply the uptake mechanism in vivo. Of course, further in vivo trafficking and uptake study needs to be done. Actually, binding exosomes through static interaction is a new way of coupling exosomes with scaffolds. The contact-dependent uptake mechanism is also a new way of cell interacting with exosomes. It has been reported that ECM scaffold buried some vesicles with immunomodulatory properties that would be released during ECM degradation,[151-153] and our Exo-PEF system very much resembles this natural design.

The loading of exosomes to scaffolds did not compromise the bio-activity of the exosomes, as shown in figure 4 that Exo-PEF showed equivalent even superior properties to modulate macrophage phenotype towards M2 compared to exosome alone. The UEF showed the ability to increase anti-inflammatory cytokine gene expression in vitro (Fig. 4.5 A, B), though not as potent as exosomes. This could contribute to the reason why Exo-PEF were more potent than exosomes alone in modulating macrophage phenotypes (Fig. 4.5 B, E). However, the UEF induced long term M1-biased macrophage accumulation in the transplant sites/wound sites in both healthy and wound environment in vivo. (Fig. 4.6

A-D, Fig. 4.7) This could attribute to limited biocompatibility of PCL in vivo as PCL is a hydrophobic synthetic material. When being used in wound dressing material, PCL is usually blend with biocompatible ingredients such as collagen or treated to be more hydrophilic. From this point of consideration, PEI modification to UEF also aim to improve the hydrophilicity (Fig. 4.3 B) and biocompatibility of the PCL EF scaffolds (Supplementary figure 5), except for introducing positive charge for exosome loading.

In order to fully elucidate the intrinsic immunomodulatory properties of Exo-PEF in vivo, we first did a mechanistic study in healthy mice with no pathological immune background. The results proved our hypothesis that the presence of fibrous scaffolds would recruit more macrophage to the transplant site (Fig. 4.6 A), followed by the recruited immune cells receiving the signals from exosomes and exhibiting M2-biased immune response (Fig. 4.6 D). It was observed that the Exo-PEF recruited more macrophage compared to UEF, which could be due to the long-term existence of exosomes interfering with the macrophage recruitment. In the draining lymph nodes, the Th2 immune response and increase number of Tregs was observed in both Exo and Exo-PEF group, indicating the immunomodulatory properties brought up by exosomes. (Fig. 4.6 E-G) In contrast, only Exo-PEF showed significant immunomodulation towards DCs, macrophage and increased Treg population in the spleen. (Fig. 4.6 H-I) It was speculated that the mechanism of Th2 immune response and increased Treg population driven by Exo and Exo-PEF may be different. Exosomes injected subcutaneously diffused quickly in 24 hours (data not shown). However, as we inferred the Exo-PEF uptake mechanism is scaffold contact –dependent, the immune response caused in lymphatic organs may be mainly mediated by exosome uptaken immune cells. Therefore, the trafficking and mechanism of immunomodulation

are different for free exosomes and scaffold bound exosomes, which need to be further validated with more experiments.

In the real scenario of injury, there will be endogenous dynamic change in the immune system in response to the injury. Therefore, it is much more challenging to apply and characterize the designed material to modulate the immune system in such complicated micro-environment. The injury model we used in this study is a mice full excisional wound healing model. The skin is a tissue that could heal by itself post moderate injury. Studies have proved the indispensable role of macrophage in the skin wound healing. Especially, the macrophage phenotype converting from M1 to M2 in the mid-stage of the healing (day3-7) post injury is critical for an appropriate healing.[5, 154, 155] In our study, it is observed that the overall trend of immune response post injury through day 3 to day 14: the migration and retreat of macrophage and the shift from M1 to M2-biased immune response. (Fig.4.7) Compared to mechanistic study in the healthy mice, the wound site itself has the ability to recruit more numbers of macrophage. Even so, the results once again confirmed the first part of our hypothesis that the presence of EF scaffolds will result in more recruited immune cells to the transplant site. (Fig. 4.7 A) It is noteworthy that the Exo and Exo-PEF have advanced the transition from M1 to M2 for macrophage phenotype as early as day 3 (Fig. 4.7 D) and accelerated the wound closure pace (Fig. 4.8 A), compared to control wound. Though the M1/M2 balance is similar between Exo and Exo-PEF at day 3, the magnitude of the immune response is different as Exo-PEF have driven significant more M2 macrophage compared to Exo. (Fig.4.7 B) This may explain the better outcome of wound closure of Exo-PEF compared to Exo alone at day 3. On contrary, the UEF showed an attenuated M1-biased pro-inflammatory immune response in the wound

site (Fig. 4.7) and hindered the regeneration process (Fig. 4.8A). The integrated results proved the second part of our hypothesis in the wound healing model that the recruited immune cells received the immunomodulatory signals from exosomes and convert their phenotype towards pro-regeneration.

In the draining lymph nodes and spleen of the wound healing model, we again saw the elevated Th2 immune response and increased Treg population driven by Exo and Exo-PEF. (Fig. 4.9 A, B) Though studies have connected the adaptive immune cell behavior to the regenerative process, the role of the adaptive immune response in the lymphatic organs are hardly studied in the wound healing model. The Th2 immune response and upregulated Treg population we observed from the lymph nodes and the spleen driven by materials in the wound healing model has not been reported before. The exact role of the adaptive immune response generated by the synthetic materials coupling exosomes in the wound healing process remains to be further explored with depletion of specific immune cells.

The immune system is a complicated network, the consequence of immune response is depending on the timing, balance and the magnitude of the immune response in tissue repair/regeneration. The early pro-inflammatory immune response is relevant to debris clearance and progenitor cell proliferation. It has been reported that infiltrating M2 macrophage immediately after injury will hinder the healing process. Therefore, the immunomodulatory material design needs to consider the requirement of the tissue repair in specific time stage. The uncontrollable inflammatory immune response will hinder the healing process, whereas high intensity of Th2 and M2-biased immune response will lead to fibrosis. Thus the immune modulation by materials needs to be within a proper extent. The consideration of variation of species, age, tissue will add more dimensions for potent

pro-regenerative immunomodulatory biomaterial design. With all the challenges and promises, regenerative immunomodulation by biomaterials is a bright new direction and our study have added new clues to this realm.

CHAPTER 5. CONCLUSION AND FUTURE DIRECTIONS

5.1 Cancer immunotherapy based on tumor-derived exosomes

The key idea of cancer immunotherapy is to stimulate and education immune system for specific anti-cancer immunity, involving the participates of specific tumor antigens and immune stimulators. In chapter 2, a cancer vaccine was developed with tumor-derived exosomes as the antigen sources and TLR7/9 agonists as the immune-stimulator to fight against B lymphoma. What could be concluded from the study is that tumor-derived exosomes could be used as an antigen source for cancer immunotherapy. Tumor-derived exosomes could drive both adaptive and humoral immunity against cancer cells and showed therapeutic effects in established metastatic B lymphoma model in mice. Other than that, tumor-derived exosomes treated mice could generate memory B cells that secreting specific anti-tumor antibodies and prevent cancer recurrence. By facilitating with TLR7/9 agonists, exosome-agonist vaccine design further promoted the survival of cancer beard mice, induced better maturation of dendritic cells and T cell immune response compared exosome alone.

This study established the design of exosome-agonist system as a new modality for cancer immunotherapy in B lymphoma treatment. B cell lymphomas is a deadly disease for all age groups. Patients still suffered from life threaten and the risk of recurrence of the B lymphoma after conventional clinical treatments, such as a rituximab (a monoclonal anti-CD20 antibody). This vaccine not only showed therapeutic effects in a B lymphoma model established for 7 days, but also protected mice from tumor re-challenge, showing great potential for further clinical translation. Cancer immunotherapy requires the source of

specific antigens of tumor and identifying neo-antigen for each patient is time and money consuming. Our study showed the possibilities of using exosomes to display full spectrum of cancer antigens to the immune system and this method could be generalized to the therapy of other types of cancer. Other than survival, this study also carefully characterized the immune response driven by the tumor derived exosomes in a comprehensive way and unraveled the mechanisms of the anti-tumor immunity driven by tumor-derived exosome, which have paved the way for better design of cancer vaccine based on tumor-derived exosomes.

In the future, the safety of using exosomes in the cancer immunotherapy needs to be considered with highest priority. Studies have shown that the exosomes have the ability to promote angiogenesis and aid metastasis of the cancer. Thus, the materials design should avoid the probable pro-cancer side effects of the exosomes, by considering the way of administration such as i.v./i.p./s.c. injection, or the facilitate of immune stimulators such as growth factors or agonists. Another concern would be that tumor cell-derived exosomes contain not only tumor antigens but also other endogenous autologous antigens, which might induce autoimmune reaction after their presentation by dendritic cells. Although clinical trial of tumor cell-derived exosomes for cancer immunotherapy did not report severe adverse effect including autoimmune reactions, consideration should be given to the autoimmune response after the immunization with tumor cell-derived exosomes.

Another worth exploring strategy is to couple tumor-derived exosomes to the scaffolds with immune stimulating design, as the immune system have natural foreign body reaction to transplanted materials and could thus increase the chance for uptake of exosomes by antigen-presenting cells. This material design is very tricky, as shown in our

study in appendix that coupling the tumor-derived exosomes to the microparticles would compromise the therapeutic efficacy of the vaccine. However, it has been reported that the porous scaffolds loaded with tumor antigen and GM-CSF or TLR agonist have showed improved therapeutic efficacy against cancer. From this point view, coupling exosomes to materials with more immune stimulatory properties might be a promising strategy to further increase the efficacy and decrease the required dose for cancer vaccine design based on tumor-derived exosomes.

5.2 Fibrous scaffolds for enhanced immunomodulatory properties of MSC

In chapter 3, fibrous scaffolds with varied topologic cues were designed utilizing electrospinning techniques for enhancement of MSCs paracrine functions. Three basic conclusions may be drawn in this material-MSCs interaction system compared to polystyrene cultured MSCs. First, the fibrous scaffolds have the capability to elevate the secretion of immunomodulatory and pro-angiogenic molecules of MSCs through activation of NFκB signaling pathway. Second, the varied topological architectures of the scaffolds could regulate the immunomodulatory paracrine activities differently, with the scaffolds of lattice-like structure the most potent. Third, the paracrine products derived from the scaffolds-MSCs system showed the ability to skew macrophage towards pro-regenerative M2 phenotype and showed therapeutic effects in the wound healing model in vivo.

This study reveals the impact of the scaffolds materials and their topological architectures on MSCs paracrine functions. As have been proved that the paracrine factors of MSCs contribute the most in their therapeutic effects by treating degenerative diseases,

this study brought insights for a new dimension of regenerative medicine design regarding the MSCs. Due to the low viability, retention rate and uncontrollable behavior of MSCs post in vivo transplantation, this study also proved the possibilities to use the paracrine product of material-primed MSCs collected in vitro as a substitute of MSCs for in vivo treatments.

In the future, how to design more potent materials to potentiate MSCs paracrine function need to be considered. By exploring how scaffolds and the topological cues affect MSC paracrine function, we could have more understanding in the mechanisms of crosstalk in materials-MSCs system. Besides topological cues, many other aspects of material design could be untiled and tested in the materials-MSCs interaction system focusing on the improvement of paracrine function of MSCs, including chemical, physical properties, biological cues of the materials.

paved the way of better designed materials. In this study, the immunomodulation properties of scaffolds-MSCs were only examined on macrophage phenotype. Though macrophage plays the central role in the immune network, other immune cells, especially adaptive immune cells, were also identified as key mediators of tissue repair/regeneration, Therefore, to study the immunomodulation function of material-MSCs system on the full spectrum of immune systems also worth exploring.

In recent years, the EVs released from MSCs showed immunomodulatory possibilities and therapeutic effects in many tissues resembling the functions of cells. Moreover, EVs purified from the supernatants of MSC culture have simplified components compared to the conditioned medium we used in the study. Thus it will be of great interest

to study how the material will affect MSC EVs, in terms of the released amount, functional components and targeting properties of the EVs. Furthermore, materials could be further designed for coupling EVs for in vivo therapy, just as the work in the chapter 4. Of course, more standards regarding the isolation methods, marker identification, component characterization need to be established for EVs future wide-scale translation in clinical modality in the future.

5.3 Exosome-loaded scaffolds for regenerative immunomodulation.

On the basis of previous two studies, we developed a MSC exosome-loaded scaffolds for regenerative immunomodulation in the chapter 4. By surface modification of PEI to the fibrous scaffolds, we realized the material design of loading exosomes to the scaffolds with relatively controllable and stable way. The in vivo study verified three basic hypothesis based on this Exo-EF materials. First, the scaffolds have the ability to recruit more immune cells to the transplanted sites. Second, due to the immunomodulatory properties of MSCs exosomes, the Exo-EF could convert the recruited macrophage towards pro-regenerative M2 phenotype. Third, the local transplanted Exo-EF could drive systemic Th2 immune response and increased Tregs in the remote lymphatic organs, which were considered as pro-regenerative.

In this study, the martial design has borrowed the concept from cancer vaccine that the materials were used to recruit the immune cells and the carried exosomes were aimed at educating the recruited immune cells towards regenerative phenotype. Compared to the conventional material design emphasis the inert properties of materials and prevention of triggering immune response, this study utilized the immune response towards materials,

properly modulate the immune response with scaffolds structure design and coupling of immune modulator. Therefore, brings new thoughts to the development of immunomodulatory material for regeneration. Moreover, studies in regenerative medicine usually focused on the local immune response and innate immune response in the injured sites but neglect the immune response happened in the remote lymphatic organs. This study has explored the immune response driven by Exo-EF, looking at both innate and adaptive immune responses, in both local sites and lymphatic organs, thus revealed the immunomodulatory functions of the materials in more comprehensive spectrum.

In the future, the study of trafficking and uptake of exosomes loaded on the scaffolds by immune cells and other cell types in vivo is worth considering. It would be interesting to compare the cell types that uptake exosomes between scaffold loaded exosomes and free exosomes. This will reveal the role of materials to interfere the exosome uptake in vivo with more solid proof. Exosomes contains versatile components that could affect many immune cells as well as other cell types that involved in regeneration such as endothelial cells. To study which specific cell types are uptaking the exosomes and how would their behavior be affected due to the exosome uptake in vivo will also elucidate the fundamental mechanism for exosomes in regenerative medicine.

Moreover, the crosstalk between the adaptive immune cells and the innate immune cells and the role Exo-EF material plays in it is still vague. We have seen both innate and adaptive immune response are driven by Exo-EF in vivo, but how is the message passed between adaptive immune cells and innate immune cells in the presence of materials is an intriguing point to be explored in the future.

APPENDIX A. SUPPEMENTARY MATERIALS

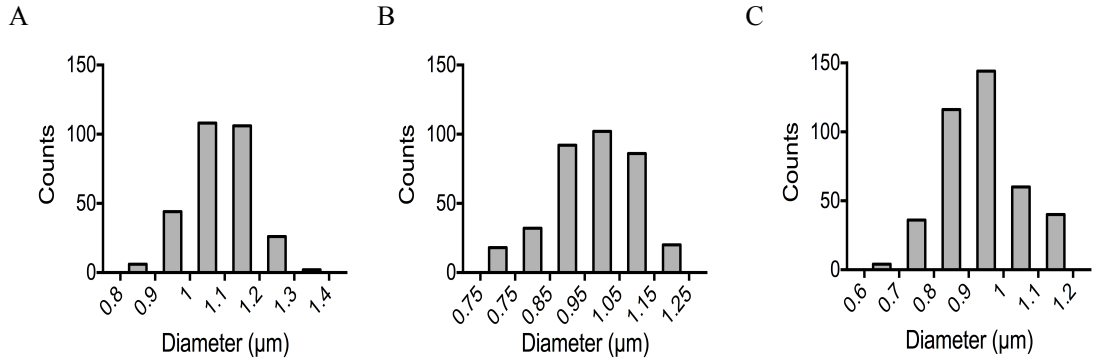

Supplementary figure 1. Electrospun fiber diameter distribution for REF (A), AEF (B) and MEF(C).

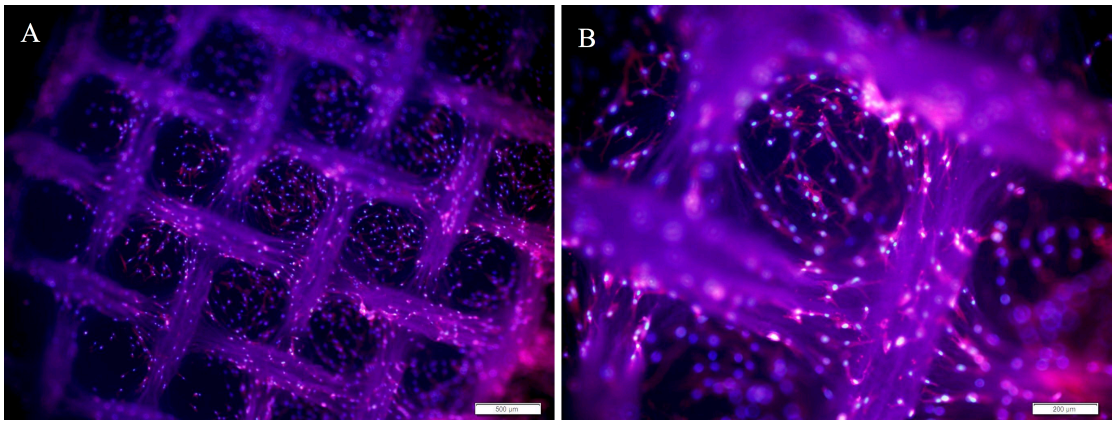

Supplementary figure 2. Fluorescent microscopy picture of Ad-MSCs seeded on the MEF scaffolds. In a low magnification view, the cells were organized into this whirlpool-like repeated units. Scale bar indicates 500µm and 200µm in A and B, respectively.

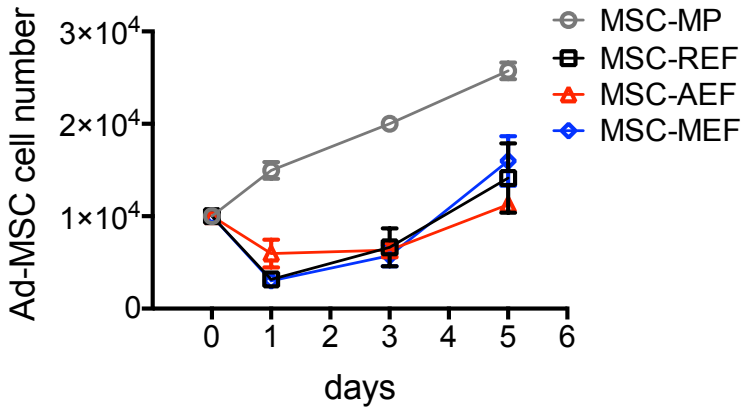

Supplementary figure 3. Ad-MSCs proliferation cultured on either microplate or fibrous scaffolds.

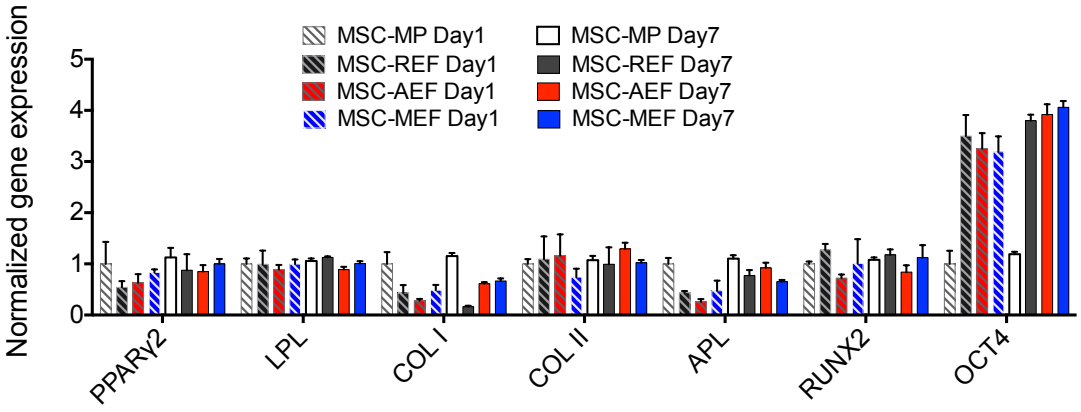

Supplementary figure 4. Ad-MSCs gene expression of differentiation marker and stemness marker at day1 and day7. The ddCt of qPCR were calculated versus MSC-MP Day1 group.

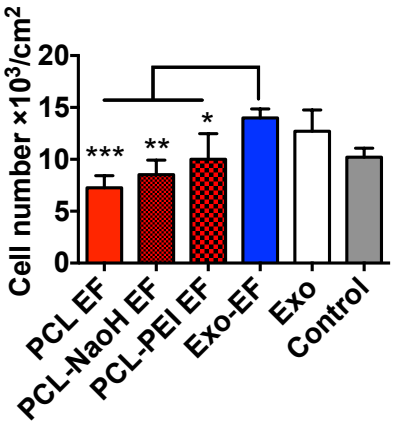

Supplementary figure 5. HUVEC cells were cultured on different EF scaffolds or in microplates supplemented with or without exosomes for 24 hours. The cell number were calculated by DAPI staining and cell count using image J

Supplementary table 1. Primer sequence for qPCR

	Gene	Forward primer	Reverse primer
Mouse	TNF-α	GACCCTCACACTCAGATCATCTTCT	CCTCCACTTGGTGGTTTGCT
	IL-10	ATGCTGCCTGCTCTTACTGACTG	CCCAAGTAACCCTTAAAGTCCTGC
	β-actin	AGAGGGAAATCGTGCGTGAC	CAATAGTGATGACCTGGCCGT
	Arg-1		
Rat	GAPDH	GTATGACTCTACCCACGGCAAGT	TTCCCGTTGATGACCAGCTT
	bFGF-2	GTCAAACTACAGCTCCAAGCAGAA	AGGTACCGGTTCGCACACA
	HGF	CAATCCAGAGGTACGCTACGAA	TTTCACCGTTGCAGGTCATG
	VEGF	GAGGAAAGGGAAAGGGTCAAAA	CACAGTGAACGCTCCAGGATT
	COX-2	AAGGGAGTCTGGAACATTGTGAAC	CAAATGTGATCTGGACGTCAACA
	TGF-β	CCTGGAAAGGGCTCAACAC	CAGTTCTTCTCTGTGGAGCTGA

PUBLICATIONS

[1] **Su N**, Gao PL, Wang K, Wang JY, Zhong Y, Luo Y. Fibrous scaffolds potentiate the paracrine function of mesenchymal stromal cells: A new dimension in cell-material interaction. **Biomaterials**. 2017;141:74-85.

[2] Wang K, Hou WD, Wang X, Han C, Vuletic I, **Su N**, et al. Overcoming foreign-body reaction through nanotopography: Biocompatibility and immunoisolation properties of a nanofibrous membrane. **Biomaterials**. 2016;102:249-58.

[3] **Su N**[1], Jiang LY[1], Wang X[1], Gao PL, Zhou J, et al. Membrane-binding adhesive particulates enhance the viability and paracrine function of mesenchymal stromal cells for cell-based therapy. (**Biomacromolecules, in preparation**)

[4] **Su N**, Pradhan P, Liu JY, Leleux J, Luo Y, Roy K. Tumor-derived exosomes-agonist vaccine shows long-term anti-tumor immunity in pre-established metastatic B lymphoma model. (**in preparation**)

[5] **Su N**, Hao YY, Hou WD, Wang F, Luo Y. Exosome-loaded electrospun fibers: design of tissue scaffolds towards regenerative immunomodulation (**in preparation**)

REFERENCES

[1] Aurora AB, Porrello ER, Tan W, Mahmoud AI, Hill JA, Bassel-Duby R, et al. Macrophages are required for neonatal heart regeneration. J Clin Invest. 2014;124:1382-92.

[2] Tidball JG. Regulation of muscle growth and regeneration by the immune system. Nat Rev Immunol. 2017;17:165-78.

[3] Wynn TA, Vannella KM. Macrophages in Tissue Repair, Regeneration, and Fibrosis. Immunity. 2016;44:450-62.

[4] Bouchery T, Harris NL. Specific repair by discerning macrophages. Science. 2017;356:1014.

[5] Shook B, Xiao E, Kumamoto Y, Iwasaki A, Horsley V. CD301b+ Macrophages Are Essential for Effective Skin Wound Healing. J Invest Dermatol. 2016;136:1885-91.

[6] Jetten N, Roumans N, Gijbels MJ, Romano A, Post MJ, de Winther MP, et al. Wound administration of M2-polarized macrophages does not improve murine cutaneous healing responses. PLoS One. 2014;9:e102994.

[7] Lucas T, Waisman A, Ranjan R, Roes J, Krieg T, Muller W, et al. Differential roles of macrophages in diverse phases of skin repair. J Immunol. 2010;184:3964-77.

[8] Burzyn D, Kuswanto W, Kolodin D, Shadrach JL, Cerletti M, Jang Y, et al. A special population of regulatory T cells potentiates muscle repair. Cell. 2013;155:1282-95.

[9] Ali N, Zirak B, Rodriguez RS, Pauli ML, Truong HA, Lai K, et al. Regulatory T Cells in Skin Facilitate Epithelial Stem Cell Differentiation. Cell. 2017;169:1119-29 e11.

[10] Ali N, Rosenblum MD. Regulatory T cells in skin. Immunology. 2017;152:372-81.

[11] Dombrowski Y, O'Hagan T, Dittmer M, Penalva R, Mayoral SR, Bankhead P, et al. Regulatory T cells promote myelin regeneration in the central nervous system. Nat Neurosci. 2017;20:674-80.

[12] Nosbaum A, Prevel N, Truong HA, Mehta P, Ettinger M, Scharschmidt TC, et al. Cutting Edge: Regulatory T Cells Facilitate Cutaneous Wound Healing. J Immunol. 2016;196:2010-4.

[13] Ben Ya'acov A, Lichtenstein Y, Zolotarov L, Ilan Y. The gut microbiome as a target for regulatory T cell-based immunotherapy: induction of regulatory lymphocytes by oral administration of anti-LPS enriched colostrum alleviates immune mediated colitis. BMC Gastroenterol. 2015;15:154.

[14] Schiaffino S, Pereira MG, Ciciliot S, Rovere-Querini P. Regulatory T cells and skeletal muscle regeneration. FEBS J. 2017;284:517-24.

[15] Chen G, Tang L, Wei W, Li Z, Li Y, Duan X, et al. mTOR regulates neuroprotective effect of immunized CD4+Foxp3+ T cells in optic nerve ischemia. Sci Rep. 2016;6:37805.

[16] Hendrix S, Nitsch R. The role of T helper cells in neuroprotection and regeneration. J Neuroimmunol. 2007;184:100-12.

[17] Chen F, Liu Z, Wu W, Rozo C, Bowdridge S, Millman A, et al. An essential role for TH2-type responses in limiting acute tissue damage during experimental helminth infection. Nat Med. 2012;18:260-6.

[18] Liu Y, Wang L, Kikuiri T, Akiyama K, Chen C, Xu X, et al. Mesenchymal stem cell-based tissue regeneration is governed by recipient T lymphocytes via IFN-gamma and TNF-alpha. Nat Med. 2011;17:1594-601.

[19] Linero I, Chaparro O. Paracrine effect of mesenchymal stem cells derived from human adipose tissue in bone regeneration. PLoS One. 2014;9:e107001.

[20] Ranganath SH, Levy O, Inamdar MS, Karp JM. Harnessing the mesenchymal stem cell secretome for the treatment of cardiovascular disease. Cell Stem Cell. 2012;10:244-58.

[21] Gnecchi M, Zhang Z, Ni A, Dzau VJ. Paracrine mechanisms in adult stem cell signaling and therapy. Circ Res. 2008;103:1204-19.

[22] Nauta AJ, Fibbe WE. Immunomodulatory properties of mesenchymal stromal cells. Blood. 2007;110:3499-506.

[23] Nemeth K, Leelahavanichkul A, Yuen PS, Mayer B, Parmelee A, Doi K, et al. Bone marrow stromal cells attenuate sepsis via prostaglandin E(2)-dependent reprogramming of host macrophages to increase their interleukin-10 production. Nat Med. 2009;15:42-9.

[24] Kang K, Ma R, Cai W, Huang W, Paul C, Liang J, et al. Exosomes Secreted from CXCR4 Overexpressing Mesenchymal Stem Cells Promote Cardioprotection via Akt Signaling Pathway following Myocardial Infarction. Stem Cells Int. 2015;2015:659890.

[25] Shabbir A, Cox A, Rodriguez-Menocal L, Salgado M, Van Badiavas E. Mesenchymal Stem Cell Exosomes Induce Proliferation and Migration of Normal and Chronic Wound Fibroblasts, and Enhance Angiogenesis In Vitro. Stem Cells Dev. 2015;24:1635-47.

[26] Xin H, Li Y, Cui Y, Yang JJ, Zhang ZG, Chopp M. Systemic administration of exosomes released from mesenchymal stromal cells promote functional recovery and neurovascular plasticity after stroke in rats. J Cereb Blood Flow Metab. 2013;33:1711-5.

[27] Collier TO, Anderson JM, Brodbeck WG, Barber T, Healy KE. Inhibition of macrophage development and foreign body giant cell formation by hydrophilic interpenetrating polymer network. J Biomed Mater Res A. 2004;69:644-50.

[28] Jain S, Pitoc GA, Holl EK, Zhang Y, Borst L, Leong KW, et al. Nucleic acid scavengers inhibit thrombosis without increasing bleeding. Proc Natl Acad Sci U S A. 2012;109:12938-43.

[29] Lee J, Jackman JG, Kwun J, Manook M, Moreno A, Elster EA, et al. Nucleic acid scavenging microfiber mesh inhibits trauma-induced inflammation and thrombosis. Biomaterials. 2017;120:94-102.

[30] Jackman JG, Juwarker H, Poveromo LP, Levinson H, Leong KW, Sullenger BA. Polycationic Nanofibers for Nucleic Acid Scavenging. Biomacromolecules. 2016;17:3706-13.

[31] Dumont CM, Park J, Shea LD. Controlled release strategies for modulating immune responses to promote tissue regeneration. J Control Release. 2015;219:155-66.

[32] Li M, Gao L, Chen J, Zhang Y, Wang J, Lu X, et al. Controllable Release of Interleukin-4 in Double-Layer Sol-Gel Coatings on TiO2 Nanotubes for Modulating Macrophage Polarization. Biomed Mater. 2017.

[33] Lin CC, Metters AT, Anseth KS. Functional PEG-peptide hydrogels to modulate local inflammation induced by the pro-inflammatory cytokine TNFalpha. Biomaterials. 2009;30:4907-14.

[34] Sy JC, Seshadri G, Yang SC, Brown M, Oh T, Dikalov S, et al. Sustained release of a p38 inhibitor from non-inflammatory microspheres inhibits cardiac dysfunction. Nat Mater. 2008;7:863-8.

[35] Reeves AR, Spiller KL, Freytes DO, Vunjak-Novakovic G, Kaplan DL. Controlled release of cytokines using silk-biomaterials for macrophage polarization. Biomaterials. 2015;73:272-83.

[36] Morishita Y, Imai T, Yoshizawa H, Watanabe M, Ishibashi K, Muto S, et al. Delivery of microRNA-146a with polyethylenimine nanoparticles inhibits renal fibrosis in vivo. Int J Nanomedicine. 2015;10:3475-88.

[37] Swartzlander MD, Blakney AK, Amer LD, Hankenson KD, Kyriakides TR, Bryant SJ. Immunomodulation by mesenchymal stem cells combats the foreign body response to cell-laden synthetic hydrogels. Biomaterials. 2015;41:79-88.

[38] Chen Z, Wu C, Gu W, Klein T, Crawford R, Xiao Y. Osteogenic differentiation of bone marrow MSCs by beta-tricalcium phosphate stimulating macrophages via BMP2 signalling pathway. Biomaterials. 2014;35:1507-18.

[39] Chen Z, Bachhuka A, Han S, Wei F, Lu S, Visalakshan RM, et al. Tuning Chemistry and Topography of Nanoengineered Surfaces to Manipulate Immune Response for Bone Regeneration Applications. ACS Nano. 2017;11:4494-506.

[40] Al-Maawi S, Orlowska A, Sader R, James Kirkpatrick C, Ghanaati S. In vivo cellular reactions to different biomaterials-Physiological and pathological aspects and their consequences. Semin Immunol. 2017;29:49-61.

[41] Veiseh O, Doloff JC, Ma M, Vegas AJ, Tam HH, Bader AR, et al. Size- and shape-dependent foreign body immune response to materials implanted in rodents and non-human primates. Nat Mater. 2015;14:643-51.

[42] Lebre F, Sridharan R, Sawkins MJ, Kelly DJ, O'Brien FJ, Lavelle EC. The shape and size of hydroxyapatite particles dictate inflammatory responses following implantation. Sci Rep. 2017;7:2922.

[43] Chen Z, Ni S, Han S, Crawford R, Lu S, Wei F, et al. Nanoporous microstructures mediate osteogenesis by modulating the osteo-immune response of macrophages. Nanoscale. 2017;9:706-18.

[44] Han S, Chen Z, Han P, Hu Q, Xiao Y. Activation of Macrophages by Lipopolysaccharide for Assessing the Immunomodulatory Property of Biomaterials(). Tissue Eng Part A. 2017;23:1100-9.

[45] Hsieh JY, Smith TD, Meli VS, Tran TN, Botvinick EL, Liu WF. Differential regulation of macrophage inflammatory activation by fibrin and fibrinogen. Acta Biomater. 2017;47:14-24.

[46] Vasconcelos DM, Goncalves RM, Almeida CR, Pereira IO, Oliveira MI, Neves N, et al. Fibrinogen scaffolds with immunomodulatory properties promote in vivo bone regeneration. Biomaterials. 2016;111:163-78.

[47] Purwada A, Roy K, Singh A. Engineering vaccines and niches for immune modulation. Acta Biomater. 2014;10:1728-40.

[48] Leleux JA, Pradhan P, Roy K. Biophysical Attributes of CpG Presentation Control TLR9 Signaling to Differentially Polarize Systemic Immune Responses. Cell Rep. 2017;18:700-10.

[49] Mora-Solano C, Collier JH. Engaging adaptive immunity with biomaterials. J Mater Chem B. 2014;2:2409-21.

[50] Adjei IM, Blanka S. Modulation of the tumor microenvironment for cancer treatment: a biomaterials approach. J Funct Biomater. 2015;6:81-103.

[51] Tamber H, Johansen P, Merkle HP, Gander B. Formulation aspects of biodegradable polymeric microspheres for antigen delivery. Adv Drug Deliv Rev. 2005;57:357-76.

[52] Bracho-Sanchez E, Xia CQ, Clare-Salzler MJ, Keselowsky BG. Micro and Nano Material Carriers for Immunomodulation. Am J Transplant. 2016;16:3362-70.

[53] Zhu M, Ding X, Zhao R, Liu X, Shen H, Cai C, et al. Co-delivery of tumor antigen and dual toll-like receptor ligands into dendritic cell by silicon microparticle enables efficient immunotherapy against melanoma. J Control Release. 2018;272:72-82.

[54] Singh A, Pradhan P, Roy K. Immunobioengineering Approaches Towards Combinatorial Delivery of Immune-Modulators and Antigens. 2013:161-81.

[55] Madan-Lala R, Pradhan P, Roy K. Combinatorial Delivery of Dual and Triple TLR Agonists via Polymeric Pathogen-like Particles Synergistically Enhances Innate and Adaptive Immune Responses. Sci Rep. 2017;7:2530.

[56] Bencherif SA, Warren Sands R, Ali OA, Li WA, Lewin SA, Braschler TM, et al. Injectable cryogel-based whole-cell cancer vaccines. Nat Commun. 2015;6:7556.

[57] Kim J, Li WA, Choi Y, Lewin SA, Verbeke CS, Dranoff G, et al. Injectable, spontaneously assembling, inorganic scaffolds modulate immune cells in vivo and increase vaccine efficacy. Nat Biotechnol. 2015;33:64-72.

[58] Spits H, Di Santo JP. The expanding family of innate lymphoid cells: regulators and effectors of immunity and tissue remodeling. Nat Immunol. 2011;12:21-7.

[59] Ramirez K, Witherden DA, Havran WL. All hands on DE(T)C: Epithelial-resident gammadelta T cells respond to tissue injury. Cell Immunol. 2015;296:57-61.

[60] Hubbell JA, Thomas SN, Swartz MA. Materials engineering for immunomodulation. Nature. 2009;462:449-60.

[61] Leleux J, Roy K. Micro and nanoparticle-based delivery systems for vaccine immunotherapy: an immunological and materials perspective. Adv Healthc Mater. 2013;2:72-94.

[62] Kharaziha P, Ceder S, Li Q, Panaretakis T. Tumor cell-derived exosomes: a message in a bottle. Biochim Biophys Acta. 2012;1826:103-11.

[63] Oksvold MP, Kullmann A, Forfang L, Kierulf B, Li M, Brech A, et al. Expression of B-cell surface antigens in subpopulations of exosomes released from B-cell lymphoma cells. Clin Ther. 2014;36:847-62 e1.

[64] Sun Y, Liu J. Potential of cancer cell-derived exosomes in clinical application: a review of recent research advances. Clin Ther. 2014;36:863-72.

[65] Tran TH, Mattheolabakis G, Aldawsari H, Amiji M. Exosomes as nanocarriers for immunotherapy of cancer and inflammatory diseases. Clin Immunol. 2015;160:46-58.

[66] Chen W, Wang J, Shao C, Liu S, Yu Y, Wang Q, et al. Efficient induction of antitumor T cell immunity by exosomes derived from heat-shocked lymphoma cells. Eur J Immunol. 2006;36:1598-607.

[67] Chaput N, Schartz NEC, Andre F, Taieb J, Novault S, Bonnaventure P, et al. Exosomes as Potent Cell-Free Peptide-Based Vaccine. II. Exosomes in CpG Adjuvants Efficiently Prime Naive Tc1 Lymphocytes Leading to Tumor Rejection. The Journal of Immunology. 2004;172:2137-46.

[68] Gehrmann U, Naslund TI, Hiltbrunner S, Larssen P, Gabrielsson S. Harnessing the exosome-induced immune response for cancer immunotherapy. Semin Cancer Biol. 2014;28:58-67.

[69] Xie Y, Bai O, Zhang H, Yuan J, Zong S, Chibbar R, et al. Membrane-bound HSP70-engineered myeloma cell-derived exosomes stimulate more efficient CD8(+) CTL- and NK-mediated antitumour immunity than exosomes released from heat-shocked tumour cells expressing cytoplasmic HSP70. J Cell Mol Med. 2010;14:2655-66.

[70] Singer NG, Caplan AI. Mesenchymal stem cells: mechanisms of inflammation. Annu Rev Pathol. 2011;6:457-78.

[71] An Y, wei W, Jing H, Ming L, Liu S, Jin Y. Bone marrow mesenchymal stem cell aggregate: an optimal cell therapy for full-layer cutaneous wound vascularization and regeneration. Sci Rep. 2015;5:17036.

[72] Chen L, Tredget EE, Wu PY, Wu Y. Paracrine factors of mesenchymal stem cells recruit macrophages and endothelial lineage cells and enhance wound healing. PLoS One. 2008;3:e1886.

[73] Ylostalo JH, Bartosh TJ, Coble K, Prockop DJ. Human mesenchymal stem/stromal cells cultured as spheroids are self-activated to produce prostaglandin E2 that directs stimulated macrophages into an anti-inflammatory phenotype. Stem Cells. 2012;30:2283-96.

[74] Shao Z, Zhang X, Pi Y, Wang X, Jia Z, Zhu J, et al. Polycaprolactone electrospun mesh conjugated with an MSC affinity peptide for MSC homing in vivo. Biomaterials. 2012;33:3375-87.

[75] Capkin M, Cakmak S, Kurt FO, Gumusderelioglu M, Sen BH, Turk BT, et al. Random/aligned electrospun PCL/PCL-collagen nanofibrous membranes: comparison of neural differentiation of rat AdMSCs and BMSCs. Biomed Mater. 2012;7:045013.

[76] Kilian KA, Bugarija B, Lahn BT, Mrksich M. Geometric cues for directing the differentiation of mesenchymal stem cells. Proc Natl Acad Sci U S A. 2010;107:4872-7.

[77] Kim IL, Khetan S, Baker BM, Chen CS, Burdick JA. Fibrous hyaluronic acid hydrogels that direct MSC chondrogenesis through mechanical and adhesive cues. Biomaterials. 2013;34:5571-80.

[78] Pijnappels DA, Schalij MJ, Ramkisoensing AA, van Tuyn J, de Vries AA, van der Laarse A, et al. Forced alignment of mesenchymal stem cells undergoing cardiomyogenic

differentiation affects functional integration with cardiomyocyte cultures. Circ Res. 2008;103:167-76.

[79] Wang Y, Gao R, Wang PP, Jian J, Jiang XL, Yan C, et al. The differential effects of aligned electrospun PHBHHx fibers on adipogenic and osteogenic potential of MSCs through the regulation of PPARgamma signaling. Biomaterials. 2012;33:485-93.

[80] Oh S, Brammer KS, Li YS, Teng D, Engler AJ, Chien S, et al. Stem cell fate dictated solely by altered nanotube dimension. Proc Natl Acad Sci U S A. 2009;106:2130-5.

[81] Zhang D, Chang J. Patterning of Electrospun Fibers Using Electroconductive Templates. Advanced Materials. 2007;19:3664-7.

[82] Wang K, Wang X, Han C, Hou W, Wang J, Chen L, et al. From Micro to Macro: The Hierarchical Design in a Micropatterned Scaffold for Cell Assembling and Transplantation. Adv Mater. 2017;29.

[83] Rustad KC, Wong VW, Sorkin M, Glotzbach JP, Major MR, Rajadas J, et al. Enhancement of mesenchymal stem cell angiogenic capacity and stemness by a biomimetic hydrogel scaffold. Biomaterials. 2012;33:80-90.

[84] Li Z, Tian X, Yuan Y, Song Z, Zhang L, Wang X, et al. Effect of cell culture using chitosan membranes on stemness marker genes in mesenchymal stem cells. Mol Med Rep. 2013;7:1945-9.

[85] Chew SY, Mi R, Hoke A, Leong KW. The effect of the alignment of electrospun fibrous scaffolds on Schwann cell maturation. Biomaterials. 2008;29:653-61.

[86] Gao L, McBeath R, Chen CS. Stem cell shape regulates a chondrogenic versus myogenic fate through Rac1 and N-cadherin. Stem Cells. 2010;28:564-72.

[87] Wu Y, Chen L, Scott PG, Tredget EE. Mesenchymal stem cells enhance wound healing through differentiation and angiogenesis. Stem Cells. 2007;25:2648-59.

[88] Kinnaird T, Stabile E, Burnett MS, Lee CW, Barr S, Fuchs S, et al. Marrow-derived stromal cells express genes encoding a broad spectrum of arteriogenic cytokines and promote in vitro and in vivo arteriogenesis through paracrine mechanisms. Circ Res. 2004;94:678-85.

[89] Miyahara Y, Nagaya N, Kataoka M, Yanagawa B, Tanaka K, Hao H, et al. Monolayered mesenchymal stem cells repair scarred myocardium after myocardial infarction. Nat Med. 2006;12:459-65.

[90] Williams AR, Hare JM. Mesenchymal stem cells: biology, pathophysiology, translational findings, and therapeutic implications for cardiac disease. Circ Res. 2011;109:923-40.

[91] Zimmermann JA, McDevitt TC. Pre-conditioning mesenchymal stromal cell spheroids for immunomodulatory paracrine factor secretion. Cytotherapy. 2014;16:331-45.

[92] Bouffi C, Bony C, Courties G, Jorgensen C, Noel D. IL-6-dependent PGE2 secretion by mesenchymal stem cells inhibits local inflammation in experimental arthritis. PLoS One. 2010;5:e14247.

[93] Wang K, Hou WD, Wang X, Han C, Vuletic I, Su N, et al. Overcoming foreign-body reaction through nanotopography: Biocompatibility and immunoisolation properties of a nanofibrous membrane. Biomaterials. 2016;102:249-58.

[94] Pumberger M, Qazi TH, Ehrentraut MC, Textor M, Kueper J, Stoltenburg-Didinger G, et al. Synthetic niche to modulate regenerative potential of MSCs and enhance skeletal muscle regeneration. Biomaterials. 2016;99:95-108.

[95] Yang J, Chen X, Yuan T, Yang X, Fan Y, Zhang X. Regulation of the secretion of immunoregulatory factors of mesenchymal stem cells (MSCs) by collagen-based scaffolds during chondrogenesis. Materials Science and Engineering: C. 2016.

[96] Jiang LY, Lv B, Luo Y. The effects of an RGD-PAMAM dendrimer conjugate in 3D spheroid culture on cell proliferation, expression and aggregation. Biomaterials. 2013;34:2665-73.

[97] Thomas D, Fontana G, Chen X, Sanz-Nogués C, Zeugolis DI, Dockery P, et al. A shape-controlled tuneable microgel platform to modulate angiogenic paracrine responses in stem cells. Biomaterials. 2014;35:8757-66.

[98] Valles G, Bensiamar F, Crespo L, Arruebo M, Vilaboa N, Saldana L. Topographical cues regulate the crosstalk between MSCs and macrophages. Biomaterials. 2015;37:124-33.

[99] Muscari C, Giordano E, Bonafè F, Govoni M, Pasini A, Guarnieri C. Priming adult stem cells by hypoxic pretreatments for applications in regenerative medicine. Journal of Biomedical Science. 2013;20:63.

[100] Afzal MR, Haider HK, Idris NM, Jiang S, Ahmed RP, Ashraf M. Preconditioning promotes survival and angiomyogenic potential of mesenchymal stem cells in the infarcted heart via NF-kappaB signaling. Antioxid Redox Signal. 2010;12.

[101] Crisostomo PR, Wang Y, Markel TA, Wang M, Lahm T, Meldrum DR. Human mesenchymal stem cells stimulated by TNF-α, LPS, or hypoxia produce growth factors by an NFκB-but not JNK-dependent mechanism. American Journal of Physiology-Cell Physiology. 2008;294:C675-C82.

[102] Hocking AM, Gibran NS. Mesenchymal stem cells: paracrine signaling and differentiation during cutaneous wound repair. Exp Cell Res. 2010;316:2213-9.

[103] von Bonin M, Stolzel F, Goedecke A, Richter K, Wuschek N, Holig K, et al. Treatment of refractory acute GVHD with third-party MSC expanded in platelet lysate-containing medium. Bone Marrow Transplant. 2009;43:245-51.

[104] Hu X, Yu SP, Fraser JL, Lu Z, Ogle ME, Wang JA, et al. Transplantation of hypoxia-preconditioned mesenchymal stem cells improves infarcted heart function via enhanced survival of implanted cells and angiogenesis. J Thorac Cardiovasc Surg. 2008;135:799-808.

[105] Rosenblum S, Wang N, Smith TN, Pendharkar AV, Chua JY, Birk H, et al. Timing of intra-arterial neural stem cell transplantation after hypoxia-ischemia influences cell engraftment, survival, and differentiation. Stroke. 2012;43:1624-31.

[106] Maxson S, Lopez EA, Yoo D, Danilkovitch-Miagkova A, Leroux MA. Concise review: role of mesenchymal stem cells in wound repair. Stem Cells Transl Med. 2012;1:142-9.

[107] Ruffell D, Mourkioti F, Gambardella A, Kirstetter P, Lopez RG, Rosenthal N, et al. A CREB-C/EBPbeta cascade induces M2 macrophage-specific gene expression and promotes muscle injury repair. Proc Natl Acad Sci U S A. 2009;106:17475-80.

[108] Gordon S, Martinez FO. Alternative activation of macrophages: mechanism and functions. Immunity. 2010;32:593-604.

[109] Sindrilaru A, Peters T, Wieschalka S, Baican C, Baican A, Peter H, et al. An unrestrained proinflammatory M1 macrophage population induced by iron impairs wound healing in humans and mice. J Clin Invest. 2011;121:985-97.

[110] Zhu Z, Ding J, Ma Z, Iwashina T, Tredget EE. Systemic depletion of macrophages in the subacute phase of wound healing reduces hypertrophic scar formation. Wound Repair Regen. 2016;24:644-56.

[111] Choi H, Lee RH, Bazhanov N, Oh JY, Prockop DJ. Anti-inflammatory protein TSG-6 secreted by activated MSCs attenuates zymosan-induced mouse peritonitis by decreasing TLR2/NF-kappaB signaling in resident macrophages. Blood. 2011;118:330-8.

[112] Aurora AB, Olson EN. Immune modulation of stem cells and regeneration. Cell Stem Cell. 2014;15:14-25.

[113] Li T, Yan Y, Wang B, Qian H, Zhang X, Shen L, et al. Exosomes Derived from Human Umbilical Cord Mesenchymal Stem Cells Alleviate Liver Fibrosis. Stem Cells & Development. 2013;22:845.

[114] Lee C, Mitsialis SA, Aslam M, Vitali SH, Vergadi E, Konstantinou G, et al. Exosomes mediate the cytoprotective action of mesenchymal stromal cells on hypoxia-induced pulmonary hypertension. Circulation. 2012;126:2601-11.

[115] Semedo P, Palasio CG, Oliveira CD, Feitoza CQ, Goncalves GM, Cenedeze MA, et al. Early modulation of inflammation by mesenchymal stem cell after acute kidney injury. Int Immunopharmacol. 2009;9:677-82.

[116] Hu L, Wang J, Zhou X, Xiong Z, Zhao J, Yu R, et al. Exosomes derived from human adipose mensenchymal stem cells accelerates cutaneous wound healing via optimizing the characteristics of fibroblasts. Sci Rep. 2016;6:32993.

[117] Aali E, Mirzamohammadi S, Ghaznavi H, Madjd Z, Larijani B, Rayegan S, et al. A comparative study of mesenchymal stem cell transplantation with its paracrine effect on control of hyperglycemia in type 1 diabetic rats. J Diabetes Metab Disord. 2014;13:76.

[118] Timmers L, Lim SK, Hoefer IE, Arslan F, Lai RC, van Oorschot AA, et al. Human mesenchymal stem cell-conditioned medium improves cardiac function following myocardial infarction. Stem Cell Res. 2011;6:206-14.

[119] Xu YX, Chen L, Hou WK, Lin P, Sun L, Sun Y, et al. Mesenchymal stem cells treated with rat pancreatic extract secrete cytokines that improve the glycometabolism of diabetic rats. Transplant Proc. 2009;41:1878-84.

[120] Fukuoka H, Suga H, Narita K, Watanabe R, Shintani S. The latest advance in hair regeneration therapy using proteins secreted by adipose-derived stem cells. The American Journal of Cosmetic Surgery. 2012;29:273-82.

[121] Zhou BR, Xu Y, Guo SL, Xu Y, Wang Y, Zhu F, et al. The effect of conditioned media of adipose-derived stem cells on wound healing after ablative fractional carbon dioxide laser resurfacing. Biomed Res Int. 2013;2013:519126.

[122] Batrakova EV, Kim MS. Development and regulation of exosome-based therapy products. Wiley Interdiscip Rev Nanomed Nanobiotechnol. 2016;8:744-57.

[123] Fais S, O'Driscoll L, Borras FE, Buzas E, Camussi G, Cappello F, et al. Evidence-Based Clinical Use of Nanoscale Extracellular Vesicles in Nanomedicine. ACS Nano. 2016;10:3886-99.

[124] Gyorgy B, Hung ME, Breakefield XO, Leonard JN. Therapeutic applications of extracellular vesicles: clinical promise and open questions. Annu Rev Pharmacol Toxicol. 2015;55:439-64.

[125] Chung L, Maestas DR, Jr., Housseau F, Elisseeff JH. Key players in the immune response to biomaterial scaffolds for regenerative medicine. Adv Drug Deliv Rev. 2017;114:184-92.

[126] Mescher AL, Neff AW, King MW. Inflammation and immunity in organ regeneration. Dev Comp Immunol. 2017;66:98-110.

[127] Julier Z, Park AJ, Briquez PS, Martino MM. Promoting tissue regeneration by modulating the immune system. Acta Biomater. 2017;53:13-28.

[128] Karin M, Clevers H. Reparative inflammation takes charge of tissue regeneration. Nature. 2016;529:307-15.

[129] Das A, Sinha M, Datta S, Abas M, Chaffee S, Sen CK, et al. Monocyte and macrophage plasticity in tissue repair and regeneration. Am J Pathol. 2015;185:2596-606.

[130] Scheib JL, Hoke A. An attenuated immune response by Schwann cells and macrophages inhibits nerve regeneration in aged rats. Neurobiol Aging. 2016;45:1-9.

[131] Chazaud B. Macrophages: supportive cells for tissue repair and regeneration. Immunobiology. 2014;219:172-8.

[132] Spiller KL, Koh TJ. Macrophage-based therapeutic strategies in regenerative medicine. Adv Drug Deliv Rev. 2017;122:74-83.

[133] Ferrante CJ, Leibovich SJ. Regulation of Macrophage Polarization and Wound Healing. Adv Wound Care (New Rochelle). 2012;1:10-6.

[134] de Girolamo L, Lucarelli E, Alessandri G, Antonietta Avanzini M, Ester Bernardo M, Biagi E, et al. Mesenchymal stem/stromal cells: a new"cells as drugs"paradigm. Efficacy and critical aspects in cell therapy. Current pharmaceutical design. 2013;19:2459-73.

[135] Fontaine MJ, Shih H, Schafer R, Pittenger MF. Unraveling the Mesenchymal Stromal Cells' Paracrine Immunomodulatory Effects. Transfus Med Rev. 2016;30:37-43.

[136] Krampera M, Cosmi L, Angeli R, Pasini A, Liotta F, Andreini A, et al. Role for interferon-gamma in the immunomodulatory activity of human bone marrow mesenchymal stem cells. Stem Cells. 2006;24:386-98.

[137] Bruno S, Deregibus MC, Camussi G. The secretome of mesenchymal stromal cells: Role of extracellular vesicles in immunomodulation. Immunol Lett. 2015;168:154-8.

[138] Ozdemir AT, Ozgul Ozdemir RB, Kirmaz C, Sariboyaci AE, Unal Halbutogllari ZS, Ozel C, et al. The paracrine immunomodulatory interactions between the human dental pulp derived mesenchymal stem cells and CD4 T cell subsets. Cell Immunol. 2016;310:108-15.

[139] Zhang B, Yin Y, Lai RC, Tan SS, Choo AB, Lim SK. Mesenchymal stem cells secrete immunologically active exosomes. Stem Cells Dev. 2014;23:1233-44.

[140] Lo Sicco C, Reverberi D, Balbi C, Ulivi V, Principi E, Pascucci L, et al. Mesenchymal Stem Cell-Derived Extracellular Vesicles as Mediators of Anti-Inflammatory Effects: Endorsement of Macrophage Polarization. Stem Cells Transl Med. 2017;6:1018-28.

[141] Chen W, Huang Y, Han J, Yu L, Li Y, Lu Z, et al. Immunomodulatory effects of mesenchymal stromal cells-derived exosome. Immunol Res. 2016;64:831-40.

[142] Zhang QZ, Su WR, Shi SH, Wilder-Smith P, Xiang AP, Wong A, et al. Human gingiva-derived mesenchymal stem cells elicit polarization of m2 macrophages and enhance cutaneous wound healing. Stem Cells. 2010;28:1856-68.

[143] Zhang S, Chuah SJ, Lai RC, Hui JHP, Lim SK, Toh WS. MSC exosomes mediate cartilage repair by enhancing proliferation, attenuating apoptosis and modulating immune reactivity. Biomaterials. 2018;156:16-27.

[144] Sadtler K, Estrellas K, Allen BW, Wolf MT, Fan H, Tam AJ, et al. Developing a pro-regenerative biomaterial scaffold microenvironment requires T helper 2 cells. Science. 2016;352:366-70.

[145] Wang Z, Cui Y, Wang J, Yang X, Wu Y, Wang K, et al. The effect of thick fibers and large pores of electrospun poly(epsilon-caprolactone) vascular grafts on macrophage polarization and arterial regeneration. Biomaterials. 2014;35:5700-10.

[146] Saino E, Focarete ML, Gualandi C, Emanuele E, Cornaglia AI, Imbriani M, et al. Effect of electrospun fiber diameter and alignment on macrophage activation and secretion of proinflammatory cytokines and chemokines. Biomacromolecules. 2011;12:1900-11.

[147] Gizaw M, Thompson J, Faglie A, Lee SY, Neuenschwander P, Chou SF. Electrospun Fibers as a Dressing Material for Drug and Biological Agent Delivery in Wound Healing Applications. Bioengineering (Basel). 2018;5.

[148] Pal P, Dadhich P, Srivas PK, Das B, Maulik D, Dhara S. Bilayered nanofibrous 3D hierarchy as skin rudiment by emulsion electrospinning for burn wound management. Biomater Sci. 2017;5:1786-99.

[149] Kim BJ, Cheong H, Choi ES, Yun SH, Choi BH, Park KS, et al. Accelerated skin wound healing using electrospun nanofibrous mats blended with mussel adhesive protein and polycaprolactone. J Biomed Mater Res A. 2017;105:218-25.

[150] Dong RH, Jia YX, Qin CC, Zhan L, Yan X, Cui L, et al. In situ deposition of a personalized nanofibrous dressing via a handy electrospinning device for skin wound care. Nanoscale. 2016;8:3482-8.

[151] Huleihel L, Bartolacci JG, Dziki JL, Vorobyov T, Arnold B, Scarritt ME, et al. Matrix-Bound Nanovesicles Recapitulate Extracellular Matrix Effects on Macrophage Phenotype. Tissue Eng Part A. 2017;23:1283-94.

[152] Xie H, Wang Z, Zhang L, Lei Q, Zhao A, Wang H, et al. Extracellular Vesicle-functionalized Decalcified Bone Matrix Scaffolds with Enhanced Pro-angiogenic and Pro-bone Regeneration Activities. Sci Rep. 2017;7:45622.

[153] An M, Kwon K, Park J, Ryu DR, Shin JA, Lee Kang J, et al. Extracellular matrix-derived extracellular vesicles promote cardiomyocyte growth and electrical activity in engineered cardiac atria. Biomaterials. 2017;146:49-59.

[154] Mirza R, DiPietro LA, Koh TJ. Selective and specific macrophage ablation is detrimental to wound healing in mice. Am J Pathol. 2009;175:2454-62.

[155] Mahdavian Delavary B, van der Veer WM, van Egmond M, Niessen FB, Beelen RH. Macrophages in skin injury and repair. Immunobiology. 2011;216:753-62.